INFORMATION TO USERS

While the most advanced technology has been used to photograph and reproduce this manuscript, the quality of the reproduction is heavily dependent upon the quality of the material submitted. For example:

- Manuscript pages may have indistinct print. In such cases, the best available copy has been filmed.
- Manuscripts may not always be complete. In such cases, a note will indicate that it is not possible to obtain missing pages.
- Copyrighted material may have been removed from the manuscript. In such cases, a note will indicate the deletion.

Oversize materials (e.g., maps, drawings, and charts) are photographed by sectioning the original, beginning at the upper left-hand corner and continuing from left to right in equal sections with small overlaps. Each oversize page is also filmed as one exposure and is available, for an additional charge, as a standard 35mm slide or as a 17"x 23" black and white photographic print.

Most photographs reproduce acceptably on positive microfilm or microfiche but lack the clarity on xerographic copies made from the microfilm. For an additional charge, 35mm slides of 6"x 9" black and white photographic prints are available for any photographs or illustrations that cannot be reproduced satisfactorily by xerography.

Malikayil, Joy Antony

A CHEMICAL AND SPECTROSCOPIC STUDY OF FERREDOXIN I FROM AZOTOBACTER VINELANDII

City University of New York PH.D. 1987

PLEASE NOTE:

In all cases this material has been filmed in the best possible way from the available copy. Problems encountered with this document have been identified here with a check mark __✓__.

1. Glossy photographs or pages _____
2. Colored illustrations, paper or print _____
3. Photographs with dark background __✓__
4. Illustrations are poor copy _____
5. Pages with black marks, not original copy _____
6. Print shows through as there is text on both sides of page _____
7. Indistinct, broken or small print on several pages __✓__
8. Print exceeds margin requirements _____
9. Tightly bound copy with print lost in spine _____
10. Computer printout pages with indistinct print _____
11. Page(s) _____ lacking when material received, and not available from school or author.
12. Page(s) _____ seem to be missing in numbering only as text follows.
13. Two pages numbered _____. Text follows.
14. Curling and wrinkled pages _____
15. Dissertation contains pages with print at a slant, filmed as received __✓__
16. Other _____

_____

_____

University
Microfilms
International

A CHEMICAL AND SPECTROSCOPIC STUDY OF FERREDOXIN I FROM AZOTOBACTER VINELANDII

by

J. ANTONY MALIKAYIL

A dissertation submitted to the Graduate Faculty in Biochemistry in partial fulfillment of the requirements for the degree of Doctor of Philosophy, The City University of New York.

1987

This manuscript has been read and accepted for the Graduate Faculty in Biochemistry in satisfaction of the dissertation requirement for the degree of Doctor of Philosophy.

1/25/86
Date

William Sawyer
Chair of Examining Committee

1/26/87
Date

Horst Schulz
Executive Officer

Thomas C. Stefas
Thomas H. Haines
William E. L. Grossman
Michelle S. Bridle
Supervisory Committee

The City University of New York

Abstract

A CHEMICAL AND SPECTROSCOPIC STUDY OF FERREDOXIN I FROM AZOTOBACTER VINELANDII

by

J. Antony Malikayil

Adviser: Prof. William Sweeney

Ferredoxin I of Azotobacter vinelandii is an iron sulfur protein containing one [4Fe-S] cluster and one [3Fe-3S] cluster. The structure and geometry of the 3Fe cluster is under dispute. The X-ray crystal structure of the protein describes the 3Fe cluster as a planar [3Fe-3S] cluster in which one of the iron atoms is ligated to a solvent accessible oxoligand, presumably from water or hydroxide (Ghosh et al., (1982) J. Mol. Biol. 158: 73-109). Efforts to displace the oxoligand were unsuccessful even when the protein was demonstrably denatured in 80% (V/V) dimethyl sulfoxide. In addition, comparison of the electron spin echo envelopes for H2O and D2O-equilibrated samples of ferredoxin I showed only a slight deuterium modulation, far less than would be expected were water to be bound as an iron ligand. These results

do not support the presence of a solvent accessible oxoligand to the 3Fe center as described in the X-ray crystal structure.

The latter part of the thesis describes studies conducted in efforts to characterize the hyperfine-shifted resonances in the proton magnetic resonance spectrum of ferredoxin I. A. vinelandii was grown on synthetic media that contained isotopically labelled cystine as the only sulfur source. In independent experiments ferredoxin I was isolated from organism that was grown on such medium that contained alpha-^{2}H-dl-cystine, beta-^{2}H-dl-cystine, or beta-^{13}C-dl-cystine. However, ferredoxins isolated from these media were devoid of the corresponding isotopic labels. Thus the experiments designed to characterize the hyperfine-shifted resonances of ferredoxin I were unsuccessful.

I dedicate this thesis to my parents and Lynn.

ACKNOWLEDGEMENT

I wish to thank my thesis advisor, Prof. William V. Sweeney for the guidance and help that he had provided in a multitude of ways during the years of my graduate carreer. I also thank the members of my thesis committee, Prof. Michelle Broido, Prof. William Grossman, Prof. Thomas Haines, and Prof. Thomas Strekas. I am very thankful to Prof. Klaus Grohman for the synthesis of isotopically labelled cysteines to assist my research. Credits are also due to Prof. Ian Armitage of Yale University for some very helpful discussions, and also for making his Bruker CXP-200 spectrometer available to me which was very implemental to the completion of this thesis. Finally, credits are due to my friend, Lynn Brostoff, partly to whom I dedicate this thesis.

TABLE OF CONTENTS

LIST OF ABBREVIATIONS

DMSO	dimethyl sulfoxide
DSS	Sodium 2,2-dimethyl-2-silapentane-5-sulfonate.
FdI	ferredoxin I of Azotobacter vinelandii.
FdIA	ferredoxin I isolated from Azotobacter vinelandii grown on cystine medium containing alpha-^{2}H-dl-cystine.
FdIB	ferredoxin I isolated from Azotobacter vinelandii grown on cystine medium containing beta-^{2}H-dl-cystine.
FdIC	ferredoxin I isolated from Azotobacter vinelandii grown on cystine medium containing beta-^{13}C-dl-cystine.
PSI	pounds per square inch.

LIST OF FIGURES

INTRODUCTION

Ferredoxins are low molecular weight iron sulfur proteins present in prokaryotic and eukaryotic organisms. They are known to function as electron transport proteins in bacteria, chloroplast and mitochondria. The prosthetic groups of these proteins, iron sulfur centers, are connected to the peptide moeity of the protein generally through cysteines as ligands to the iron atoms. Two ferredoxins are reported to have non-cysteinyl ligands to iron (1,2).

Three different kinds of iron sulfur centers are recognized in ferredoxins. [2Fe-2S] centers (Figure IA) are common both in plant and animal ferredoxins. [4Fe-4S] centers (Figure IB) are prevalent in bacterial, plant and mammalian ferredoxins. The structure of these two types of iron sulfur centers are extensively studied in various systems. [3Fe-nS] centers are of recent discovery (1,3,4,5,6). It is not certain whether the 3Fe centers exhibit structural variations among proteins in which they have been recognized. Three different structures have been proposed for this novel iron sulfur center (Figure II and Figure III).

Figure I

The structure of [2Fe-2S] center (A) and [4Fe-4S] center (B).

A

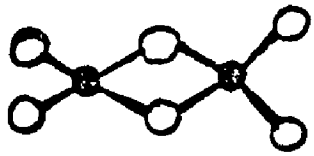

B

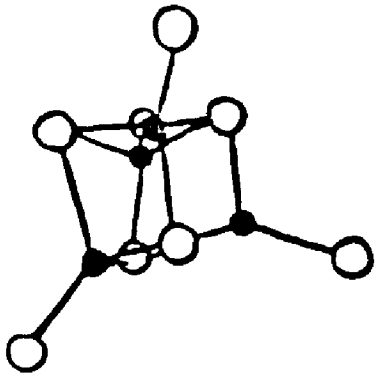

Figure II

The 2.0 A X-ray diffraction structure of the [3Fe-3S] center of FdI, Ghosh et al. (1982).

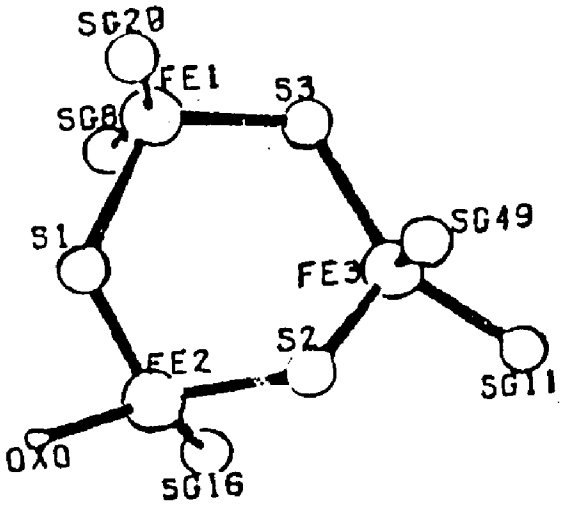
SG20
FE1
S3
SG8
S1
SG49
FE3
S2
FE2
SG11
OXO
SG16

Figure III

The common structure of [3Fe-4S] center proposed for 3Fe [Fe-S] clusters, Johnson et al. (1984).

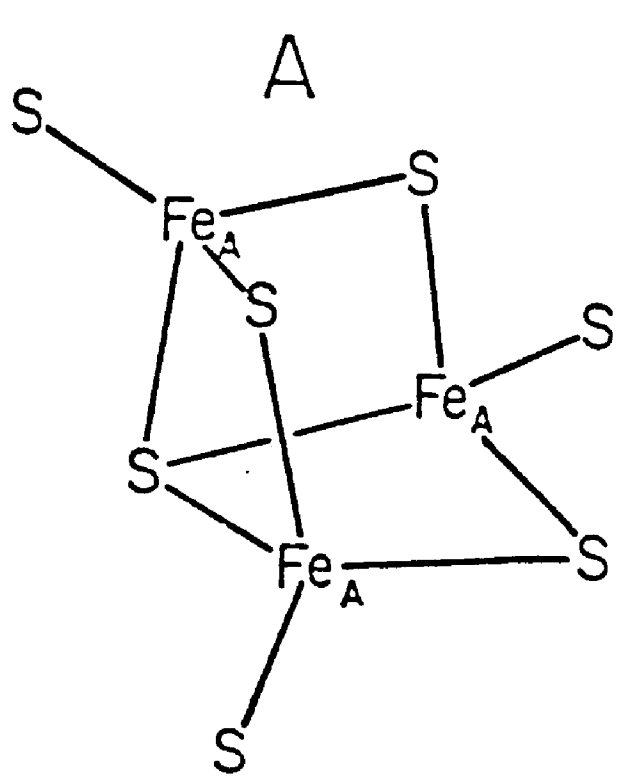

$Fe_3S_4^bS_3^t$

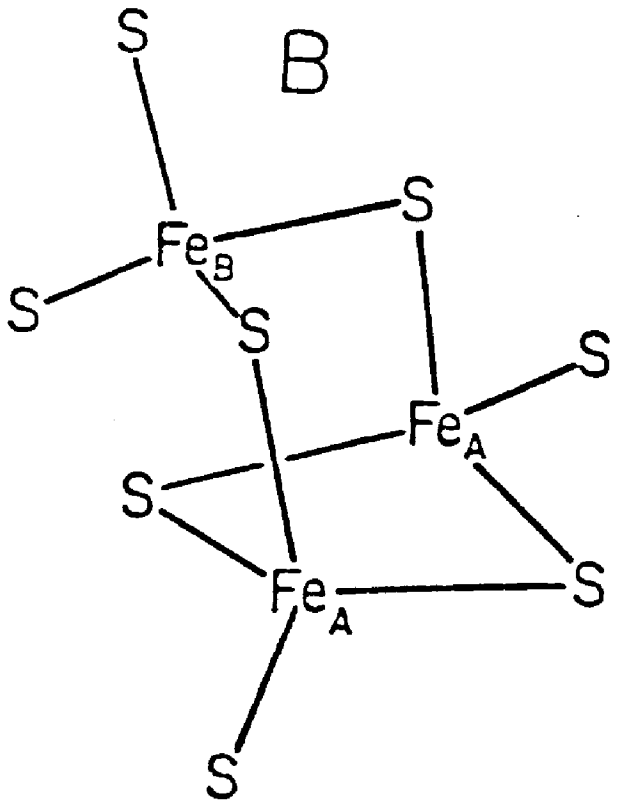

$Fe_3S_4^bS_4^t$

Three iron centers in ferredoxins

The possibility for the existence of 3Fe centers in ferredoxins was first suggested by Mossbauer studies on ferredoxin I (FdI) of Azotobacter vinelandii (6). This surprising result was promptly supported by 2.5 A X-ray diffraction studies of FdI (7). Within a short period after this initial discovery the number of proteins that are thought to contain 3Fe centers rapidly expanded. At present, ferredoxin II of Desulfovibrio gigas (FdII), the Kreb's cycle enzyme aconitase, a ferredoxin from Thermus thermophilus, a ferredoxin from Pseudomonas ovalis, a ferredoxin from Mycobacterium smegmatis, glutamate synthase from A. vinelandii and Escherichia coli, and several hydrogenases are thought to contain 3Fe centers, and the list is certain to grow at a fast rate.

Various spectroscopic data are available for proteins that contain 3Fe centers. However, X-ray diffraction data of 3Fe containing proteins are limited to FdI of A. vinelandii and aconitase of pig heart mitochondria (1,5). FdII of D. gigas and aconitase are ideally suited for the spectroscopic characterization of 3Fe centers since these proteins contain a single type of [Fe-S] clusters.

The structure of the 3Fe center of FdI reported by the 2.0 A X-ray diffraction study (1) is shown in Figure II. Accordingly, the 3Fe center is a nearly planar 3Fe-3S ring with distorted tetrahedral coordination about each iron atom. The internal angles at S(1), S(2), and S(3) are 126°, 131°, and 113° respectively. These values are 35° to 55° larger than the reported ~75° internal angles at the inorganic sulfur atoms for the [2Fe-2S] and [4Fe-4S] centers. As a consequence of these large bond angles the Fe...Fe separation is 4.01 A, a value considerably larger than the average Fe...Fe separation of 2.7 A in [2Fe-2S] and [4Fe-4S] clusters. Another distinguishing feature of the structure is the presence of an oxo ligand, water or hydroxide, coordinated to Fe(2). Thus the 3Fe center of A. vinelandii is the first ferredoxin reported to have a non-cysteinyl coordination to iron.

According to the 2.7 A X-ray diffraction studies of aconitase from pig heart mitochondria (5), the 3Fe center of this protein exhibits Fe...Fe separations and bond angles that are normal among ferredoxins and the synthetic analogues of their active sites. This result is consistent with a [3Fe-4S] structure proposed on the basis of chemical analysis and extended x-ray absorption fine structure (EXAFS) measurements of aconitase from

beef heart mitochondria (3). EXAFS studies on FdII of D. gigas also reported an Fe...Fe separation of 2.7 A for this 3Fe center (8).

The Mossbauer characteristics of the 3Fe centers of FdI of A. vinelandii, FdII of D. gigas, and beef heart aconitase are very similar (6,8,9). In the isolated state all three centers exhibit a single quadrupole doublet with an isomer shift of 0.27 mm/sec and quadrupole splittings of 0.63 mm/sec, 0.54 mm/sec, and 0.71 mm/sec respectively. Thus all three iron atoms are equivalent. The isomer shift and the quadrupole split values are consistent with high spin ferric iron atoms in tetrahedral sulfur environments. The iron atoms are antiferromagnetically spin coupled to a system spin of 1/2 (10). Thus the g = 2.01 epr signal of the 3Fe centers arise from the oxidized 3Fe center. In the one electron reduced state, the centers display a pair of doublets with intensity ratios of 2:1 with isomer shifts around 0.46 mm/sec and 0.29 mm/sec. These data have been interpreted as originating from a trinuclear center with two iron atoms in the formal oxidation state of 2.5 and the third iron atom in the formal oxidation state of 3.0. Thus the incoming electron is shared by two iron atoms while the oxidation state of the third iron atom is unaffected by reduction. In this state the system spin

assumes an integral value >1 and the cluster becomes epr silent (10). By analysis of the low temperature magnetic circular dichroism curve, a spin value of S =2, has been assigned to the dithionite reduced clusters of FdII of D. gigas and aconitase of beef heart (11,12).

Resonance Raman spectra of a number of proteins, including FdI of A. vinelandii and FdII of D. gigas, containing 3Fe centers have been reported (4). The results indicate a common [3Fe-4S] structure for the 3Fe centers of all the proteins that have been studied. Furthermore the interatomic distances and bond angles of the structure were predicted to be essentially similar to those in other ferredoxins.

Thus the [3Fe-3S] structure proposed for the 3Fe center of FdI of A. vinelandii by X-ray crystallography is in direct conflict with the common [3Fe-4S] structure proposed for 3Fe centers by a variety of spectroscopic studies.

Ferredoxin I of Azotobacter vinelandii (FdI)

Early history

Ferredoxin I of azotobacter vinelandii was independently isolated by Shethna and Yoch et.al (13,14).

Shethna designated this protein as iron sulfur protein III and described it as very similar in properties to clostridial-type ferredoxins.

Three years later Yoch and Arnon reported the partial characterization of two iron sulfur proteins from A. vinelandii (15). They called these proteins ferredoxin I and ferredoxin II. The more abundant ferredoxin I was the iron sulfur protein previously reported by Shethna and Yoch et al.. Yoch and Arnon's terminology is currently in practice.

Yoch and Arnon, while describing FdI as similar in properties to clostridial-type ferredoxins, noted some distinctions in this protein. The molecular weight of the new ferredoxin was approximately twice that of the clostridial-type ferredoxins. The sulfur groups of the new protein were only slowly and partially titrable by p-chloromercurobenzoate. The significantly higher stability of FdI to oxygen and in 4M guanidium hydrochloride was noted and was rationalized in terms of feasible biological functionality. Thus even the earliest works on FdI revealed deviations in properties from the well studied ferredoxins.

Sweeney and Rabinowitz (16) reported the first

evidence for the presence of two types of iron sulfur centers in FdI. In its isolated state FdI displayed a g = 2.01 EPR signal. On one electron reduction this signal disappeared. The midpoint potential for this reduction was -420 mV. On oxidation with potassium ferricyanide new features appeared in the EPR spectrum. Quantitative EPR showed that a second cluster in the protein became paramagnetic by yielding one electron to the oxidant (16). A midpoint- reduction potential of +360 mV was estimated for the second cluster. Thus FdI was the first known instance of an iron-sulfur protein with clusters that widely vary in reduction potentials.

Que et al. (17) demonstrated that intact [Fe-S] clusters can be extruded from proteins, under anaerobic conditions in 80% DMSO solution, by displacement of the cysteine ligands with organic thiol reagents. The extruded cluster can be easily characterized by UV visible spectroscopy. The first cluster extrusion experiments on FdI reported the removal of two [4Fe-4S] clusters from the protein (18). However, in a later experiment, one cluster was reported to extrude as a [4Fe-4S] cluster while second cluster was reported not to yield any identifiable species (19). Thus, this result was the earliest evidence for the existence of a novel [Fe-S] cluster in FdI.

Structure of FdI

The complete amino acid sequence of FdI has been determined and the sequence has been confirmed by 2A electron density maps for the residues (20). The primary structure of the protein as reported by this study is shown in Figure IV.

The protein contains 106 amino acids. FdI is thus readily distinguished from the clostridial-type ferredoxins by the increased length of its peptide moiety. However, the amino half-terminal of FdI contains all the cysteines and is related to the clostridial-type ferredoxins. In this region of 58 amino acid residues there are 40% sequence identities and 25% conservative replacements in comparison to clostridial-type ferredoxins. The important structural variations between clostridial-type ferredoxins and FdI can be rationalized in terms of the unique spatial requirements of the latter protein to accommodate an unusual 3Fe center. Despite the close similarity in cysteine distribution to clostridial-type ferredoxins, FdI more closely resembles High potential iron proteins (HiPIPs) in its spectroscopic characteristics.

The 2.0 A X-ray diffraction study of FdI reported

Figure IV

The amino acid sequence of FdI, Howard et al. (1983).

$^{+}NH_3$-Ala-Phe-Val-Val-Thr-Asp-Asn-Cys-Ile-Lys-Cys-
Lys-Tyr-Thr-Asp-Cys-Val-Glu-Val-Cys-Pro-Val-Asp-
Cys-Phe-Tyr-Glu-Gly-Pro-Asn-Phe-Leu-Val-Ile-His-
Pro-Asp-Glu-Cys-Ile--Asp-Cys-Ala-Leu-Cys-Glu-Pro-
Glu-Cys-Pro-Ala-Glu-Ala-Ile-Phe-Ser-glu-Asp-Glu-
Val-Pro-Glu-Asp-Met-Gln-Glu-Phe-Ile-Gln-Leu-asn-
Ala-Glu-Leu-Ala-Glu-Val-Trp-Pro-Asn-Ile-Thr-Glu-
Lys-Lys-Asp-Pro-Leu-Pro-Asp-Ala-Glu-Asp-Trp-Asp-
Gly-Val-Lys-Gly-Lys-Leu-Gln-His-Leu-Glu-Arg-COO^{-}

several important structural features (1). Accordingly, the protein contains a [4Fe-4S] center and a [3Fe-3S] center. The former center is a typical HiPIP type center, in terms of cluster geometry and structure. On the other hand, the 3Fe center is a hitherto unrecognized [Fe-S] center with unusual structural features. The center has a nearly planar, slightly twist boat conformation. Each Fe atom is in a distorted tetrahedral environment. Two Fe atoms are bonded to two cysteines each, and the third Fe atom is ligated by one cysteine and an oxoligand, presumably water or hydroxide. The internal angles at the inorganic sulfur atoms are 35^{o} to 55^{o} larger than the angles known for other [Fe-S] centers in proteins and in model compounds. Because of this large internal angles at the inorganic sulfurs, the Fe...Fe and Fe...S separations in the 3Fe center are much larger than what is common in other [Fe-S] centers.

In the folding of FdI little secondary structure is observed. There is no alpha helix and there is only one small segment of antiparallel beta structure. The molecule possesses a cleft that extends from the exterior to the interior of the molecule leading to the oxoligand of the 3Fe center. The cavity is hydrated to the extent that the oxoligand itself is presumed to be hydrated.

There are 36 ionizable groups in the protein. The isoelectric point of the protein is at pI ~4. At neutral pH the net charge on the protein is expected to be -22. There is a marked concentration of acidic residues in the vicinity of the 4Fe center and of basic residues near the 3Fe center. The cleft region is rich in acidic residues facilitating its high degree of hydration. There is extensive hydrogen bonding to water and there are two salt linkages in the protein.

Spectroscopic properties of FdI

Optical spectrum: The UV-visible absorption spectrum of FdI in the region of 600-240 nm is shown in Figure V. The spectrum shows an absorption shoulder around 400 nm and an absorption peak at 280 nm. The absorption around 400 nm originates from Fe S charge transfer transitions and is a common feature among ferredoxins. On reduction of the protein using sodium dithionite, there is a marked reduction in absorbance in the visible region of the spectrum. The ratio of absorbances at 425 nm between oxidized and fully reduced ferredoxins at 412 nm is 0.81. The molar extinction coefficient of the oxidized protein at 400 nm is 30 mM^{-1} cm^{-1}. The ratio of absorbances(A_{400} / A_{280}) is used as an indication of protein purity. Typically this ratio varied between 0.59 and 0.57. However, on a few

Figure V

The UV-visible absorption spectrum of FdI.

Solvent 0.1 M tris.Cl / 0.1 M NaCl, pH 7.17.

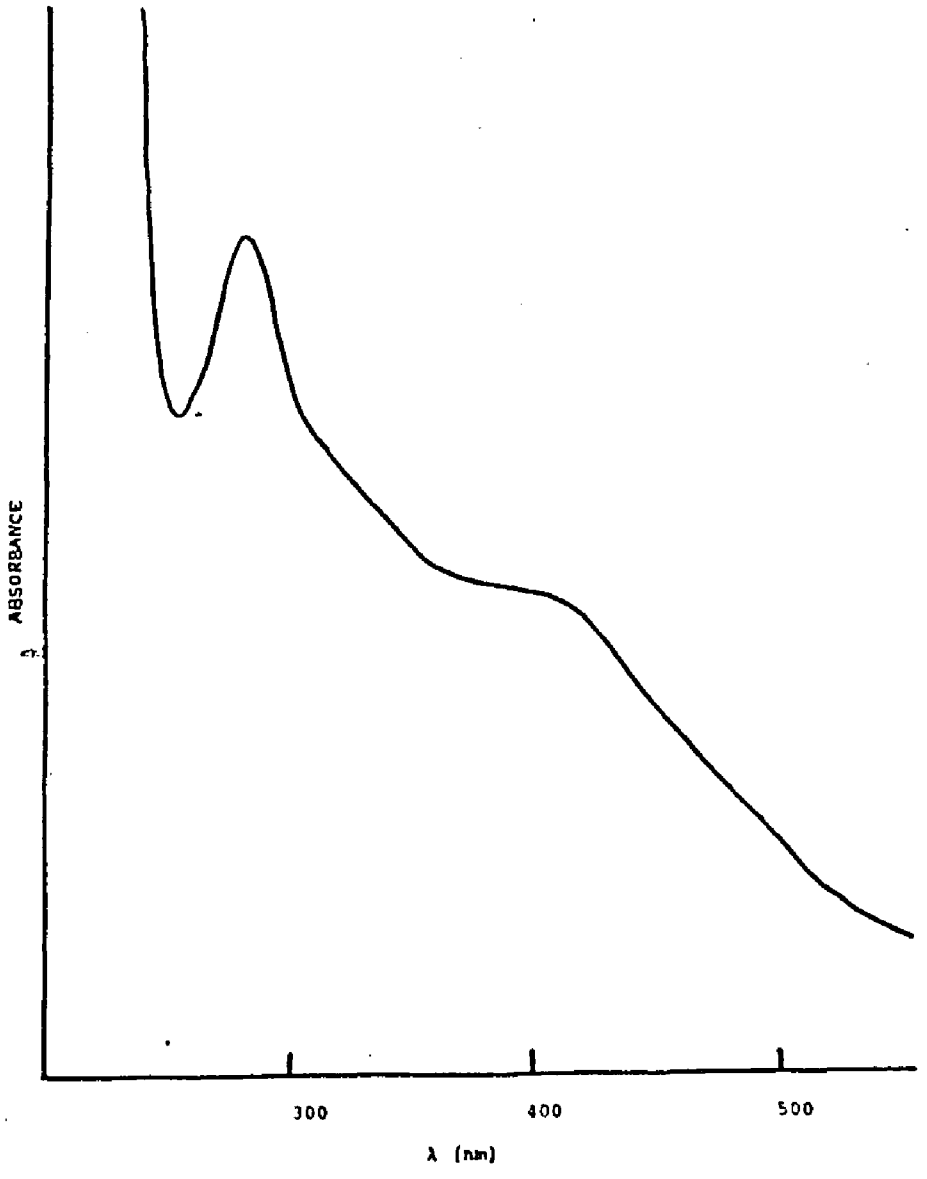
ABSORBANCE
300
400
500
λ (nm)

occasions proteins with purity ratios of 0.60 were prepared.

Electron paramagnetic resonance (EPR) spectrum: The X-band EPR spectrum of a frozen solution of FdI in the isolated state of the protein is shown in Figure VI. The spectrum shows a nearly isotropic line with a g value of 2.01. The line width at 15 K is approximately 35 gauss. The signal becomes undetectable above 18 K due to fast electron relaxation. On one electron reduction of the protein with sodium dithionite, the signal disappears and no new signal was detected.

Figure VII shows the epr spectrum of a sample of FdI reduced with sodium borohydride. The spectrum shows a line at g = 1.94 which is characteristic of reduced [4Fe-4S] centers in ferredoxins. Thus it appears that the 4Fe center of FdI is reducable to the +1 oxidation state in the presence of a strong reducing agent (21).

Proton magnetic resonance (PMR) spectrum: The 400 MHz proton magnetic resonance spectrum of FdI is shown in Figure VIII. The aliphatic region of the spectrum, i.e. 0 to +5 ppm from DSS, is virtually featureless due to excessive overlap of resonances. The spectral region of +5 ppm to +10 ppm presumably contains resonance lines

Figure VI

The X-band EPR spectrum of FdI. Solvent 0.1 M tris.Cl / 0.1 M NaCl, pH 7.17. Temperature 13 K; gain 630; modulation amplitude, 2.5 G; power 2 mW; frequency 9.4 GHz.

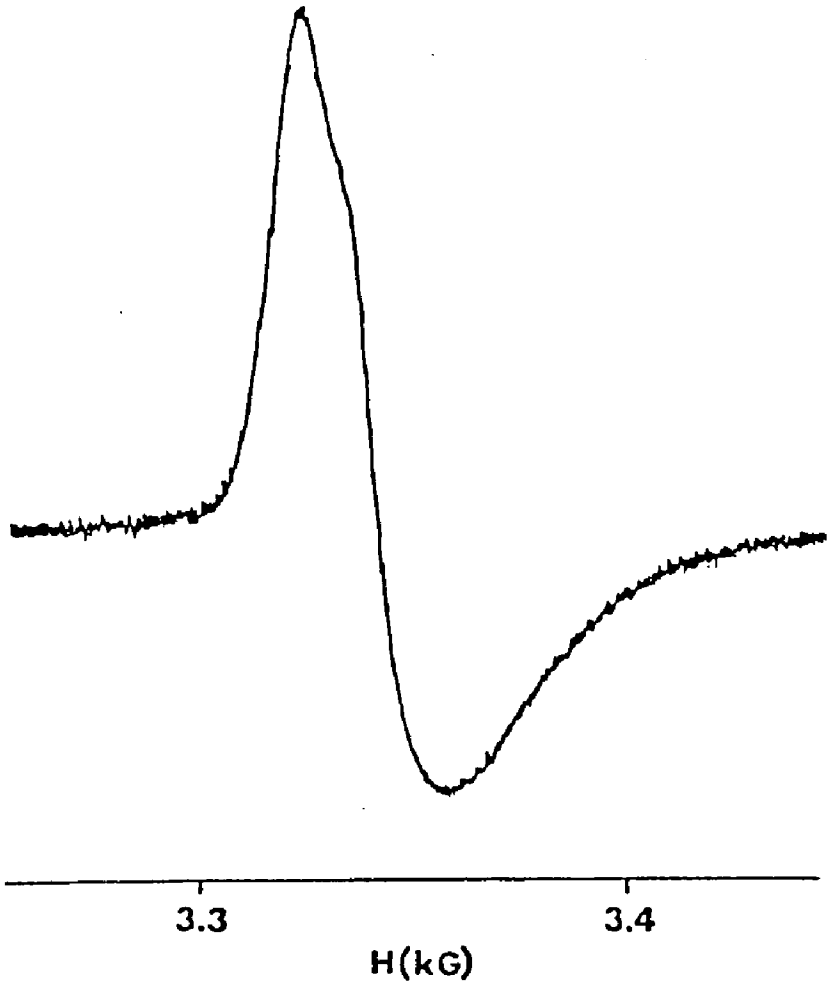
3.3
3.4
H(kG)

Figure VII

X-band EPR spectrum of fully reduced FdI (both clusters reduced). Solvent 0.1 M tris.Cl / 0.1 M NaCl, pH 7.17. Temperature 13 K; gain 630; modulation amplitude, 2.5 G; power 2 mW; frequency 9.4 GHz.

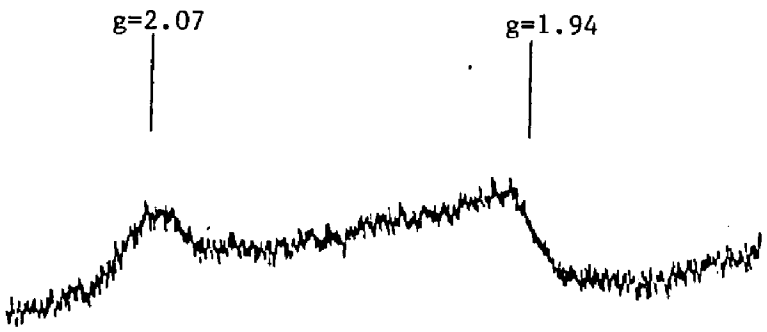
g=2.07
g=1.94

Figure VIII

400 MHz PMR spectrum of FdI. Solvent 50 mM potassium deuterium phosphate buffer, pD 7.39. Temperature, 25^{o}C; Spectral width, 40000 Hz; Points 65336; Acquisition time, 0.819 seconds; pulse delay, 0.681 seconds; window, exponential, BF, 0.3 Hz. HDO = 4.8 ppm.

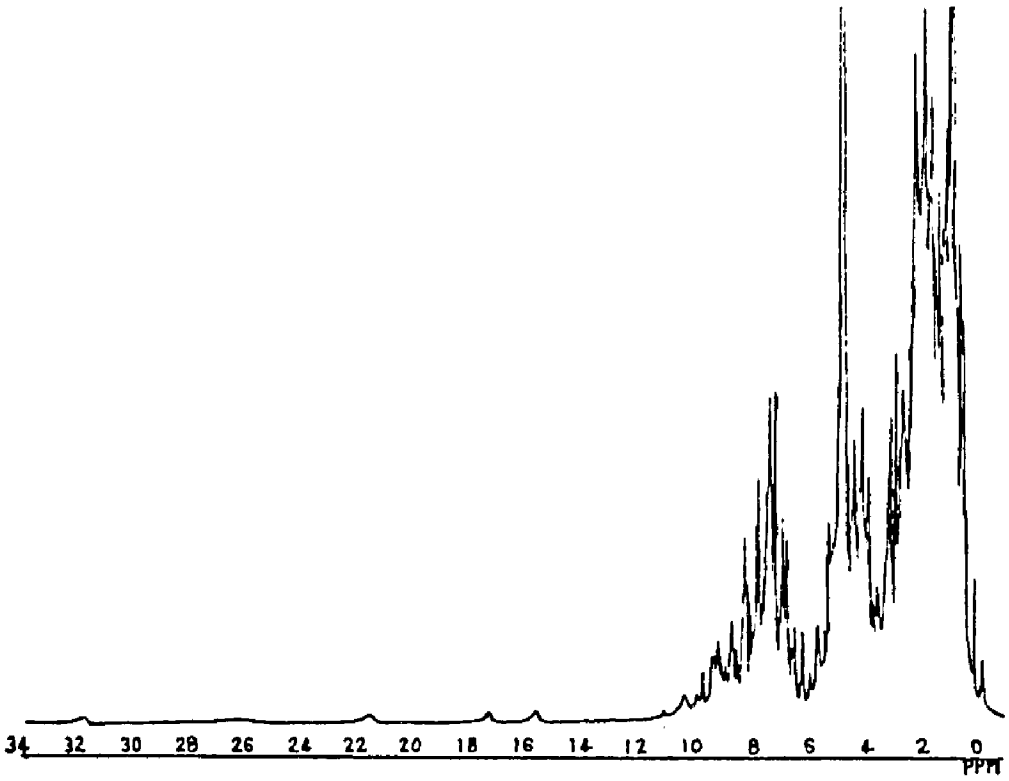
34
32
30
28
26
24
22
20
18
16
14
12
10
8
6
4
2
0
PPM

originationg from the aromatic amino acids, the dipolar shifted lines of hydrogens on residues in the vicinity of the [Fe-S] centers and backbone amide hydrogens.

The far downfield region, +15 ppm to +35 ppm, of the spectrum displays five hyperfine shifted resonances. On reduction of the 3Fe center, the three most downfield resonances disappear. Thus these three lines were expected to originate from protons in the vicinity of the 3Fe center. On reduction of the p+rotein with sodium borohydride the three most downfield resonances completely disappear and the two resonances near 15 ppm reduce in intensity. Therefore the resonances near 15 ppm presumably arise from protons near the 4Fe center. A detailed study of the PMR spectrum of FdI is reported later.

GENERAL METHODS

Growth of Azotobacter vinelandii

Azotobacter vinelandii was regularly grown in a Fermatron-150 fermentor in 100 liter batches. The growth medium contained per hundred liters,

$MgSO_4.7H_2O$	20.0g
$CaSO_4.2H_2O$	5.0g
$FeSO_4$	0.42g
$NaMoO_4$	0.1g
Sucrose	2.0Kg
K_2HPO_4	64.0g
KH_2PO_4	16.0g

The fermentor was autoclaved at 121 ^{o}C for 45 minutes with all the ingredients except the phosphates. The phosphates were autoclaved in 750 ml water and were added into the fermentor immediately before innoculation. The pH of this medium was generally around 7.4. The medium was innoculated with 30 g of frozen cells. The cells were grown at 30 ^{o}C with vigorous agitation and bubbling of air through the growth medium. Cells were usually harvested, using a CEPA cell harvester, 18-20 hours after innoculation or when the Klett turbidometric reading reached approximately 450. The pH was noted to drop steadily as growth progressed, to a final value of 6.5. However, no pH adjustment was necessary during the growth cycle. A typical yield was 600 g of cells from

one growth cycle. The cells were stored at -20 ^{o}c in air-tight plastic bags.

Isolation of ferredoxin I

600 g of frozen cells were smashed with a hammer into small chunks in a 4 liter plastic bucket. 1200 ml of 0.05 M Tris.Cl, pH 7.17, were added and the cells were suspended in the buffer by gentle agitation with an overhead paddle. The cell suspension was placed in an ice bath and 600 ml of n-butanol was added portionwise as fast as mixing occurred. After the complete addition of the butanol, the cell suspension was stirred for an additional 60 minutes at the ice bath temperature. This whole operation was carried out at 5 - 10 ^{o}C. During this time the viscosity of the solution gradually increased presumably due to the release of nucleic acids.

The cell extract from the previous step was centrifuged at 12000 X G for 2 hours. Three distinct layers were obtained in the centrifuge bottle- a yellow lipid layer, a dark brown soluble-protein layer, and a layer of solid cell debris. The lipid layer was carefully removed by continuous suction through a Pasteur pipette. The dark brown protein layer was decanted through a multiple layer of cheese cloth into a large flask without disturbing the sedimented cell debris. The

protein solution was clarified by centrifugation at 12000 X G for 15 minutes, if necessary. The protein solution was then added to 400 ml of settled DEAE (Whatman DE 52) equilibrated with 0.05 M Tris.cl, pH 7.17. This mixture was very gently stirred with an overhead paddle at room temperature for one hour.

The mixture was centrifuged at 2500 X G for 3 minutes. The reddish supernatant, predominantly cytochromes, was discarded. The sedimented DEAE was suspended in 0.05 M Tris.Cl, pH 7.17, and was recentrifuged as before. This procedure was repeated until the color of the supernatant became faint yellow. The DEAE from the above step was made into a thin suspension by dilution with the same buffer. This DEAE suspension was poured into a 5 cm X 30 cm column. The column was packed using the same buffer. The packed column was washed with the same buffer for at least one column volume. Then the protein was eluted with a 0.05 M Tris.Cl buffer, pH 7.17, containing 0.4 M NaCl. When the dark brown protein band reached the bottom of the column the eluant was collected. Thus all the DEAE-bound proteins were collected as one fraction. The protein solution was dialysed for 40 hours at 4 ^{o}C against distilled water, pH adjusted to 7.0 with 0.1 M Tris.Cl, pH 7.17.

The dialyzed protein was applied to a 3 cm X 15 cm DEAE(Sephacel) column pre-equilibrated with 0.05 M Tris.Cl, 0.05 M NaCl, pH 7.17. The column was first washed with the same buffer for 2-3 column volumes. Then the column was washed with the same buffer of 0.1 M NaCl concentration. At this stage three distinct bands were observable in the column. A diffuse reddish brown band, which was predominantly cytochromes and other iron sulfur proteins, a yellowish flavin band and a tightly bound grayish FdI band. The washing was continued until all of the reddish brown band was eluted. Then the salt concentration of the buffer was increased to 0.15 M NaCl. This washing was continued until all of the flavin band eluted off and the ferredoxin band reached the bottom of the column. The ferredoxin band was collected as a concentrated solution with the buffer of 0.4 M NaCl concentration.

At this stage the protein showed a high 260 nm absorbance due to RNA contamination. Therefore the solution was transferred into an amicon ultrafiltration vessel equipped with a YM 10 membrane for RNA digestion. 5.0 mg of ribonuclease was added and the solution was concentrated at a nitrogen gas pressure of 40 psi. When the solution level reached below the stirrer more of 0.1 M Tris.Cl, pH 7.17, was added. The process was

repeated several times. The protein was finally concentrated to a volume of 5 ml and stored under argon overnight at 4 ^{o}C.

The nucleased protein was applied on a 5 cm X 100 cm sephadex G75 (superfine) column, that was preequilibrated with 0.1 M tris.Cl, 0.1 M NaCL, pH 7.4(4 ^{o}C). Sephadex chromatography was carried out in a cold room that was maintained at 4 ^{o}C. The protein reached the bottom of the column usually in 3 1/2 days. 5 ml fractions were collected. All fractions with a A_{400nm} / A_{280nm} ratio of 0.48 and above were pooled together and were concentrated to a volume of 20 ml. The solution was brought to 80% saturation with grade 1 $(NH_4)_2SO_4$ (Sigma Chemicals), under a constant flow of argon over the solution surface. Before addition, the solid $(NH_4)_2SO_4$ was thoroughly powdered with 2.2 mg of trizma base, per gram of ammonium sulfate, to counteract the pH effect of $(NH_4)_2SO_4$. The solution was thoroughly deaired by repeated evacuation and flushing with argon gas and was stored at 4 ^{o}C until further use. The protein usually precipitated on overnight standing. The protein at this stage usually had a A_{400nm} / A_{280nm} ratio of 0.57 - 0.59. A typical yield was 7 mg of ferredoxin I.

Growth of Clostridium pasteurianum

Clostridium pasteurianum cells were grown, by the procedure of Rabinowitz (22) for the isolation of hydrogenase. Cultures were started by innoculation of lyophilized cells into a potato medium in a 25 ml culture tube fitted with an anaerobic cotton plug (cotton plug soaked with alkaline pyragallol). The fully grown potato tube culture was used to innoculate a 125 ml synthetic medium in a 250 ml volumetric flask. The synthetic medium contained, per liter,

Sucrose (supermarket brand Domino)	200g
$MgCl_2.6H_2O$	0.15g
$NaCl$	0.10g
$Na_2MoO_4.2H_2O$ (10% w/v)	0.10ml
Biotin + p-aminobenzoic acid (solution 0.01% in each)	0.05ml
Na_2SO_4	0.07g
NH_4Cl	16.0g
$CaCO_3$	1.5g
$FeCl_3$ (5% in absolute ethanol)	4.0ml and
K_2HPO_4 (sterile solution in water)	4.45g.

The medium was autoclaved at 121 ^{o}C for 45 minutes with all the components, except $FeCl_3$ and K_2HPO_4 which were added just prior to innoculation. Cells were harvested by centrifugation while the cells were actively evolving hydrogen and when the growth medium showed a high turbidity.

Partial purification of Hydrogenase.

The general procedure of Lode et. al (23) was

strictly followed for the preparation of hydrogenase. Extreme precautions were taken against atmospheric oxygen throughout the preparation.

Approximately fifty grams of freshly harvested cells were suspended in 50 ml of 0.01 M potassium phosphate buffer (pH 7.4) that had been previously saturated with hydrogen gas and subsequently made 0.01M in $Na_2S_2O_4$. The cell suspension was sonicated at 0 ^{o}C (Sonifier cell disruptor Model W140, Heat systems Ultrasonics) at 80% full power for 20 minutes. The cell extract thus obtained was centrifuged at 14000 X g for one hour. The supernatant was applied to a DEAE column (Whatman DE52). This column had been equilibrated first with 0.1 M potassium phosphate (pH 7.4), and then with several column volumes of the same buffer saturated with hydrogen gas and finally with the same buffer saturated with hydrogen and containing 0.01 M Na_2S2O_4. The green 'pass-thru' was collected in centrifuge tubes under a constant flow of hydrogen gas over the solution surface. The peak fractions were placed in a water bath at 60 ^{o}C for 10 minutes fitted with serum caps on the containers. The tubes were centrifuged at 3000 x G for 45 minutes. The supernatant was anaerobically transferred into 0.5ml sample tubes equipped with serum caps. The sample tubes were flushed with hydrogen gas through inlet and outlet

needles on the serum cap and were frozen in liquid nitrogen. The samples were stored in liquid nitrogen until the time of use.

Preparation of inert atmosphere glove box

A argon/hydrogen atmosphere glove box was prepared to carry out the oxygen sensitive treatments of the protein.

A mixture of prepurified grade argon (Linde) and prepurified grade hydrogen (Linde), (10 parts : 1 part), entered the main chamber of the glove box. During the initial stage of the glove box preparation, this incoming gas was allowed to exit through the glove box outlet, a bubbler equipped with a float-check valve filled with oil, in gentle bubbling. Two to three hours prior to use, the inside atmosphere was further refined by circulation through a tower of reduced BASF catalyst at 150 ^{o}C. The gas was circulated, by a diaphragm pump, through the oxygen scrubbing tower and a cold trap and was then readmitted into the main chamber of the glove box. During use of the box, the continuous atmosphere-recirculation was in effect and the bubbler was closed to the glove box. All entries and exits into the glove box were through the small anteport of the glove box. The anteport , with the samples in, was purged by repeated

evacuation and flushing cycles. The integrity of the glove box was generally checked by the ability to maintain the blue color of a dilute solution of chromous chloride or reduced methyl viologen.

The oxygen scrubbing tower was reduced in a fume hood before assembly into the glove box system. The catalyst was loosely packed in a 30 cm column equipped with a heating tape and a thermometer at the top of the packing. The tower was slowly heated to 100 ^{o}C with a gentle flow of nitrogen gas, in the bottom to top direction. A small amount of hydrogen was then allowed to mix with the nitrogen before it entered the column. Gradually the hydrogen partial pressure was increased. The temperature of the column was not allowed to rise above 250 ^{o}C at any time. The tower was finally reduced with undiluted hydrogen. On reduction the green catalyst turned black ($CuO + H_2 \rightarrow Cu + H_2O$). During use of the box, the argon gas entering the glove box was mixed with hydrogen (10 parts / 1 part), to maintain the tower in a reduced state.

Preparation of NMR samples

A 0.05 M K2DPO4/KD2PO4 buffer (potassium deuterium phosphate buffer) was prepared by the titration of a solution of K2DPO4 in D_2O (99.8 atom%) with a 40% (w/v)

solution of KOD in D_2O. The pD of the solution was estimated by the method of Covington (24).

Ferredoxin precipitate from 80% ammonium sulfate solution was collected by centrifugation at 10000 X G for 20 minutes. The pellet was dissolved in 0.05 M potassium phosphate buffer, pH 7.4. The protein solution was then dialyzed against the same buffer for at least one hour to remove the last traces of ammonium sulfate, using a spectropore dialysis bag (molecular weight cutoff 6000-8000 daltons). The dialyzed solution was then transferred into an amicon ultrafiltration unit equipped with a YM 10 membrane. The solution was concentrated to an approximate volume of 0.35 ml. 1.5 ml of 0.05 M potassium deuterium phosphate buffer was added and the solution was concentrated to approximately 0.35 ml again. This cycle was repeated five times. The solution was finally transferred into a 5mm OD NMR tubes (Wilmad).

Preparation of EPR samples

Samples of FdI (0.5 mM) were usually prepared in 0.1 M tris.Cl buffer, pH 7.4 for EPR measurements. For spectra of the protein in the isolated state, protein was transferred into the epr tube and the solution surface was flushed with argon for 10-20 minutes. The tubes were sealed with serum caps and were frozen in liquid

nitrogen.

In the preparation of reduced samples and samples treated with other reagents, special precautions against oxygen were taken. Samples were thoroughly deaired by the repeated evacuation and flushing with nitrogen before the reductants or other reagents were added. When denaturing solvents were used, samples were prepared in an argon atmosphere glove box.

Partially reduced samples (only the 3Fe center reduced) of FdI were obtained by the addition of a four fold molar excess of methyl viologen and a twenty fold molar excess of sodium dithionite. Fully reduced samples (3Fe and 4Fe centers reduced) of FdI were obtained by the addition of a twenty fold molar excess of sodium borohydride to a deaired solution of FdI in an EPR tube. The solution was allowed to stand, in the glove box, with an outlet needle on the serum cap until the bubbling due to hydrogen evolution subsided. The samples were then frozen as before.

Measurement of the reduction potential of FdI

The reduction potential of FdI was measured by the procedure of Lode et. al (23). FdI was reduced with a H_2-hydrogenase system at atmospheric pressure. An

equimolar amount of methyl viologen was used as a redox mediator. The extent of protein reduction was followed by monitoring the absorbance change at 425 nm. Corrections were made for the absorbance of reduced methyl viologen by using a value of 0.61 for the A_{425}^{nm} / A_{740}^{nm} ratio of reduced methyl viologen. FdI exhibits negligible absorbance at 740 nm.

A solution of FdI and methyl viologen, both 1.5×10^{-5} M, in 0.1M tris-Cl/Nacl, pH 7.4, was thoroughly deaired in an anaerobic cuvette fitted with a serum cap, by bubbling the solution with hydrogen gas (prepurified grade) through inlet and outlet needles. The hydrogen gas was bubbled through a tower of pyrogallic solution, 15% pyragallic acid in 50% KOH (W/V), and then through a tower of water. The former tower was used to purge oxygen from the gas, and the latter tower was used to remove any dissolved pyragallol in the gas. After 30 minutes of bubbling the protein solution with H_2, the absorbances at 425 nm (A_{ini}) and 740 nm were recorded. 0.010 ml of hydrogenase was added using an air-tight syringe and the solution was thoroughly mixed. The absorbance of the reducing sample at 425 nm was monitered. When this reading stabilized, absorbances at 425 nm and 740 nm were recorded.

The absorbance of the protein, at 425 nm, at redox equilibrium (A_{eq}) was calculated by subtracting the absorbance of reduced methyl viologen from A_{rd}. Under identical experimental conditions, a value of $A_{425nm} / A_{740nm} = 0.61$ was measured for reduced methyl viologen. A value of 0.81 was determined for the ratio of extinction coefficients at 425 nm for reduced / oxidized FdI. This value was obtained by similar reduction of FdI at a pH of 8.88. At this pH the solution potential, under the experimental conditions, was calculated to be -524 mV. Therefore essentially full reduction of the protein was assumed (reported E_m of FdI is 420 mV).

The reduced protein was reoxidized by gentle bubbling of N_2 (prepurified grade) through the solution. This N_2 was passed through a tower of water before entering the protein solution, to obviate the concentrating effects of the dry gas. Bubbling was continued until a constant absorbance reading at 425 nm was observed (A_{ox}). If this value was less than 99% of A_{ini}, data were discarded because of assumed protein degradation during the reduction. Usually protein was recovered quantitatively after reduction. The pH of the reoxidized solution was measured.

The reduction potential of fdI was calculated by applying the Nernst equation (n = 1) of the form:

$$E_{soln} = E_{fd} + 59(\log fd_{ox} / fd_{rd})$$

with the solution potential (E_{soln}) equal to the hydrogen potential. All measurements were carried out at atmospheric pressure. Therefore solution potential at 25 ^{o}C could be approximated as:

$$E_{soln} = -59 \text{ X pH}$$

The ratio of oxidized to reduced FdI was calculated by applying the following expression:

$$[fd_{ox}] / [fd_{rd}] = (A_{eq} - 0.81A_{ox}) / (A_{ox} - A_{eq}) \quad (23).$$

A reduction potential of -422.5 mV was determined for FdI by the above method. This value is in agreement with the reported value of 420 mV (16,24).

DENATURATION STUDIES

The unusual stability of ferredoxin I was noted very early in its studies (15). FdI was reported to be significantly more stable in 4 M guanidium hydrochloride than other ferredoxins. Unlike other ferredoxins, the sulfur groups of this protein were only slowly and incompletely titrable by p-chloromercuribenzoate (15).

The stability of FdI under aerobic and anaerobic conditions are reported here. Protein stability in DMSO, urea, guanidium hydrochloride and glycerol were characterized. Reactivities of FdI with cyanide and with 2,2'-bipyridyl were investigated. These reagents were reported to degrade the [Fe-S] centers of clostridial-type ferredoxins (26,27).

The absorbance shoulder at 400 nm in the optical spectrum of FdI originates from S Fe charge transfer band of the [Fe-S] clusters. Therefore the loss of chromophore from the protein can be followed by monitoring the change in absorbance at this wavelength. When FdI was converted to apoferredoxin, the absorbance at 400 nm was completely bleached. The reaction of ferredoxin with 2,2'-bypyridyl in the presence of sodium

dithionite can be followed by monitoring the absorbance change at 520 nm (27). The product of the reaction, Fe(II)-bipyridyl complex, absorbs strongly at this wavelength.

Materials and methods

Procedures for the growth of A. vinelandii, for the isolation of FdI and for the preparation of the inert atmosphere glove box were described previously. Protein concentrations were calculated assuming an extinction coefficient of 30000 $M^{-1}cm^{-1}$ at 400 nm. Ferredoxin used in the experiments had a A_{400nm} / A_{280nm} ratio of 0.57 to 0.59. Fe(11)-bipyridyl complex formed by reaction with FdI was quantitated by using an extiction coefficient of 6.9 X 10^3 $M^{-1}cm^{-1}$ for the complex. This value was verified by reaction of 2,2'-bipyridyl with potassium ferrous ammonium sulfate.

Urea was recrystallised from ethanol. Deuterated urea was prepared by three sequential dissolution and evaporation cycles from D_2O. d_6-DMSO was obtained from Stohler Isotopes. All experiments were conducted using 0.1M trisma.Cl/0.1 M NaCl, pH 7.17 (tris buffer), unless otherwise stated. Ferredoxin was dialyzed in Spectrapore dialysis bags (6000 - 8000 MW cut off). Protein was

concentrated to the appropriate volume in an Amicon ultrafiltration setup equipped with YM10 membranes at an argon pressoure of 40 psi.

Absorbance measurements were made on a Cary 219 spectrophotometer. 400 MHz NMR spectra were recorded using a JEOL GX-400 Fourier transform spectrometer. X-band EPR spectra were recorded using a Varian V-4500 spectrometer equipped with a Heli-tran liquid helium transfer system (Air Products). pH measurements were made using a Radiometer pH meter.

Results and discussion

Stability of FdI under anaerobic conditions

Stability of FdI in 95% DMSO: Ammonium sulfate precipitated ferredoxin was dissolved in 0.1 ml tris buffer (see materials and methods). The protein solution was dialyzed for one hour against the same buffer and was then concentrated to 0.250 ml by ultrafiltration. The solution was thoroughly deaired by repeated evacuation and flushing with nitrogen in an anaerobic cuvette and was then transferred into the glove box. 1.9 ml of deoxygenated DMSO was added. The optical spectrum of the protein solution was recorded. The absorbance at 400 nm was monitored for 1 hour.

Figure IX shows the optical spectrum of FdI in 95% (V/V) DMSO. The absorbance shoulder at 400 nm has shifted to ~420 nm and has become deeper. Some spectral change is expected due to the absence of peptide constraints on the [Fe-S] clusters in DMSO. Under strictly anaerobic conditions, the absorbance at 420 nm was stable for 1 hour.

Stability in 8 M urea: Ammonium sulfate precipitated ferredoxin was dissolved in 1.5 ml of tris buffer . The solution was dialyzed for one hour against the same buffer and was deoxygenated by repeated evacuation and flushing with oxygen free nitrogen in an anaerobic cuvette. The cuvette was then transferred into an inert atmosphere glove box. Solid urea was added to a final concentration of 8 M. The cuvette was removed from the glove box and the optical spectrum of the solution was recorded. Absorbance at 400nm was monitored for 1 hour.

Figure X shows the optical spectrum of FdI in 8 M urea under anaerobic conditions. The absorbance at 280 nm has increased in comparison to the native ferredoxin. Thus the A_{400nm} /A_{280nm} ratio has dropped from 0.58 to 0.50. However, the absorbance at 400 nm remained steady for 1 hour.

Figure IX

UV-visilble spectrum of FdI in 95% DMSO / 5% 0.1 M tris.Cl / 0.1 M NaCl, pH 7.17 (V/V).

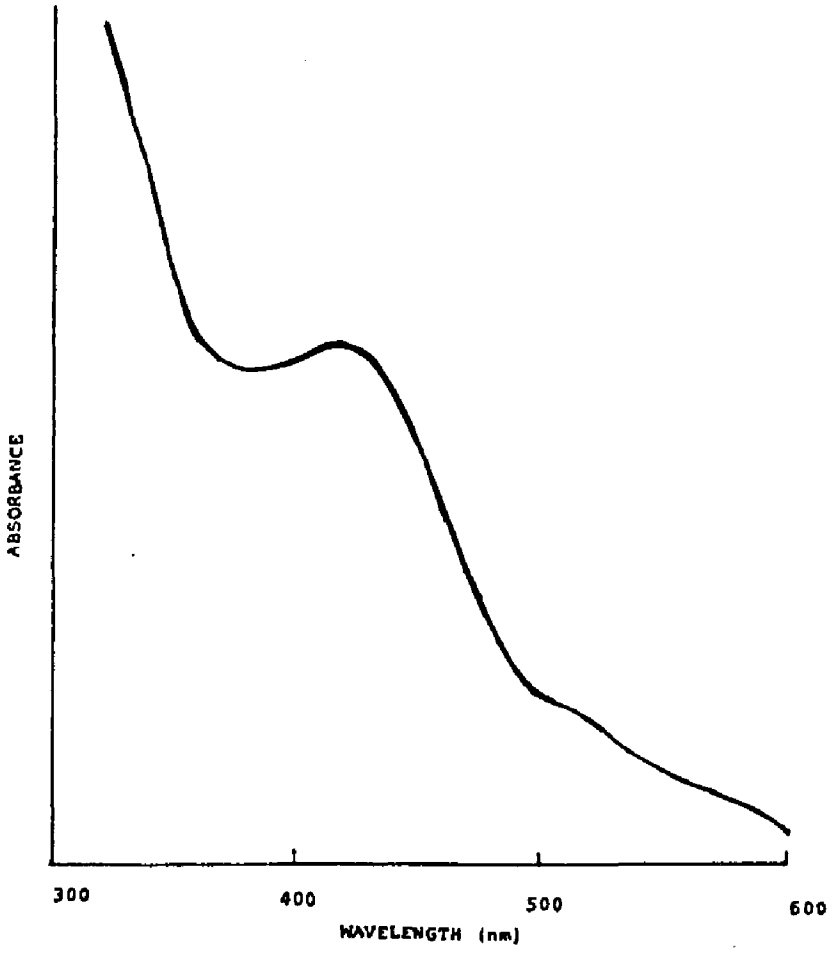
ABSORBANCE
300
400
500
600
WAVELENGTH (nm)

Figure X

UV-visible spectrum of FdI in 8M urea. Buffer, 0.1 M tris.Cl / 0.1 M NaCl, pH 7.17.

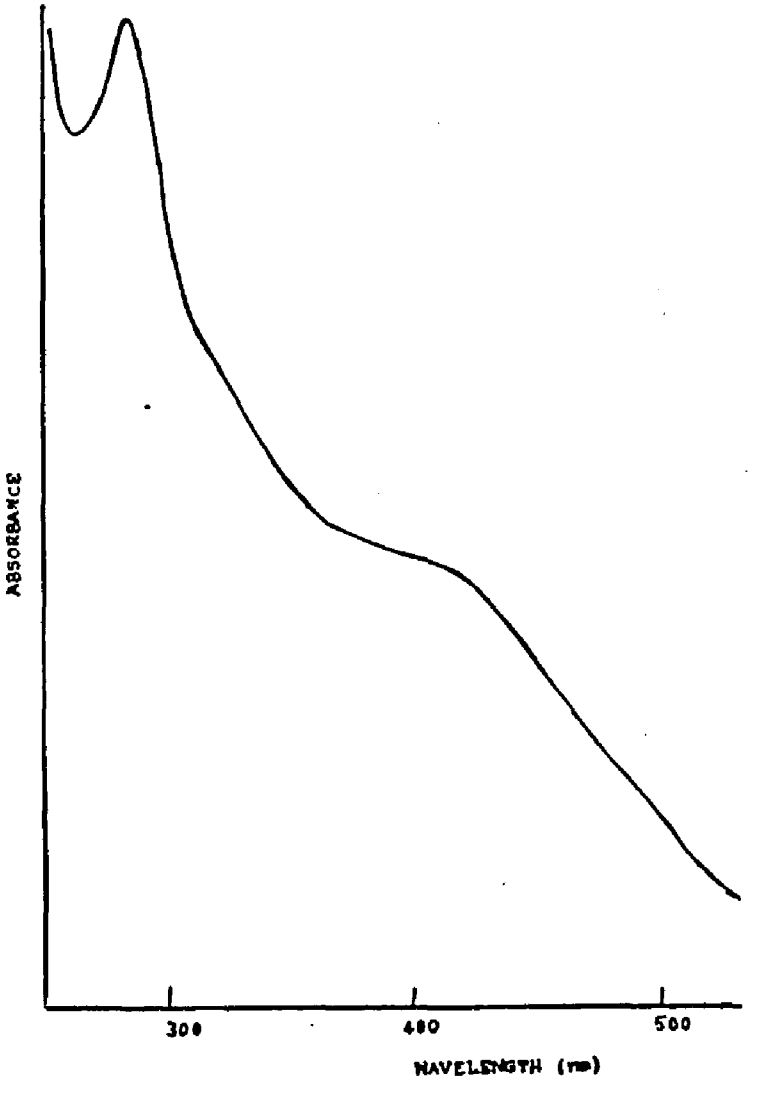
ABSORBANCE
300
400
500
WAVELENGTH (nm)

Stability of FdI in 6 M Guanidium hydrochloride or 60% glycerol: A ferredoxin solution in tris buffer containing 6 M guanidium hydrochloride was prepared by the method used for the preparation of the urea solution. In another experiment a FdI solution in 60% glycerol (V/V) was similarly prepared. In either experiment the absorbance of the protein solution at 400 nm remained steady for one hour.

Stability of FdI in the presence of cyanide

Ammonium sulfate precipitated FdI was dissolved in 1.5 ml of 0.1M tris-Cl containing 0.1M NaCl, pH8.88, to a concentration of 2.9×10^{-5} M. Aliquots of NaCN, freshly prepared in the same buffer, were added to a final concentration of 2.9×10^{-3} M. The reaction vessel was sealed with a serum cap and was incubated at room temperature for 18 hours. The reaction mixture was applied on a small DEAE column (sephacel) preequilibrated with 0.1 M tris-Cl containing 0.1 M NaCl, pH 7.4. The column was washed with several column volumes of the same buffer. FdI was eluted with tris-Cl buffer containing 0.4 M NaCl.

The optical spectrum of the cyanide treated ferredoxin was compared with that of a control sample that underwent the same treatment except for the presence

of cyanide. The two spectra compared well, both in absorbances at 400 nm and in purity ratios. Figure XI compares the EPR spectrum of FdI that was incubated in 80% DMSO (V/V) with a ten fold molar excess of sodium cyanide for 30 minutes with that of the EPR spectrum of FdI in 80% DMSO. No differences are obvious between these spectra. Thus cyanide seems to have no effect on FdI under the conditions employed in the experiment.

Stability of FdI in the presence of an iron-chelator

Stability in the presence of 2,2'-bipyridyl: A solution of 0.5 mM ferredoxin in 0.1 M tris containing 0.1 M NaCl, pH 7.2, was thoroughly deaired in an anaerobic cuvette. A hundred fold molar excess of sodium dithionite and 2,2'-bipyridyl, both freshly prepared in the same buffer and deaired, were added. The contents of the reaction vessel were mixed and the absorbance at 520 nm was recorded for 1 hour.

No change in absorbance was detected. The stability of absorbance at 520 nm indicate the lack of formation of any Fe(II)-bipyridyl complex. Thus the reagent was unable to extract iron from the protein unlike in clostridial-type ferredoxins (26).

Reactivity of FdI with bipyridyl in the presence of

Figure XI

Effect of sodium cyanide on the g = 2.01 EPR signal of FdI. (A) X-band EPR spectrum of FdI in 80% DMSO and a ten fold molar excess of cyanide. (B) X-band EPR spectrum of FdI in 80% DMSO. Solvent: 80% DMSO / 20% 0.1 M tris.Cl / 0.1 M NaCl, pH 7.17.

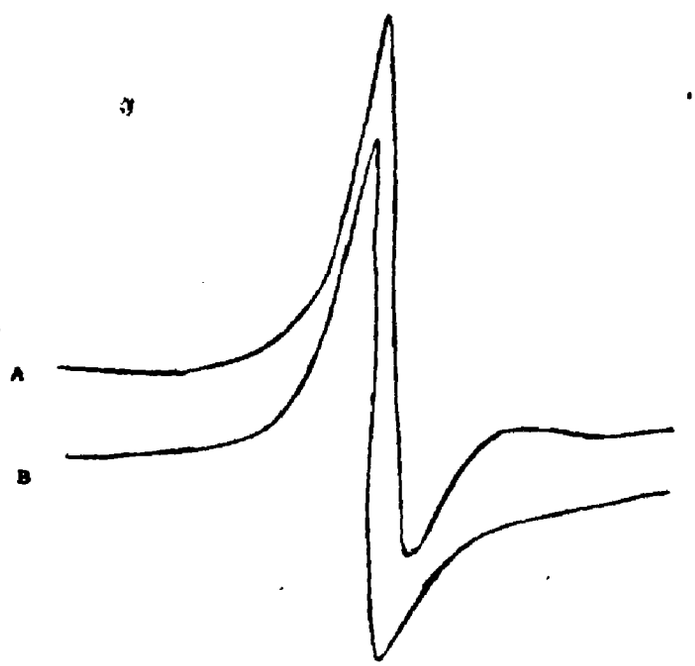
A
B

95% DMSO and in the presence of 8 M urea: A solution of approximately 1 mg of ferredoxin in 0.075 ml of buffer was thoroughly deaired in an anaerobic cuvette and was transferred into the glove box. A hundred fold molar excess of sodium dithionite in 0.025 ml of the same buffer was added followed by 1.9 ml of DMSO containing 1.1 mg of 2,2'-bipyridyl. The reaction mixture was mixed thoroughly and was transferred out of the glove box into the spectrophotometer. Absorbance at 520 nm was recorded for 12 hours. Similarly a solution of FdI in 8 M urea was treated with bipyridyl and the reaction was followed as before.

Figure XII compares the reactivity of FdI with bipyridyl in the presence of 95% (V/V) DMSO with the reactivity of of the same reagent in 8 M urea. In the presence of 95% DMSO approximately 70% of the protein bound iron reacted with bipyridyl within the first six minutes of the reaction time. In the absence of bipyridyl six hours were required for the same extent of reaction when an anaerobic solution of FdI in 80% DMSO was opened to air and allowed to react with atmospheric oxygen (Figure XIII). In the presence of 8 M urea, under anaerobic conditions, approximately 36% of the protein bound iron reacted with bipyridyl within six minutes of the reaction (Figure XIII). In the absence of bipyridyl,

Figure XII

Reactivity of FdI with 2,2'-bipyridyl.

A. Reactivity in 95% DMSO / 5% 0.1 M tris.Cl/ NaCl, pH 7.17 (V/V).

B. Reactivity in 8 M Urea, prepared in 0.1 M tris.Cl/ NaCl, pH 7.17.

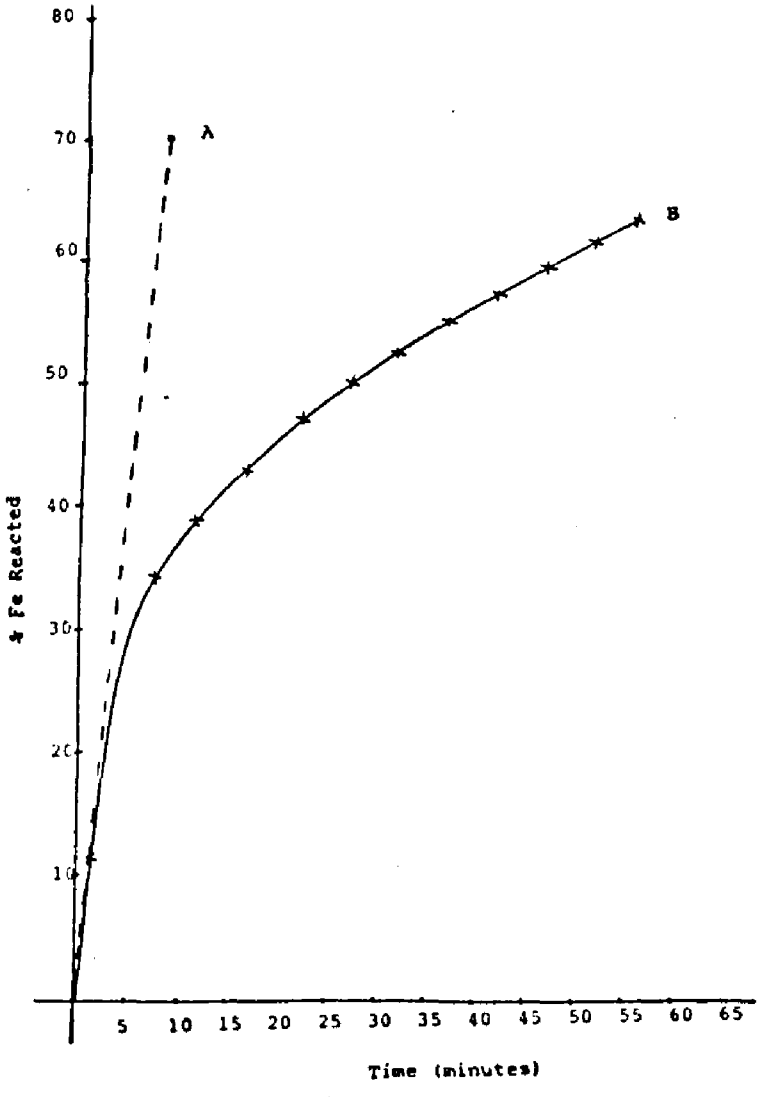
80
70
60
50
40
30
20
10
A
B
% Fe Reacted
5
10
15
20
25
30
35
40
45
50
55
60
65
Time (minutes)

Figure XIII

Reactivity of FdI with atmospheric oxygen

A. Reactivity in 80% DMSO / 20% 0.1 M tris.Cl/ NaCl, pH 7.17.

B. Reactivity in 8M urea, prepared in 0.1 M tris.Cl/ NaCl, pH 7.17.

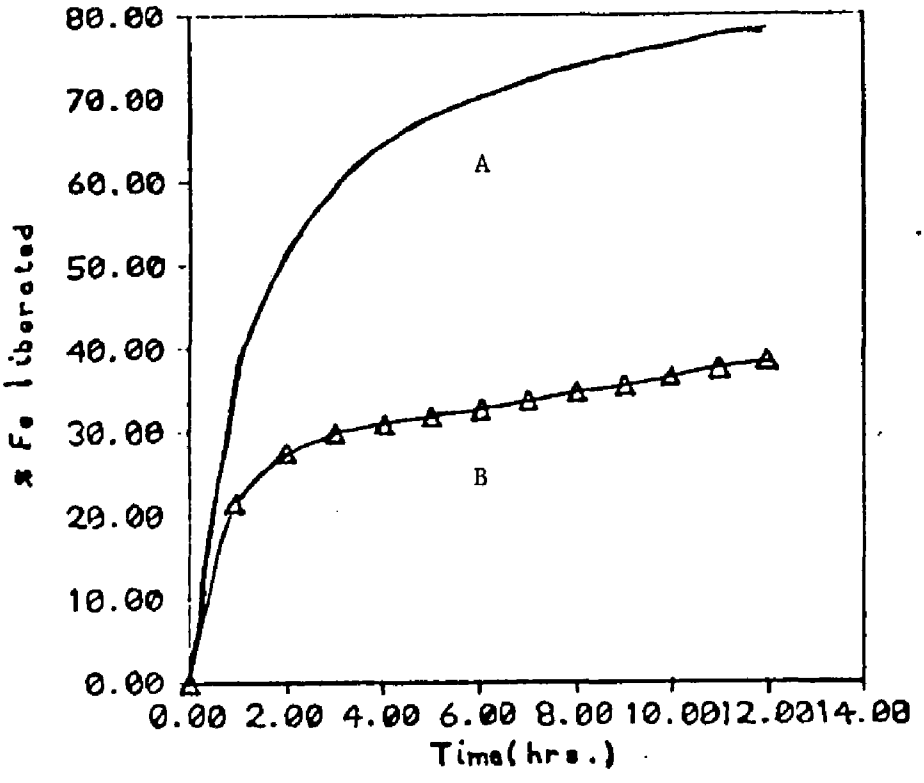
80.00
70.00
60.00
50.00
40.00
30.00
20.00
10.00
0.00
% Fe liberated
A
B
0.00 2.00 4.00 6.00 8.00 10.00 12.00 14.00
Time(hrs.)

8 hours were required for the same extent of reaction when an anaerobic solution of FdI in 8 M urea was opened to air and allowed to react with atmospheric oxygen (Figure XIII). Thus in the presence of 95% (V/V) DMSO and 8 M urea, the reactivity of FdI with bipyridyl and with oxygen was greatly enhanced.

PMR spectra of FdI in DMSO and in urea

Figure XIV compares the proton magnetic resonance spectra of FdI in potassium deuterium phosphate buffer, in 80% DMSO and in 8 M urea. The spectra in DMSO and in 8 M urea are similar but not identical. In both spectra the resonances below 10 ppm are not observed, presumably due to broadening of these low intensity lines. A peak near 1 ppm has increased in intensity and there is considerable coalescence of resonances in the aromatic region. These spectral changes have been also reported for unfolded C. pasteurianum ferredoxin (28). Thus FdI unfolds both in DMSO and in urea solutions. However, as is evident from the spectra, the nature of denaturation appears to be different between the two denaturants. This result is consistent with a higher reactivity of FdI with oxygen and bipyridyl in DMSO than in urea.

Figure XIV

PMR spectra of FdI in 80% DMSO and in 8M urea. Buffer: 50 mM $KD_2PO_4/KDPO_4$, pD 7.39. (A) In buffer, (B) in 8M urea, and (C) in 80% DMSO / 20% buffer (V/V).

Conditions: Points 32768, Spectral width 40000 Hz, Pulse repeat time 0.3 seconds and Line broadening 3.0 Hz. The HDO resonance in A was set to 4.8 ppm.

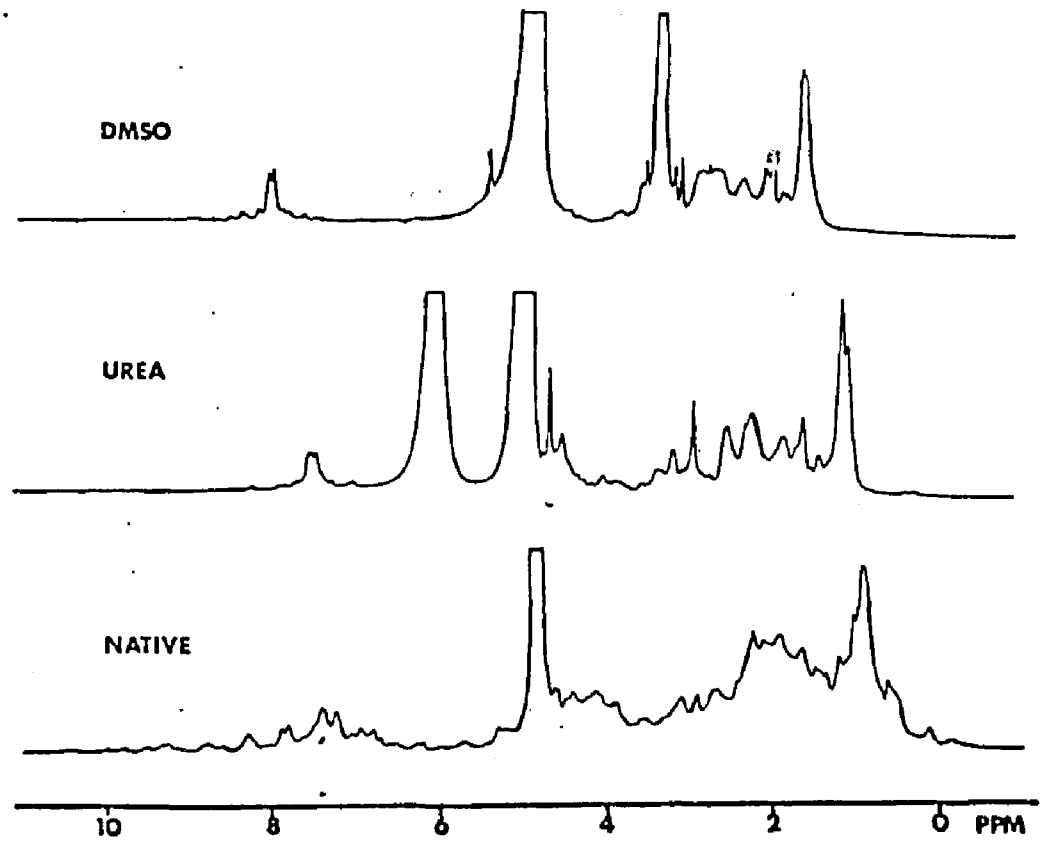
DMSO
UREA
NATIVE
10
8
6
4
2
0
PPM

Conclusions

Ferredoxin I is significantly more stable in the presence of denaturants than the clostridial-type ferredoxins. Under strictly anaerobic conditions the protein was found stable in 95% DMSO (V/V), 8 M urea, 6 M guanidium hydrochloride and 60% (V/V) glycerol. In the presence of oxygen there is rapid chromophore loss in 95% DMSO and in 8 M urea. The protein degradation in DMSO occurs at a significantly higher rate than in urea. Sodium cyanide and 2,2'-bipyridyl had no effect on FdI in the absence of denaturants. In the presence of DMSO and urea 2,2'-bipyridyl reacted very rapidly with protein bound iron. The reaction in DMSO occurs more rapidly than in urea. Proton magnetic resonance spectra of FdI in DMSO and in urea indicate protein unfolding in the presence of these reagents. The unfolding is different between these solvents. This result is consistent with the different rates of the reactions of the [Fe-S] clusters of FdI with 2,2'-bipyridyl in DMSO and in urea.

STUDIES OF THE OXOLIGAND

According to the 2.0 A X-ray structure of Ghosh et. al (1), Fe(3) of the 3Fe center of FdI is coordinated by Cys^{24} and by an oxoligand, presumably water or hydroxide (Figure II). The protein molecule possesses a cleft as a result of the loop of residues 80 to 90 that form a flap at the end of the molecule opposite to the [Fe-S] centers.

> "...This cavity extends into the interior of the molecule to the conserved glutamate E_{18} and the oxo atom. The cleft allows for the hydration of this interior portion to the extent that the [3Fe-3S] center itself is apparently hydrated. The cleft is suggestive of an enzymatic function. It represents an obvious direction of approach for solvent molecules to the [3Fe-3S] cluster, if exchange reactions at this site take place..." (1).

Thus the oxo ligand was expected to be solvent accessible. Mössbauer studies had demonstrated that the three iron atoms of the cluster are in high spin ferric states (6). Therefore attempts were made to exchange the oxoligand with substituent ligands that are known to form kinetically and thermodynamically stable complexes with Fe(III). For example the water ligand of methemoglobin and metmyoglobin are easily exchanged in the presence of cyanide (Figure XV and Figure XVI).

Figure XV

Reaction of methemoglobin with sodium cyanide. Buffer: 0.1 M tris.Cl/0.25 M NaCl, pH 7.17. [Hemoglobin] = 1.74 X 10^{-9} M. [Cyanide] = 3.97 X 10^{-2} M. Reaction time = 2 minutes.

Solid line spectrum: before the addition of cyanide.

Broken line spectrum: after the addition of cyanide.

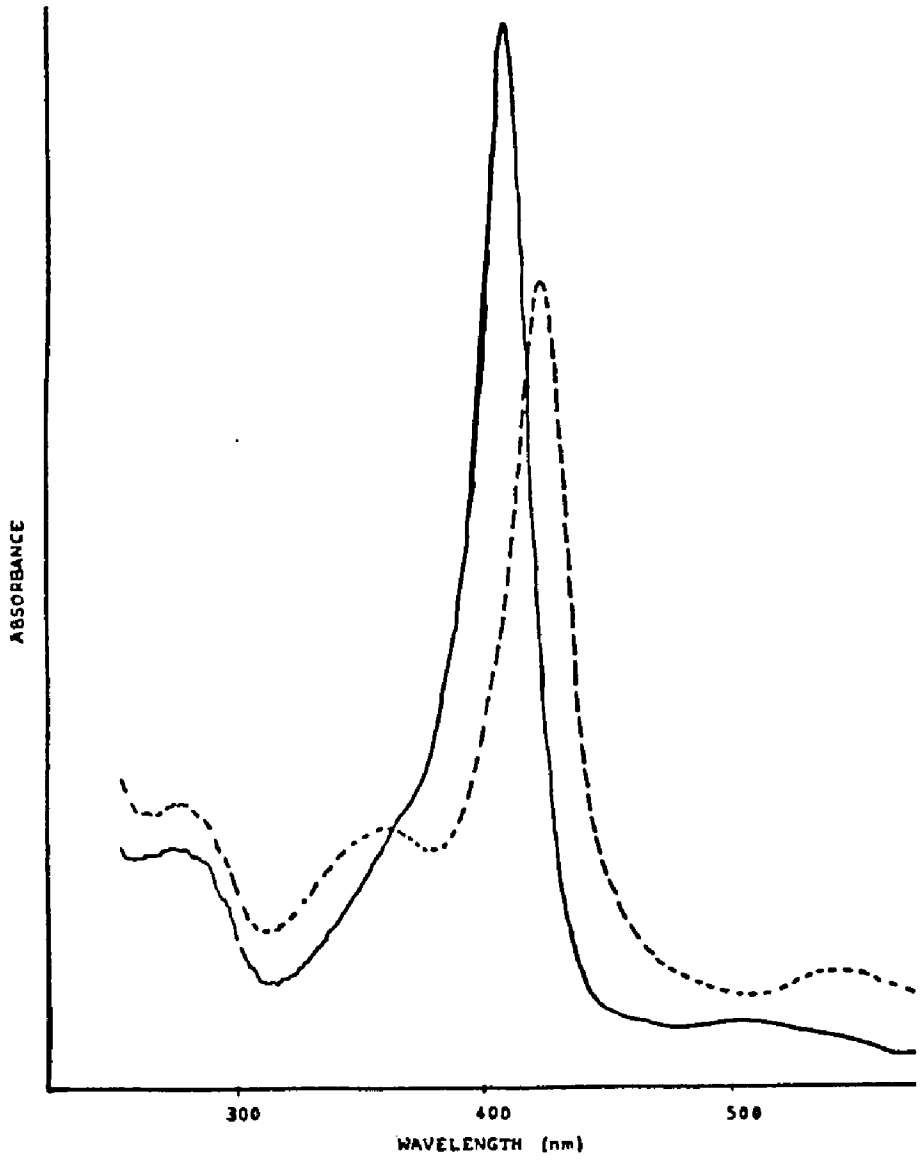
ABSORBANCE
300
400
500
WAVELENGTH (nm)

Figure XVI

Reaction of metmyoglobin with sodium cyanide. Buffer: 0.1 M tris.Cl/NaCl, pH 7.17. [Myoglobin] = 7.45 X 10^{-5} M. [Cyanide] = 6 X 10^{-3} M. Reaction time: 5 minutes.

Solid line spectrum: without cyanine.

Broken line spectrum: with cyanide.

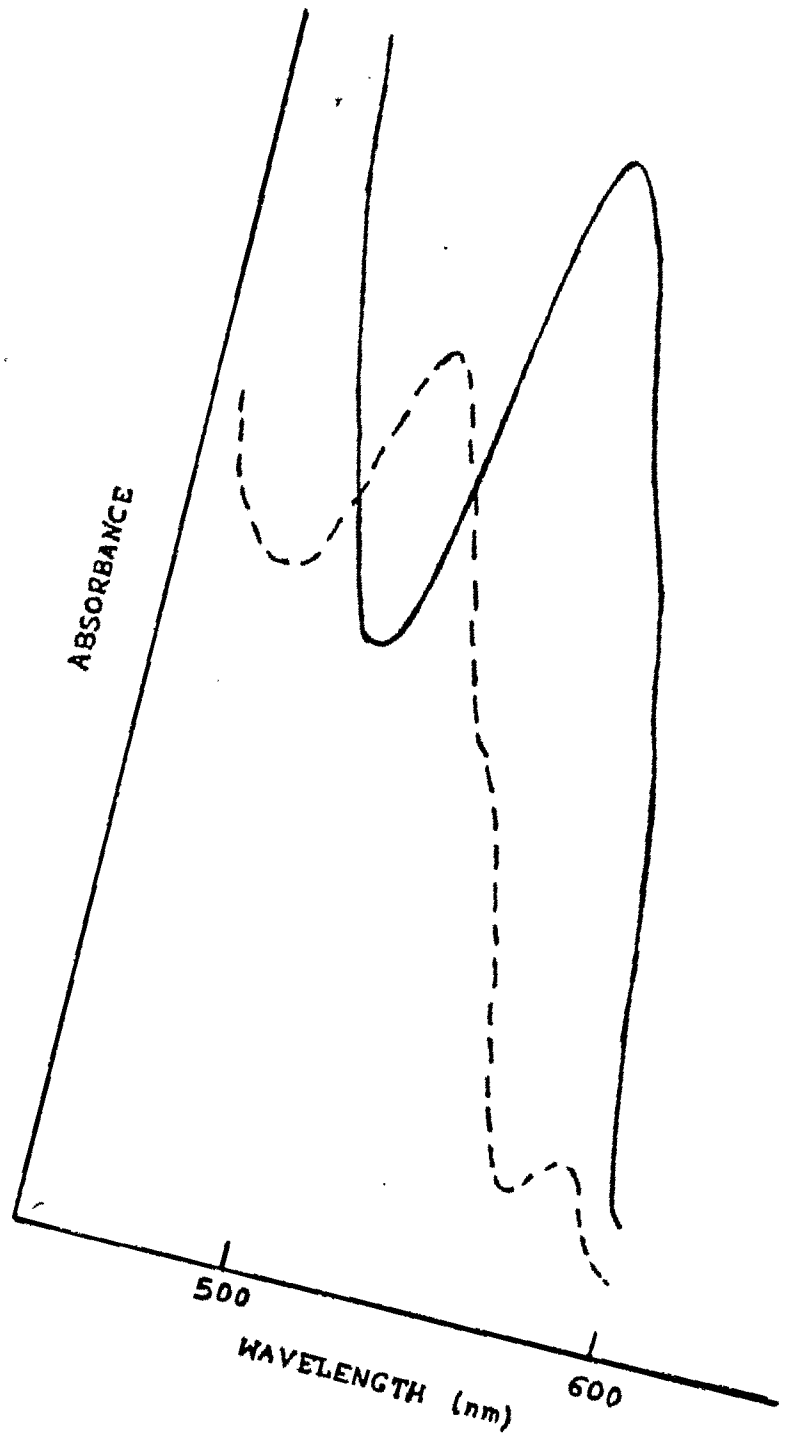
ABSORBANCE
500
600
WAVELENGTH (nm)

The proton(s) of the oxoligand was expected to be exchangeable with deuterium on incubation of the protein in D_2O. The water protons in metmyoglobin is exchangeable with deuterium from D_2O (30). Attempts were made to exchange the oxoligand protons with deuterium in an effort to find experimental verification for the existence of a solvent accessible oxoligand as reported by the X-ray analysis.

Materials and methods

Procedures for the growth of A. vinelandii, for the isolation of FdI, and for the preparation of the anaerobic glove box were described previously. Reactions at low pH, high pH, and reactions in the presence of denaturants were carried out in the inert atmosphere glove box. Ferredoxin concentration in individual reaction was approximately 10^{-5} M. The A_{400} / A_{280} ratio of the FdI solutions varied between 0.57 and 0.59.

Absorbance measurements were made with a Cary 219 UV-visible spectrophotometer. NMR spectra were recorded on a 400 MHz JEOL JX400 Fourier transform spectrometer. EPR spectra were obtained using a Varian V-4500 X-band spectrometer equipped with a Heli-Tran liquid helium transfer system (Air Products). X-band electron spin

echo measurements were carried out using both two pulse and three pulse methods as described elsewhere (31,32,33).

Results and discussion

I.Chemical exchange studies

Figure XV and Figure XVI, respectively. demonstrate the spectral changes that occurred to methemoglobin and metmyoglobin, in o.1 M tris.Cl/NaCl buffer, pH 7.17, upon addition of a hundred fold moalr excess of sodium cyanide. The observed spectral changes are expected to accompany the replacement of the water ligand of the heme with cyanide. However, under a variety of reaction conditions, neither the oxoligand exchanged with other ligands nor did the protons on the oxoligand exchange with deuteriums from the solvent.

Attempts were made to exchange the oxoligand with cysteine, cyanide, thiocyanate, ATP, acetonitrile, carbon monoxide, fluoride and azide. Exchange reactions were attempted at at different pH and also in the presence of denaturing reagents.

Cysteine

Ammonium sulfate precipitated FdI was dissolved in

0.1M tris.Cl/0.1M NaCl, pH 7.4 (previously deaired). The protein solution, 4 X 10^{-5} M, was deoxygenated in an anaerobic cuvette by repeated evacuation and flushing with oxygen-free nitrogen. The optical spectrum was recorded in the range of 600 nm to 240 nm. A hundred fold molar excess of l-cysteine, prepared in the same buffer and deaired, was anaerobically added and the optical spectrum was recorded at regular intervals for a period of 6 hours. The sample was anaerobically transferred into an EPR tube and the tube was frozen in liquid nitrogen. The X-band epr spectrum of the sample was recorded.

The experiment was repeated at pH 8.9 using the same buffer, and at pH 4.25 using 0.1 M glutamic acid buffer. Due to protein instability incubation at the low pH was carried out only for thirty minutes.

No change in optical spectra was detected in all three cases. The EPR spectra also revealed no detectable difference (Figure XVII, Figure XVIII, and Figure XIX).

Carbon monoxide

0.5 ml of a 4 X 10^{-5} M FdI solution, in 0.1 M tris.Cl/NaCl buffer, pH 7.4, was saturated with ^{13}C-CO. The reaction vessel, a 20 ml test tube, was evacuated and

Figure XVII

A. X-band EPR spectrum of FdI in 0.1 M tris.Cl/ NaCl, pH 7.17.

B. X-band EPR spectrum of FdI in 0.1 M tris.Cl/ NaCl, pH 7.17 in the presence of a hundred fold molar excess of l-cysteine.

conditions: [Fd] 4 X 10^{-5} M, temperature 9 K, field modulation 250, power 1 mW, gain 500.

The g = 2.01 signal is shown in both cases.

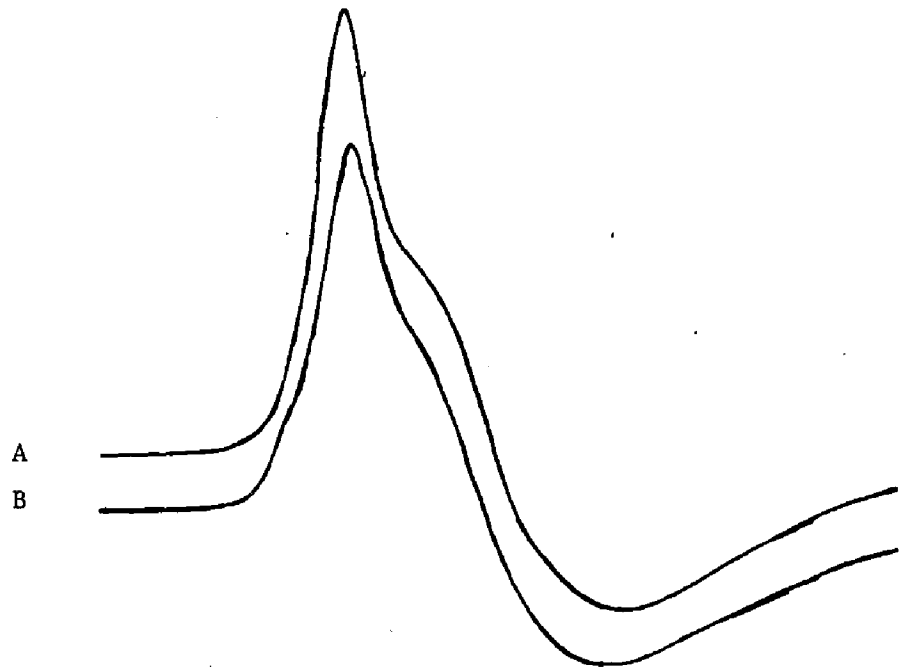
A
B

Figure XVIII

A. X- band EPR spectrum of FdI in 0.1 M tris.Cl/ NaCl, pH 8.9.

B. X-band EPR spectrum of FdI in 0.1 M tris.Cl/ NaCl, pH 8.9 in the presence of a hundred fold molar excess of l-cysteine.

conditions: [Fd] 4 X 10^{-5} M, temperature 9^{o} K, field modulation 250, power 1 mW, gain 500.

The g = 2.01 signal is shown in both cases.

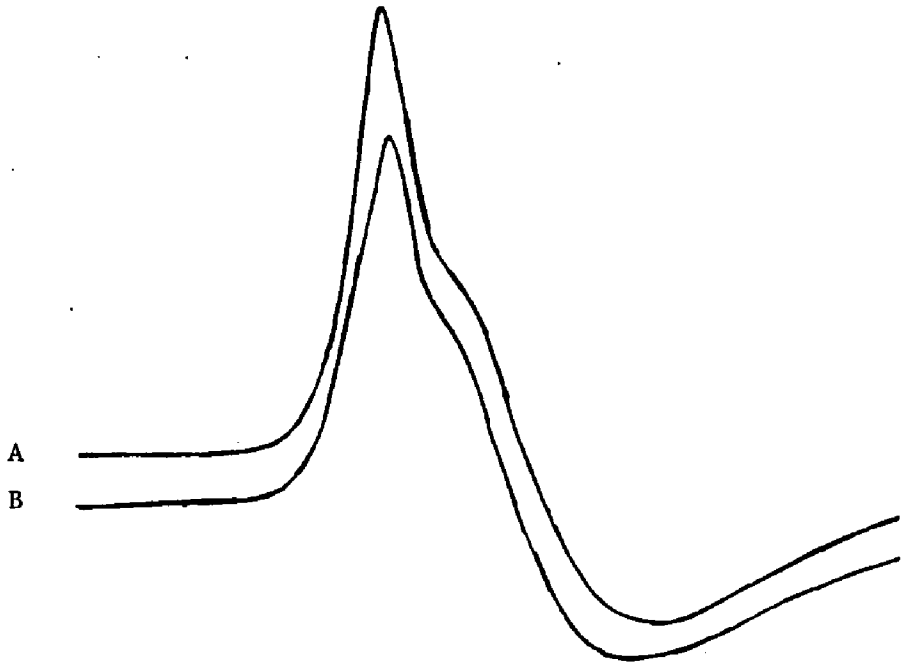
A
B

Figure XIX

A. X-band EPR spectrum of FdI in 0.1 M glutamic acid buffer, pH 4.25

B. X-band EPR spectrum of FdI in 0.1 M glutamic acid buffer, pH 4.25 in the presence of a hundred fold molar excess of l-cysteine.

conditions: [Fd] 4 X 10^{-5} M, temperature 9^{o} K, field modulation 250, power 1 mW, gain 500.

The g = 2.01 signal is shown in both cases.

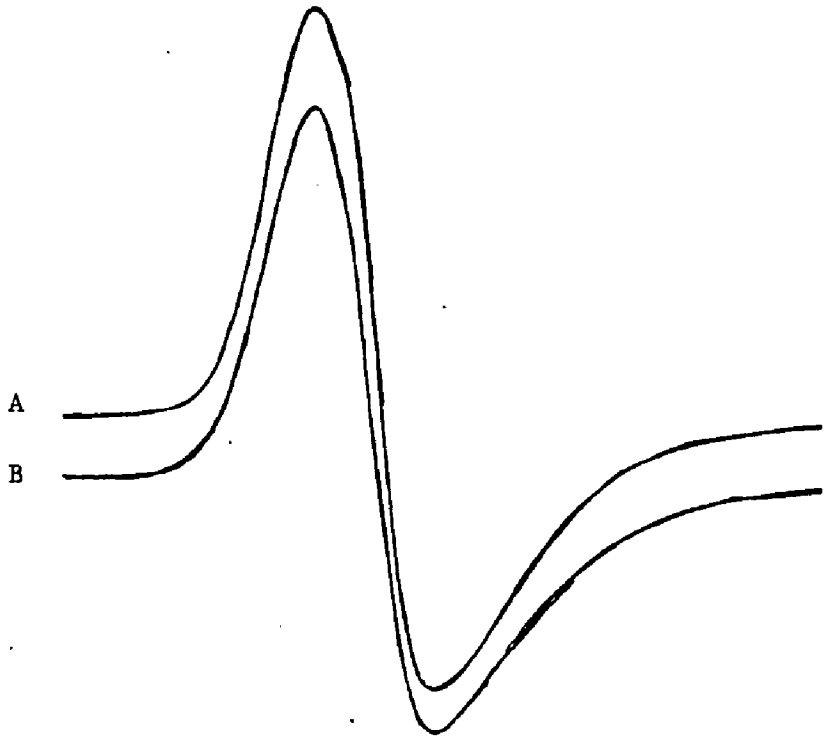
A
B

filled with ^{13}C-CO. The process was repeated with intermittent incubation and mixing in between. The sample was then transferred into an EPR tube and the X-band spectrum of the frozen sample was recorded.

The experiment was repeated at pH 8.9 in the same buffer, and at pH 4.25 in 0.1 M glutamic acid buffer. The EPR spectra did not show any indication of ligand exchange (Figure XX, Figure XXI, and Figure XXII).

Cyanide

Incubation at pH 7.4 and at pH 4.25: Ammonium sulfate precipitated FdI was dissolved in 0.1M tris.Cl/0.1M NaCl, pH 8.9. Approximately ten fold molar excess of NaCN, final concentration 1.2 X 10^{-4} M, in the same buffer was added and the optical spectrum from 600 nm to 240 nm was recorded at regular intervals for six hours. The sample was then transferred into an EPR tube. The X-band epr spectrum of the frozen solution was recorded.

Ligand exchange with cyanide was also attempted in 0.1M glutamic acid buffer, pH 4.25, with extreme caution against oxygen. Due to protein instability incubation at this low pH was carried out only for thirty minutes.

Figure XX

A. X-band EPR spectrum of FdI in 0.1 M tris.Cl/ NaCl, pH 7.17.

B. X-band EPR spectrum of FdI in 0.1 M tris.Cl/ NaCl, pH 7.17 saturated with ^{13}C- CO.

conditions: [Fd] 4 X 10^{-5} M, temperature 9^{o} K, field modulation 250, power 1 mW, gain 500.

The g = 2.01 signal is shown in both cases.

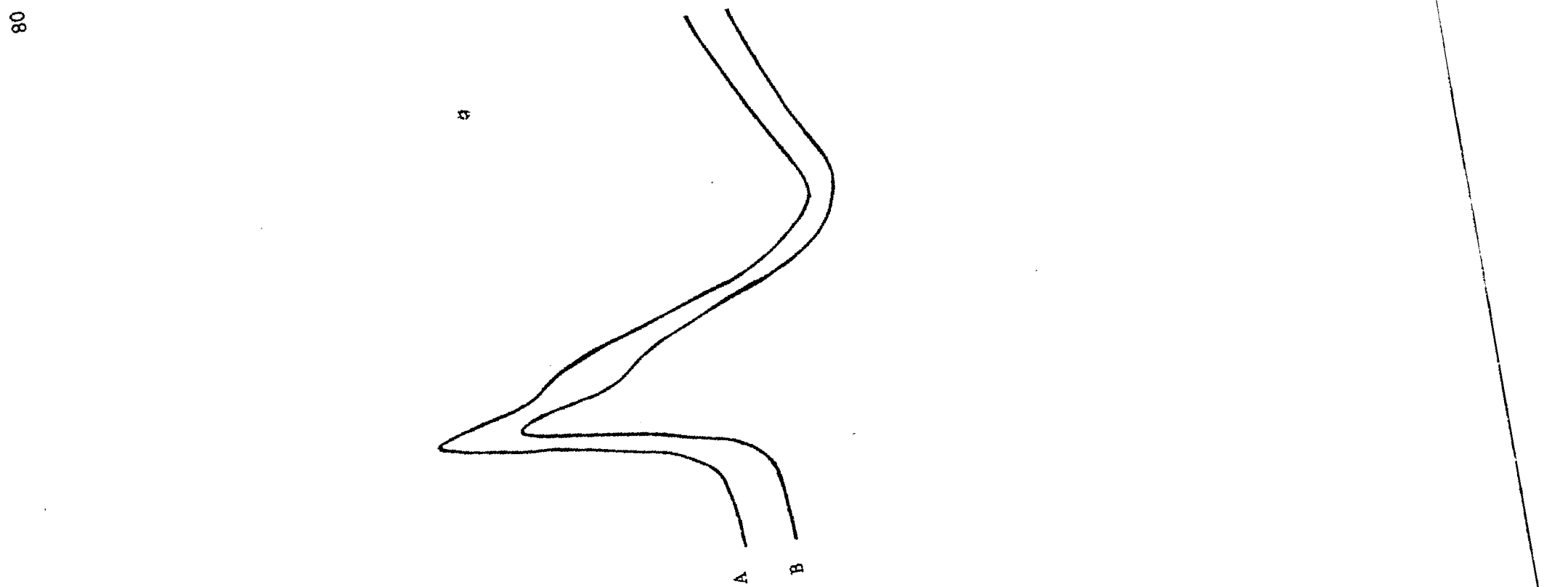
80
A
B

Figure XXI

A. X-band EPR spectrum of FdI in 0.1 M tris.Cl/ NaCl, pH 8.9.

B. X-band EPR spectrum of 0.1 M tris.Cl/ NaCl, pH 8.9 saturated with ^{13}C- CO.

conditions: [Fd] 4 X 10^{-5} M, temperature 9^{o} K, field modulation 250, power 1 mW, gain 500.

The g = 2.01 signal is shown in both cases.

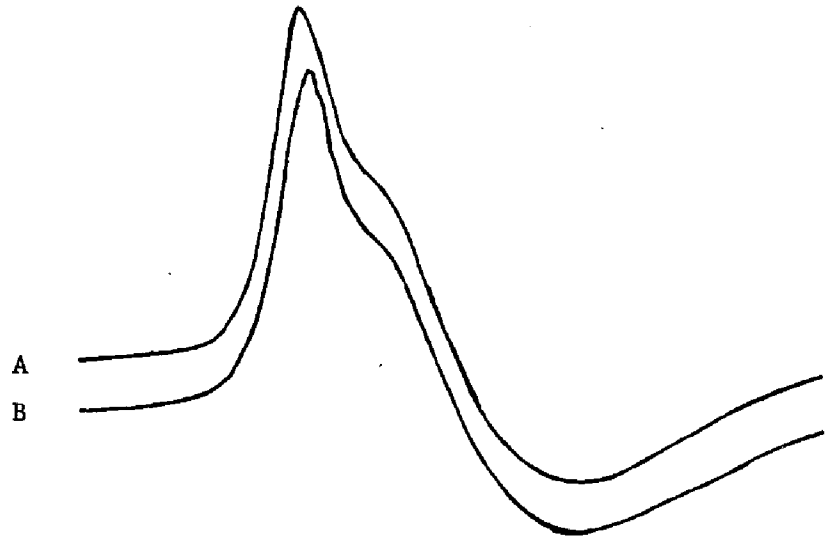
A
B

Figure XXII

A. X-band EPR spectrum of FdI in 0.1 M glutamic acid buffer, pH 4.25.

B. X-band EPR spectrum of FdI in 0.1 M glutamic acid buffer, pH 4.25 saturated with ^{13}C- CO.

conditions: [Fd] 4 X 10^{-5} M, temperature 9^{o} K, field modulation 250, power 1 mW, gain 500.

The g = 2.01 signal is shown in both cases.

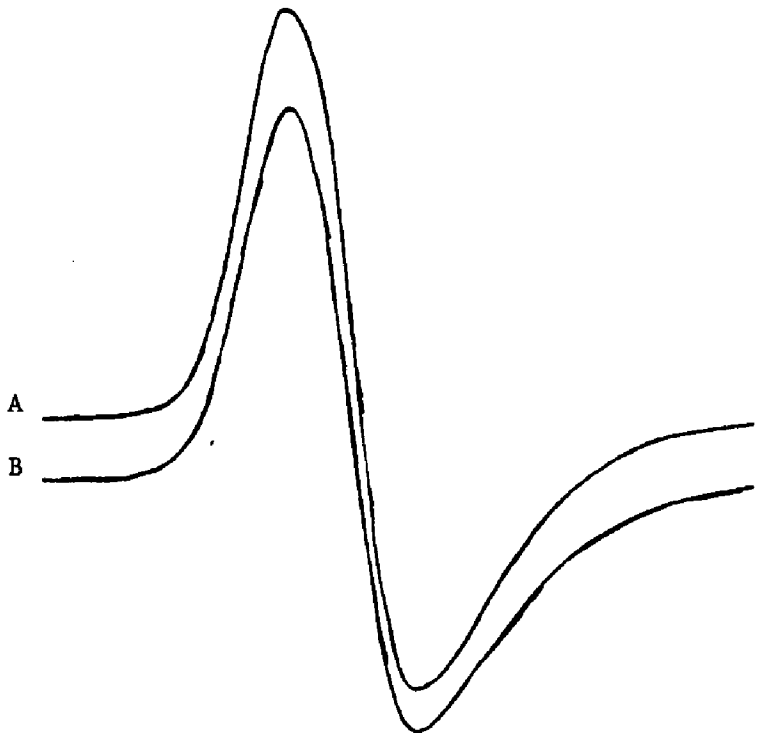
A
B

No change in the optical or EPR spectrum was detected (Figure XXIII and Figure XXIV).

Incubation in the presence of urea and guanidium hydrochloride: Ammonium sulfate precipitated ferredoxin was dissolved in 0.1M tris.Cl/0.1M NaCl, pH 7.4 and was transferred into an anaerobic cuvette. The buffer was previously deaired and saturated with oxygen free nitrogen. The solution was gently bubbled with oxygen free nitrogen to purge the oxygen present in the reaction vessel. To four of these samples, deaired denaturants were anaerobically added to final concentrations of 2M guanidium hydrochloride, 6M guanidium hydrochloride, 4M urea and 8M urea. A hundred fold molar excess of NaCN, anaerobically prepared in the same buffer, was added and the cuvettes were transferred into the spectrophotometer and the optical spectra were recorded at regular intervals for six hours. No change in the optical spectra was detected.

Incubation in the presence of DMSO: Ammonium sulfate precipitated ferredoxin was dissolved in 0.1M tris.Cl/NaCl, pH = 7.4, and was transferred into the inert atmosphere glove box. A hundred fold molar excess of sodium cyanide, 4×10^{-3} M, prepared in the same buffer was added followed by the addition of DMSO to a

Figure XXIII

A. X-band EPR spectrum of FdI in 0.1 M tris.Cl/ NaCl, pH 8.9.

B. X-band EPR spectrum of FdI in 0.1 M tris.Cl/ NaCl, pH 8.9 in the presence of ten fold molar excess of sodium cyanide.

conditions: [Fd] 4 X 10^{-5} M, temperature 9^{o} K, field modulation 250, power 1 mW, gain 500.

The g = 2.01 signal is shown in both cases.

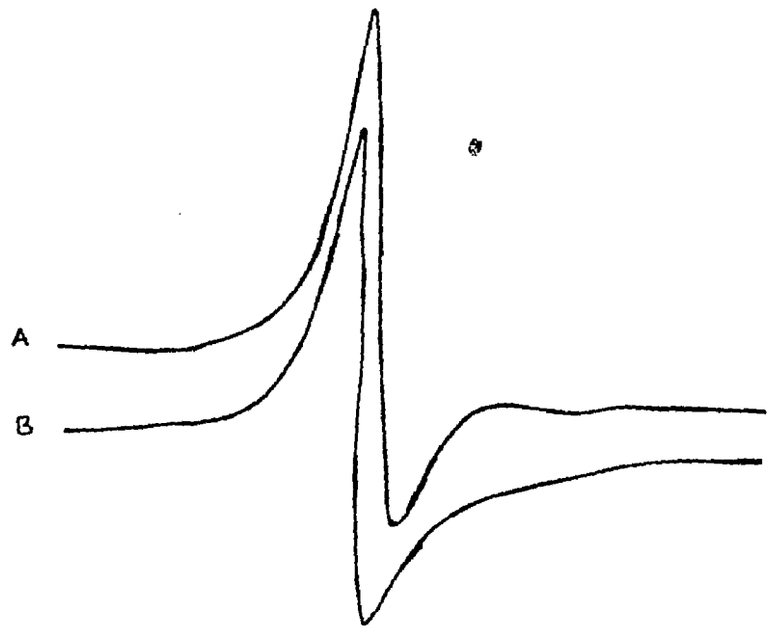
A
B

Figure XXIV

A. X-band EPR spectrum of FdI in 0.1 M glutamic acid buffer, pH 4.25

B. X-band EPR spectrum of FdI in 0.1 M glutamic acid buffer, pH 4.25in the presence of ten fold molar excess of sodium cyanide.

conditions: [Fd] 4 X 10^{-5} M, temperature 9^{o} K, field modulation 250, power 1 mW, gain 500.

The g = 2.01 signal is shown in both cases.

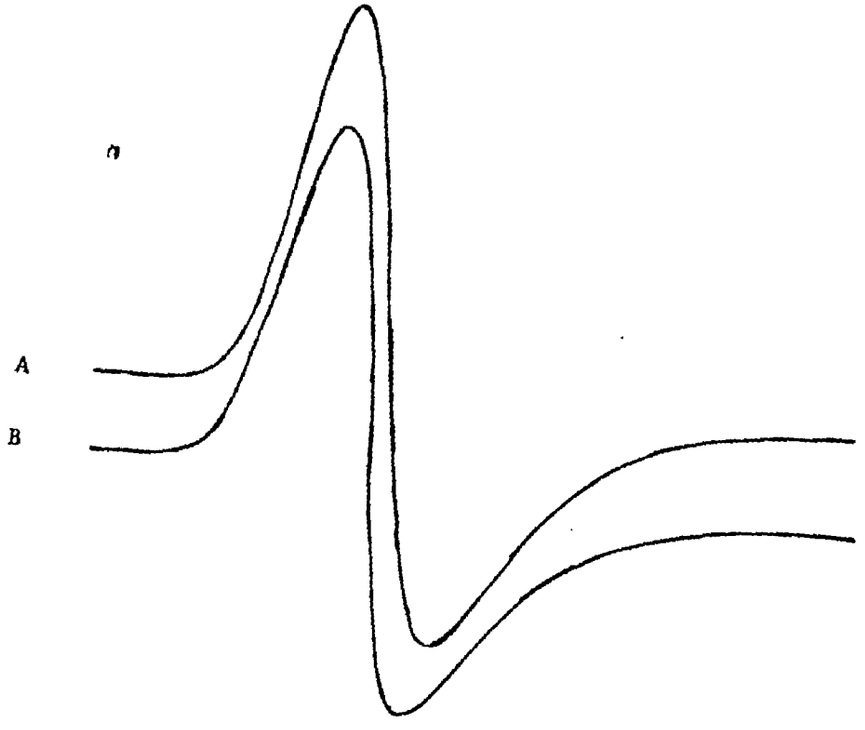
A
B

final concentration of 88% (V/V). The contents were mixed by gentle shaking and was allowed to stand for thirty minutes. The reaction mixture was concentrated to a final volume of approximately 0.35 ml by ultrafiltration. The solution was then transferred into an EPR tube. The epr tube was promptly frozen in liquid nitrogen and the X-band spectrum of the sample was recorded. The spectrum did not display any evidence for a ligand exchange (Figure XXV).

Acetonitrile, sodium azide, potassium thiocyanate, ATP and sodium fluoride

Ammonium sulfate precipitated ferredoxin was dissolved in 0.1M tris.Cl/0.1M NaCl, pH = 7.4. The protein solution, 4 X 10^{-5} M, was transferred into an anaerobic cuvette and was rendered anaerobic by repeated evacuation and flushing with oxygen free nitrogen. Aliquots of deaired acetonitrile, potassium thiocyanate, ATP, or sodium fluoride was added to a final concentration of 0.3M, 0.1 M, 0.1M, and 0.5 M respectively. Optical spectrum of the reaction mixture was recorded at regular intervals for six hours. No change was observed in the optical spectra. EPR samples of the azide, and the acetonitrile samples were prepared as described before. However, no detectable signs of ligand exchange was present in the spectra (Figure XXVI).

Figure XXV

A. X-band EPR spectrum of FdI in 88% DMSO / 12% 0.1 M tris.Cl/ NaCl, pH 7.17 (V/V).

B. X-band EPR spectrum of FdI in 88% DMSO / 12% 0.1 M tris.Cl/ NaCl, pH 7.17 (V/V) in the presence of a ten fold molar excess of sodium cyanide.

conditions: [Fd] 4 X 10^{-5} M, temperature 9^{o} K, field modulation 250, power 1 mW, gain 500.

The g = 2.01 signal is shown in both cases.

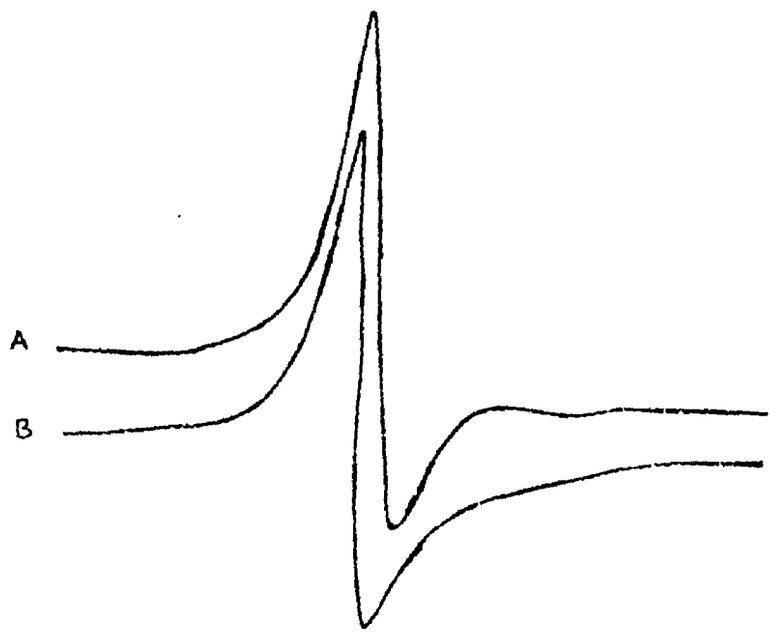
A
B

Figure XXVI

A. X-band EPR spectrum of FdI in 0.1 M tris buffer.

B. X-band EPR spectrum of FdI in 0.1 M tris buffer in the presence of 0.1 M sodium azide.

C. X-band EPR spectrum of FdI in 0.1 M tris buffer in the presence of 0.3 M acetonitrile.

Conditions: Temperature 16.8 K, power 1mW, gain 2000, field modulation 2000, frequency 9.4 GHz.

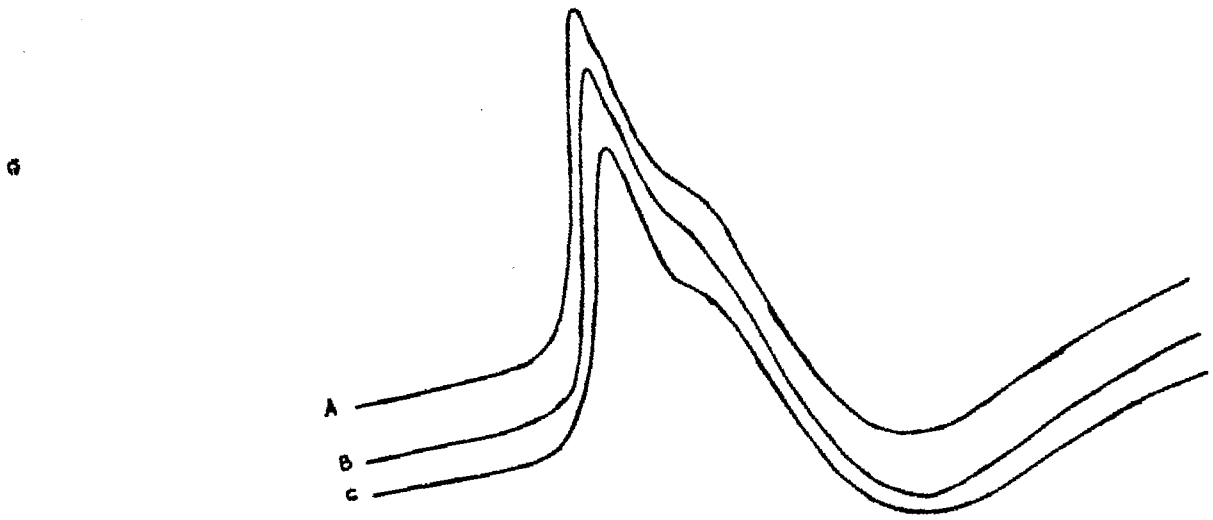
A
B
C

Thus no change in the optical absorption or EPR spectrum was observed when a solution of 4 X 10^{-5} M FdI in tris buffer was incubated with NaCN (1.2 X 10^{-4} M), NaN_3 (0.1 M), acetonitrile (0.3M), ^{13}C -CO, or l-cysteine (4 X 10^{-3} M). No spectral change was observed in the presence of a 100 fold molar excess of cysteine at pH 4.25 and pH 9.0. Incubations at pH 7.4 with thiocyanate (0.1 M, and sodium fluoride (0.3M), and incubations with cyanide at pH 4.25 also yielded uniformly negative results.

II. Electron spin echo studies

Electron spin echo spectroscopy is a powerful method for the detection of exchangeable protons in the vicinity of paramagnetic centers. This technique is particularly suited to study the environment of the active sites of ferredoxins since all known iron sulfur centers are paramagnetic in at least one of its oxidation states.

In the simplest form of the experiment, the two pulse method, a 90^{o} pulse is applied to the spin system followed by a 180^{o} pulse with a time interval of g between the pulses. At a time g after the second pulse the spin vectors refocus to generate a spin echo. The spin echo decays due to various processes of relaxation.

Electron spin echo spectroscopy constitutes the study of the decay of the amplitude of the electron spin echo envelope as a function of the interval between the echo-generating pulses.

Generally the electron spin echo amplitude does not decay monotonically as a function of the time interval between the echo generating pulses. The spin echo decay envelope is often periodic in nature. The periodicity arises from the modulation of the electron precessional frequencies by the precessional frequencies of nuclei in the vicinity of the electron spin. The modulation frequencies are characteristic of the nuclei coupled to the electron spin. Thus in favorable circumstances the identity of the nuclei coupled to the electron spin can be determined. The depth of the nuclear modulation strongly depends on the distance between the coupled nucleus and the electron. Thus the depth parameter can be analyzed to yield distance information. If electron nuclear coupling occurs through the classical magnetic dipolar mechanism the depth parameter is proportional to the inverse sixth power of the distance between the electron and the nucleus.

Due to the higher precessional frequency, the proton modulation period is ~6.5 times longer than the

modulation period of deuteron in an identical site. The depth of modulation due to a proton is approximately 8/3 times greater than the depth of modulation due to a deuteron at the identical site. Thus the exchange of a protons with deuterons is easily detected by comparison of the electron spin echo decay envelopes of H_2O and D_2O equilibrated samples under identical conditions.

Preparation of samples for electron spin echo spectra:

H2O and D2O equilibrated samples of FdI: Ammonium sulfate precipitated ferredoxin was dissolved in 50 mM potassium phosphate buffer, pH 7.4. The protein solution was dialysed against the same buffer to remove the traces of ammonium sulfate. The protein was subsequently concentrated to a volume of approximately 400 fl and was transferred into an epr tube. The epr tube was deaired by flushing the solution surface with nitrogen.

The D_2O equilibrated sample was prepared by the same procedure using 50 mM potassium deuterium phosphate buffer, pD 7.4.

Preparation of FdI unfolded in DMSO/D_2O and refolded in D_2O: Approximately 6mg of ammonium sulfate precipitated FdI was dissolved in 0.1M tris-Cl containing 0.1M NaCl, pH 7.4. The protein solution was dialysed

against the same buffer for 2 hours. The sample was concentrated to 0.5 ml in an amicon ultrafiltration unit with a YM 10 membrane. The solvent was exchanged with 50 mM potassium deuterium phosphate buffer, pD 7.4, by repeated concentration and addition of the new buffer. The sample was thoroughly deaired by repeated evacuation and flushing with oxygen free nitrogen. The protein was then transferred into an inert atmosphere glove box. Thoroughly deaired DMSO was added portionwise to a final concentration of 80% (v/v) with intermittent mixing. The solution was allowed to stand in the glove box atmosphere for 22 hours. DMSO was removed for the solution by repeated concentration and addition of 50 mM potassium deuterium phosphate buffer in the amicon vessel. The sample was transferred into an epr tube and was removed from the glove box.

Preparation of FdI unfolded in urea/DMSO and refolded in D2O: Approximately 10 mg of ammonium sulfate precipitated FdI was dissolved in 0.1M tris-Cl containing 0.1M NaCl, pH 7.4. The protein was dialysed against the same buffer for 2 hours. The sample was concentrated to approximately 400 microliters in an amicon ultrafiltration unit. The solvent was exchanged with 50 mM potassium deuterium phosphate buffer. The protein solution was thoroughly deaired and was then transferred

into the inert atmosphere glove box. Solid urea, recrystallized from ethanol, was added to a concentration. The sample was allowed to stand in the glove box for 24 hours. The denaturant was removed from solution as before.

Results and discussion

Figure XXVIIA shows the two pulse electron spin echo decay envelope for 0.97mM FdI in H_2O solution (0.1M KH_2PO_4 / K_2HPO_4 buffer, pD 8.0), and Figure XXVIIB shows the decay envelope for the same sample after six hours of incubation in D_2O (0.1M KD_2PO_4 / K_2DPO_4 buffer, pD 8.0). The proton coupling observed here is similar to that seen for Chromatium vinosum HiPIP or Rhodopseudomonas gelatinosa HiPIP (33,34). Little, if any, coupling to deuterium is observed. It has been concluded from the crystal structure of C. vinosum HiPIP that the 4Fe center in this protein is solvent inaccessible (36) and deuterium exchange with solvent is not to be expected. If a readily exchangeable proton on an iron bound oxoligand were present in FdI, a pronounced deuterium modulation would have been evident. None was observed, clearly demonstrating that if an oxoligand exists, it has no protons at or near the 3Fe center. A deep deuterium modulation of the type expected for a ligand with

Figure XXVII

Two pulse electron spin echo decay envelope of FdI in potassium phosphate buffer.

A. FdI equilibrated with H_2O buffer. Field 3290 gauss, frequency 8.931 GHz.

B. FdI equilibrated with D_2O buffer. Field 3343 gauss, frequency 9.273 GHz.

C. FdI unfolded in urea/D_2O and then refolded in D_2O buffer. Field 3350 gauss, frequency 9.309 GHz.

D. FdI unfolded in DMSO/D_2O and then refolded in D_2O buffer.

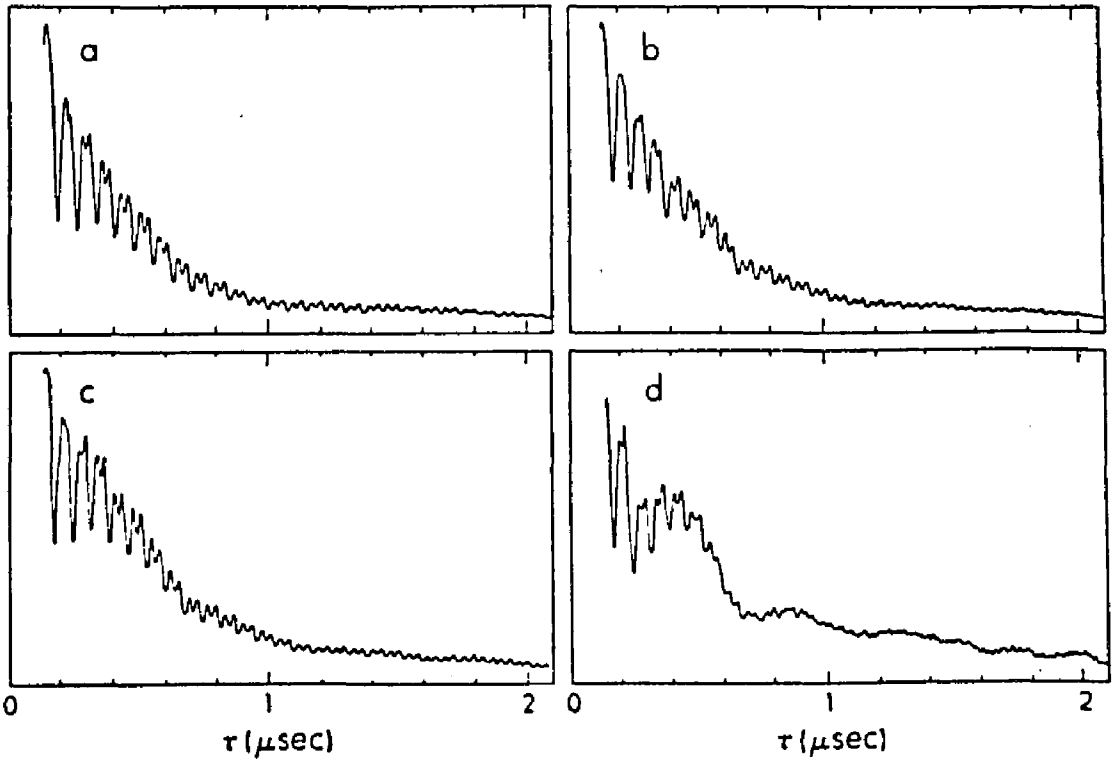
a
b
c
d
0
1
2
τ (μsec)
0
1
2
τ (μsec)

exchangeable protons near the [Fe-S] center has been previously observed for Clostridium pasteurianum ferredoxin, among others (34,35).

Even when FdI (50mM KD_2PO_4 / K_2DPO_4 buffer, pD 7.4) was incubated in D_2O solution with 8M urea for 30 minutes, only a weak deuterium modulation was observed (Figure XXVIIC). However when the protein was unfolded in DMSO and refolded in D_2O a deep deuterium modulation was seen (Figure XXVIID). In this way FdI resembles C. vinosum and R. gelatinosa HiPIPs which exhibit significant deuterium modulation in their decay envelopes after 20 minutes incubation in 80% DMSO/D_2O (V/V) (34).

Conclusion

Optical and EPR spectroscopic studies of FdI could not demonstrate ligand exchange of the oxoligand with other ligands even when the protein was demonstrably unfolded. These studies indicate that the oxoligand, if it exists, is not exchangeable. Electron spin echo decay envelope of FdI resembles those of proteins with solvent inaccessible [Fe-S] centers such as C. vinosum HiPIP. It can be firmly stated that the protons on ligands to iron in the 3Fe center of FdI are not exchangeable. Indeed, there are no exchangeable protons of any kind near the

3Fe center, including solvent protons and amide protons. Were an oxoligand present in FdI, it would be buried in the interior of the protein.

PROTON MAGNETIC RESONANCE STUDIES

All iron sulfur clusters characterized to date have been reported to be paramagnetic in at least one of their oxidation states. Because of their molecular paramagnetism, PMR spectra of [Fe-S] proteins generally display hyperfine- shifted resonances. Significant dipolar shifts were considered unlikely in [Fe-S] proteins because of the relatively small g-tensor anisotropies of the $[Fe_4S_4(S\text{-cys})_4]^{1-}$ and $[Fe_4S_4(S\text{-cys})_4]^{3-}$ clusters (37). Therefore the chemical shifts of the hyperfine shifted resonances were thought to originate from contact interaction of nuclei with the paramagnetic center.

Proton magnetic resonance data of the synthetic analogues of the 4Fe-4S clusters of the Fd_{ox} / Fd_{rd} redox couple showed that the hyperfine shifts of protons on the alkylthiolate ligands to the clusters originate from predominantly contact interactions (38,39,40). The shifts were exclusively in the downfield direction and were significantly attenuated for alpha hydrogens compared to beta hydrogens . On one electron reduction, the beta resonances moved further downfield. The absolute values of the shifts correlated well with those

observed in both oxidation states of ferredoxins and HiPIPs (38,40).

Ferredoxin from Clostridium acidi-urici is the only [Fe-S] protein for which a direct assignment of the hyperfine-shifted resonances has been reported by isotopic labelling (41). Eight downfield-shifted resonances in the spectrum of this ferredoxin has been assigned to beta hydrogens of the cysteines ligating the [Fe-S] centers. These assignments have been extended, by comparison, to the homologous ferredoxins from C. pasteurianum, C. perfringens, and Peptococcus aerogenes (41).

The significantly larger dispersion in the downfield shifts in proteins compared to their active-site analogues was explained by the dependence of the magnitude, not sign, of the hyperfine contact interaction constant, A, on the dihedral angle about the C -S axis (42). In the protein, the dihedral angle can assume several values depending on the peptide constraints on the cluster geometry. However, the angular dependence is averaged out in the analogues, because of free rotation about the C -S bond axis.

Thus it has been a practice to assign the downfield

shifted PMR resonances of [Fe-S] proteins to alpha or beta hydrogens of the cysteines coordinating the [Fe-S] centers. Hyperfine-shifted resonances were reported, both in the upfield and in the downfield regions, in the PMR spectra of HiPIPs from Chromatium vinosom and Rhodopseudomonas gelatinosa (43). The sign of the hyperfine coupling constant is independent of the relative orientation of the nucleus with respect to the paramagnetic center. Therefore in at least some of the hyperfine shifted resonances of these HiPIPs the shift mechanism must have significant dipolar contribution (43). Thus it appears that these resonances may correspond to non-cysteinyl hydrogens that are in the vicinity of the [Fe-S] centers. Saturation transfer experiments on half reduced/half oxidized HiPIPs showed that some of the upfield shifted resonances in the oxidized spectrum originate from the same protons that are downfield shifted in the reduced spectrum (43). Therefore if the upfield resonances in the spectrum of the oxidized protein arise from non-cysteinyl protons so should some of the downfield shifted protons in the spectrum of the reduced protein. These results clearly demonstrate that the general assumption of a dominantly contact mechanism for the downfield resonance shifts in [Fe-S] proteins should be reevaluated.

Proton magnetic resonance spectrum of FdI displays five hyperfine shifted resonances in the region of +15 to +32 ppm from DSS. The two most upfield resonances had been tentatively assigned to two cysteinyl beta hydrogens of the 4Fe center. The remaining three resonances were similarly assigned to the cysteinyl alpha-CH hydrogens of the 3Fe center (44). These assignments were largely based on atomic distances, cluster geometry, and cluster coordination reported by the 2.0 A X-ray structure (1). As has been already stated, the proposed X-ray structure of the 3Fe center of FdI is under dispute and the lack of experimental evidence for the putative oxoligand had been reported (45). PMR spectra of FDI were studied under various conditions in an attempt to determine the identity of protons corresponding to the downfield resonances and also to determine the nature of the hyperfine shift mechanism for these resonances.

Materials and methods

Procedures for growth of bacteria, isolation of FdI, determination of FdI concentration, preparation of glove box, preparation of NMR samples and preparation of EPR samples were described previously. A 0.4 ml solution of 0.5 mM solution of FdI in potassium deuterium phosphate buffer, pD 7.4, was generally used in the NMR

experiments. At this concentration 5000 transients were collected. A spectral width of 40000 Hz was scanned collecting 65536 points. A pulse repeat time of 1.5 seconds was generally used. Spectra were recorded with the same spectral width collecting 32768 points with a pulse repeat time of 0.5 seconds. A relaxation time measurement, by the inversion recovery, method had shown that the spectrum was completely relaxed with a pulse repeat time of 0.3 seconds. The FID was multiplied by an exponential window before Fourier transforming. The line broadening factor was set at 3.0 Hz. Reduction of both [Fe-S] centers of the protein was accomplished by the addition of a mixture of 10 mg of sodium dithionite and 3 mg of sodium borohydride to the protein solution under the strictly anaerobic conditions of the glove box. pH adjustments were made using solutions of 1M KOD or DCl (in 99.8 atom % D_2O).

400 MHz proton magnetic resonance spectra were recorded using a JEOL GX-400 Fourier transform NMR spectrometer. X-band EPR spectra were recorded using a Varian V-4500 spectrometer equipped with a Heli-tran liquid helium transfer system (Air Products). pH of NMR samples were measured in situ using a Radiometer pH meter equipped with a microelectrode.

Results and discussion

It is useful to compare the spectral characteristics of FdI with those of a ferredoxin from Pseudomonas ovalis. The ferredoxin of P. ovalis also contains a high potential 4Fe center and a low potential 3Fe center. The protein has a chain length , 106 amino acids, identical to that of FdI. There are 16 amino acid differences between the two proteins of which 4 are generally considered conservative replacements. When the similarities in the secondary structure of the two proteins were compared, by the method of Chou and Fasman, the only detected difference was the increased probability for a turn at residues 94-97 in the P. ovalis structure (20). The net charge in the vicinity of the [Fe-S] clusters in each protein is also expected to be similar. Therefore the three dimensional structure of these two proteins is expected to be essentially identical. The far downfield region of the PMR spectrum of FdI and P. ovalis ferredoxin compares well both in chemical shift pattern and in linewidths (46).

Figure XXVIII and Figure XXIX respectively show the upfield and far downfield regions of the PMR spectrum of FdI. Essentially identical data were also reported for the ferredoxin of P. ovalis (46). Because of poor

Figure XXVIII

400 MHz PMR spectrum of FdI in 50 mM potassium deuterium phosphate buffer, pD 7.39. Aromatic and aliphatic regions. HDO = 4.8 ppm.

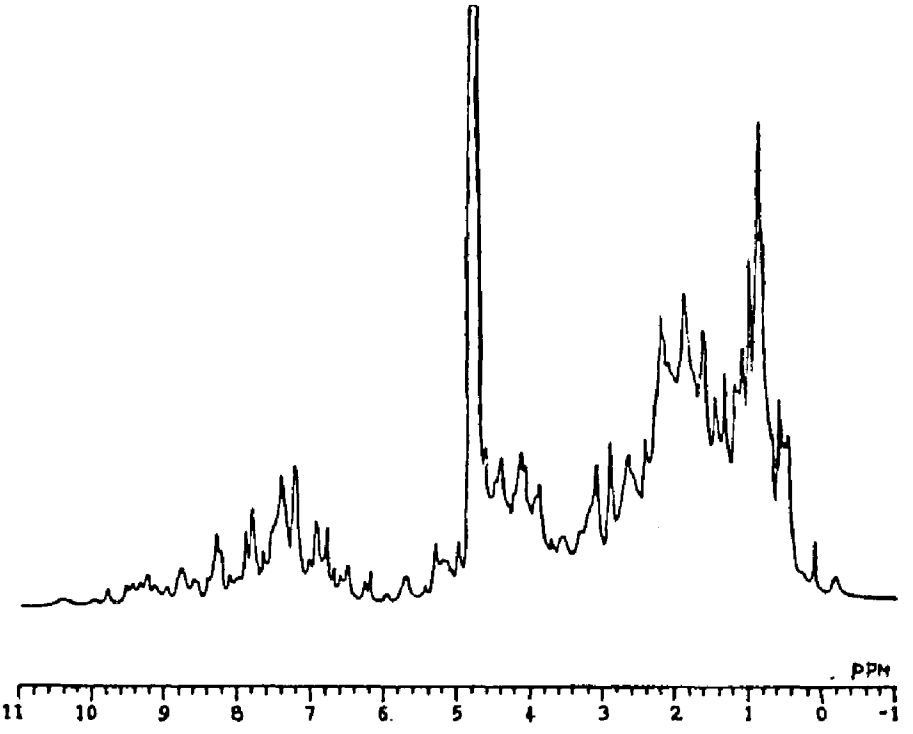
PPM
11
10
9
8
7
6
5
4
3
2
1
0
-1

Figure XXIX

400 MHz PMR spectrum of FdI in 50 mM potassium deuterium phosphate buffer, pD 7.39. The far downfield region. HDO = 4.8 ppm.

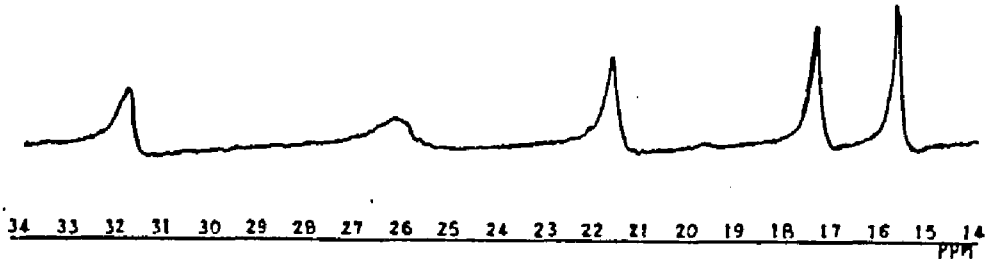
34 33 32 31 30 29 28 27 26 25 24 23 22 21 20 19 18 17 16 15 14
PPM

resolution and lack of assignments at the present time, the upfield region cannot be interpreted to provide useful insights. Despite the large linewidths, the downfield resonances are well separated from the remainder of the spectrum and are well resolved. The chemical shifts of these resonances are 15.8 ppm, 17.5 ppm, 21.8 ppm, 26.2 ppm, and 31.7 ppm at pD 7.39. The linewidths are , approximately, 40 Hz, 60 Hz, 80 Hz, 200 Hz, and 120 Hz respectively. Thus the linewidths does not uniformly increase with the magnitude of hyperfine shifts- i.e. the resonance at 26.2 ppm is significantly broader than the resonance at 31.7 ppm. The resonances around 15 ppm, 17 ppm, and 21 ppm show Curie temperature behavior, where as the two farthest shifted resonances, around 26 ppm and 32 ppm, show anti-Curie temperature dependence in their chemical shifts (Figure XXX). If the hyperfine interaction is dominated by contact interaction, then T_2^{-1}, and therefore the linewidth, must correlate with the squares of the observed shifts, since both involve A^2. The isotropic shift could be expressed as:

$$(H/H)^{iso} = - g\beta\, S(S+1)A \,/\, 3h\gamma_N kT$$

Thus for purely isotropic shifts of positive A, a Curie temperature dependence to the chemical shift is

Figure XXX

The temperature dependence of the hyperfine shifted resonances of FdI.

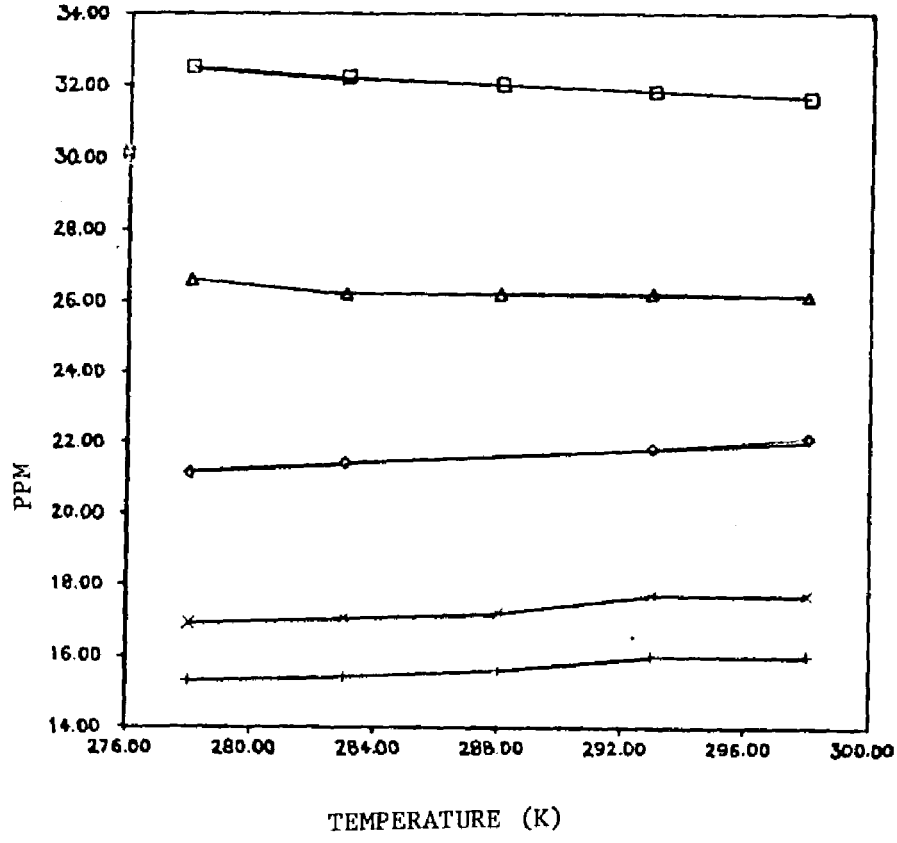
34.00
32.00
30.00
28.00
26.00
24.00
22.00
20.00
18.00
16.00
14.00
PPM
276.00
280.00
284.00
288.00
292.00
296.00
300.00
TEMPERATURE (K)

expected. And conversely in systems with negative A values, anti-Curie temperature dependence to chemical shifts would be expected. The far downfield resonances of FdI do not show a correlation of line width and chemical shifts that is expected for purely contact shifted resonances. Neither do they exhibit a uniform temperature dependence to chemical shifts. These observations could be explained in terms of the g-tensor anisotropy of the ground state or the thermally accessible excited states, unquenched orbital angular momentum in the ground state, thermal population of low-lying electronic levels, and the mixing of these levels by the applied magnetic field (47). Thus there may exist a significant pseudocontact interaction between the nucei corresponding to the downfield resonances and the paramagnetic metal center.

The three most downfield shifted resonances were not observed in the PMR spectrum of FdI reduced with methyl-viologen (44). On methyl viologen reduction, the EPR signal at g = 2.01 disappears indicating the reduction of the 3Fe center. The oxidation state of the 4Fe center is expected to be unaffected by this reduction. Therefore the resonances around 21 ppm, 26 ppm, and 32 ppm were assigned to the cysteinyl protons of the 3Fe center (44). A careful examination of the reduced spectrum also

reveals a substantial line broadening of the resonance near 15 ppm. This indicates that the reduction of the 3Fe center also affects this hyperfine shifted resonance. Similar results were also reported for P. ovalis ferredoxin (46). Therefore the association of the 3 most downfield resonances to the 3Fe center and the remaining two resonances to the 4Fe center needs to be reevaluated.

Nagayama et al. (21) reported the reduction of 4Fe clusters in 7Fe ferredoxins (ferredoxins that contain one 4Fe cluster and one 3Fe cluster) from P. ovalis, Mycobacterium smegmatis, and Thermus thermophilus using sodium borohydride as the reductant. They estimated the following order of potentials for the redox couple corresponding to the 4Fe clusters:

E_m (P. ovalis) < E_m (T. thermophilus) < E_m (M. Smegmatis) < -400 mV (21).

This estimated order is in agreement with the reported potentials of -435 mV for the 4Fe cluster of M. smegmatis and -530 mV for the 4Fe cluster of T. thermophilus (48,49). Because of the close similarities between FdI and P. ovalis ferredoxin their 4Fe clusters could be expected to have similar reduction potentials that are less than -535 mV.

Figure VII shows the X-band EPR spectrum of a sample of FdI that was reduced with a mixture of sodium dithionite and sodium borohydride. The resonance with a g value around 1.94 is typical of reduced 4Fe clusters in ferredoxins. Thus the 4Fe center presumably reduced to the C^{+1} oxidation state of the available C^{+3}, C^{+2}, and C^{+1} oxidation states predicted by Carter et. al for the 4Fe clusters in [Fe-S] proteins (50).

Several changes in the PMR spectrum is observed on reduction of the 4Fe center (Figure XXXI and Figure XXXII). The four intense resonances between +1 ppm and -1 ppm are from the reductant mixture. These lines were present in the spectrum of a control sample prepared without the protein. There is considerable line broadening and small chemical shift differences throughout the spectrum. These changes might reflect a protein conformational change that accompany the reduction. If the 4Fe center is reduced to the C^{+1} state, as anticipated by the Carter's three state hypothesis, the ground state spin of the cluster changes from S = 0 to S = 1/2. Since the vicinity of the 4Fe center shows a marked aggregation of acidic residues (1), the added charge on reduction is could impose unfavorable electrostatic interactions forcing the molecule to change its tertiary structure. Another

Figure XXXI

400 MHz PMR spectrum of FdI reduced with a mixture of sodium dithionite and sodium borohydride. Aliphatic and aromatic regions. (top)

400 MHz PMR spectrum of a control sample of FdI. Aliphatic and aromatic regions. (bottom)

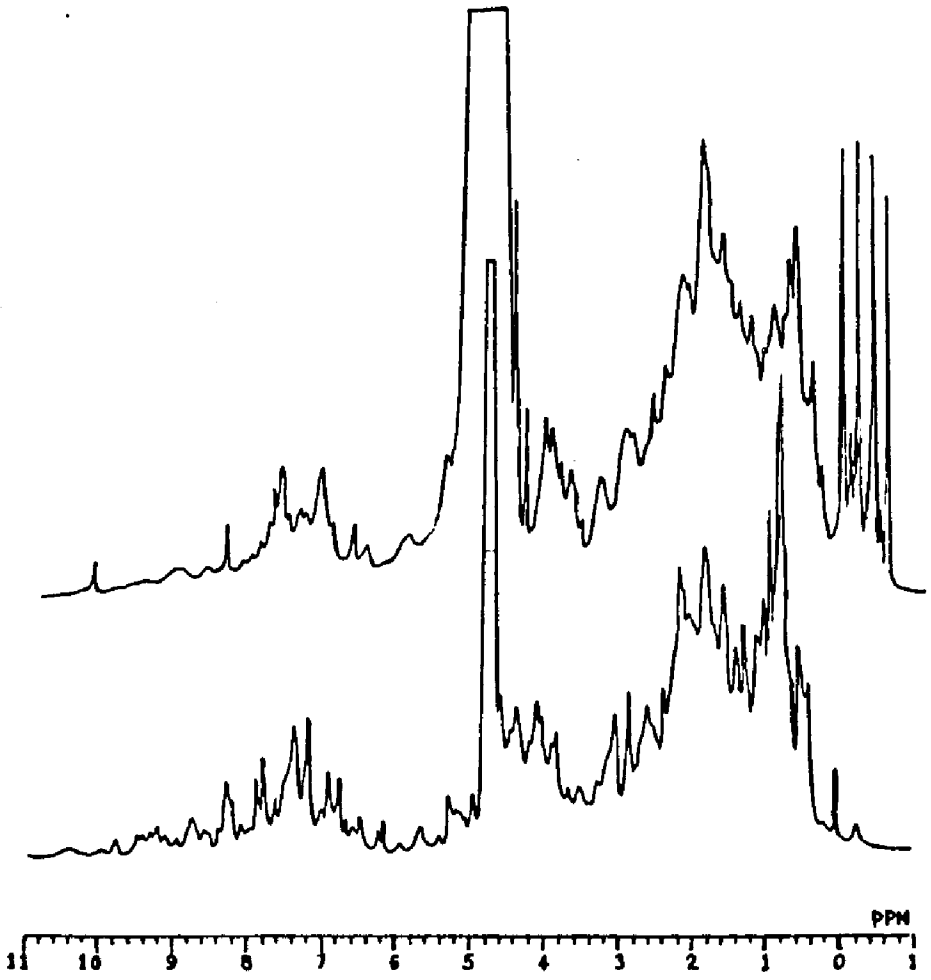
PPM
11
10
9
8
7
6
5
4
3
2
1
0
1

notable difference in the reduced spectrum is the reduction in resonance intensities in several parts of the spectrum. Intensity losses around +7.4 ppm, +2 ppm and +1 ppm are easily noticed in the spectrum on comparison with the spectrum of the protein in its isolated state. Around +10.3 ppm and around +8.5 ppm two new sharp resonances also appear in the spectrum. The spectral data of P. ovalis ferredoxin in the aliphatic region is not available for comparison.

In the far downfield region the spectra of borohydride reduced FdI and that of P. ovalis show similarities. In the reduced spectrum of FdI (Figure XXXII) resonance positions are, approximately, 15.44 ppm, 17.70 ppm, 27.13 ppm, 29.85 ppm, 37.04 ppm, and 38.61 ppm with approximate linewidths (at half height) of 100 Hz, 330 Hz, 275 Hz, 165 Hz, 275 Hz, and 220 Hz respectively. The resonances near 15 ppm and 17 ppm might reflect incomplete reduction since there are resonances in these positions in the spectrum of the protein in its isolated state also. The increase in linewidths of these resonances compared to their linewidth in the isolated state of the protein might reflect dipolar broadening as a result of a conformational change that accompany the reduction of the 4Fe center. In the protein reduced with sodium borohydride both clusters are reduced (E_m (3Fe

Figure XXXII

400 MHz PMR spectrum of FdI reduced with a mixture of sodium dithionite and sodium borohydride. Far downfield region.


PPM
40
35
30
25
20
15

cluster) = -420 mV). It has already been mentioned that the reduction of the 3Fe center results in substantial line broadening for the resonance around 15 ppm while not affecting the linewidth of the resonance near 17 ppm significantly. However, on reduction of both centers both resonances are significantly affected. These results can be explained in terms of the proximity between the two centers: the separation between the two clusters, edge to edge, is about 11.1 A (1). The lack of a significant difference in the chemical shifts while showing a large difference in linewidths indicate that the the nuclei corresponding to these resonances may have closer approach to the [Fe-S] centers in the new conformation. The far downfield shifted resonances, above +20 ppm, in the spectrum of the borohydride reduced protein must have migrated from the aliphatic and aromatic regions of the spectrum of the oxidized protein. The resonances that are reported to be missing from these regions in the spectrum of the reduced protein need to be considered in this context. The respective spin states for the 3Fe cluster and the 4Fe cluster are, presumably, S = 2 and S = 1/2 in the borohydride reduced protein. Therefore the far downfield resonances in the spectrum are not likely to correspond to the resonances around 15 ppm and 17 ppm of the isolated state of the protein.

On partial reoxidation, by opening the NMR tube to air for 30 seconds followed by incubation at room temperature for 15 minutes, small reversal of the spectrum in the upfield region and the reappearance of the resonance near 17 ppm are observed (Figure XXXIII). However, on gentle bubbling of air through the solution for 5 minutes followed by a 20 minute incubation, the downfield region of the spectrum completely reverted to the original state and the upfield region reverted to a state very close to the original spectrum (Figure XXXIV). The small differences in the upfield region is expected to be completely reversible on further standing.

Sweeney (44) reported the reversible changes in the PMR spectrum of FdI on treatment of the protein with stoichiometric amounts of potassium ferricyanide. Similar results have been reported in other 7Fe proteins as well (51). These changes are thought to arise from the oxidation of the 4Fe cluster to the C^{3+} oxidation state of Carter's three state hypothesis. In all instances excess ferricyanide produced irreversible changes in the spectra, presumably due to cluster conversions. Conversion of 4Fe clusters into 3Fe clusters had been reported in a ferredoxin from Bacillus stearothermophilus, and in a ferredoxin from C. pasteurianum on treatments with excess ferricyanide

Figure XXXIII

400 MHz PMR spectrum of borohydride reduced FdI. Upfield region. A. Native FdI. B. After mild reoxidation of the fully reduced sample. C. After bubbling air through the fully reduced sample.

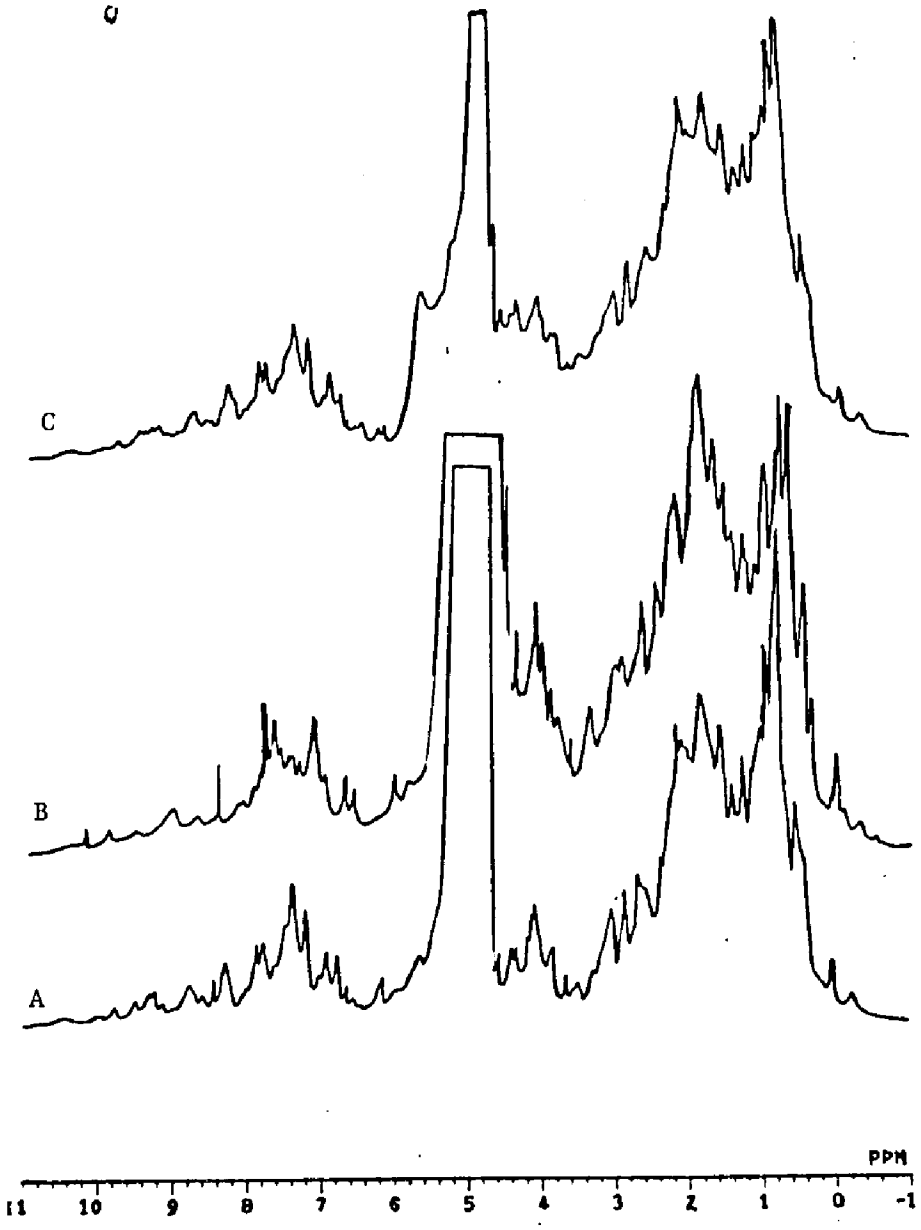
C
B
A
PPM
11
10
9
8
7
6
5
4
3
2
1
0
-1

Figure XXXIV

400 MHz PMR spectrum of borohydride reduced FdI. Downfield region. A. Native FdI. B. After mild reoxidation of the fully reduced sample. C. After bubbling air through the fully reduced sample.

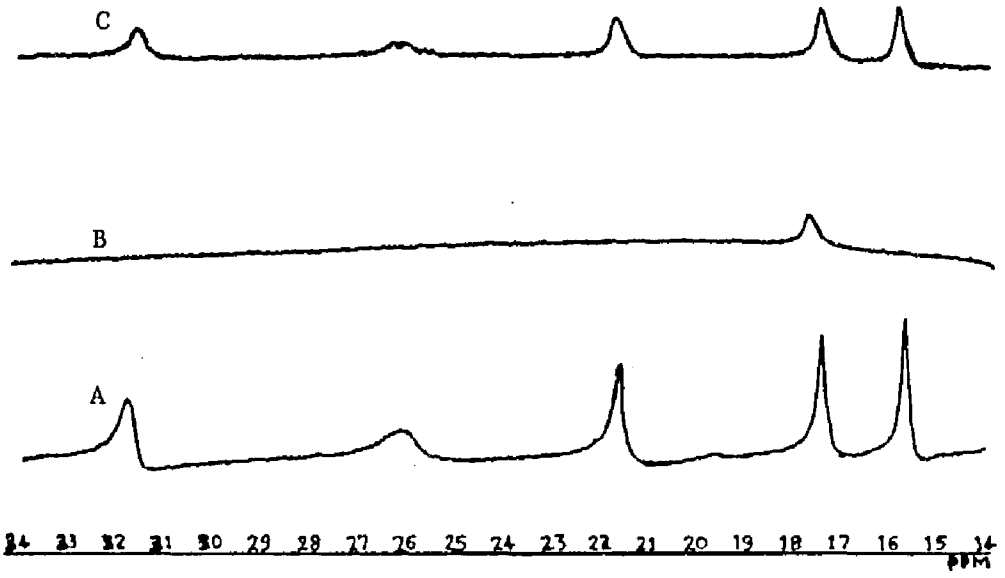
C
B
A
34 33 32 31 30 29 28 27 26 25 24 23 22 21 20 19 18 17 16 15 14
ppm

(52,53).

Figure XXXV and Figure XXXVI shows the changes in the spectral changes that occurred when a partially anaerobic solution of FdI was treated with a four fold molar excess of potassium ferricyanide under argon for 30 minutes. The spectral changes observed in the hyperfine shifted resonances are consistent with those reported by Sweeney for FdI and by Nagayama et al. for other 7Fe ferredoxins (51). The spectrum, upfield and downfield regions, reverted to the original state when the oxidant was removed from the sample by ultrafiltration. Two additional resonances, around -1 ppm and -18 ppm, are reported in the ferricyanide treated spectrum of P. ovalis (46). These resonances were not observed in FdI. However, their absence could not be stated with confidence because of the poor S/N ratio of the spectrum. On removal of the ferricyanide by ultrafiltration the spectrum completely reverted to the original state.

Conclusion

The 1H NMR spectrum of FdI, in the isolated state, shows five hyperfine shifted resonances. Three of these resonances exhibit a Curie relationship between temperature and chemical shifts in the region of 278 K to

Figure XXXV

A. 400 MHz PMR spectrum of FdI treated with a four fold molar excess of potassium ferricyanide. Aliphatic and aromatic regions. Solvent: 50 mM $KD_2PO_4/KDPO_4$, pD 7.39.

B. 400 MHz PMR spectrum of control FdI.

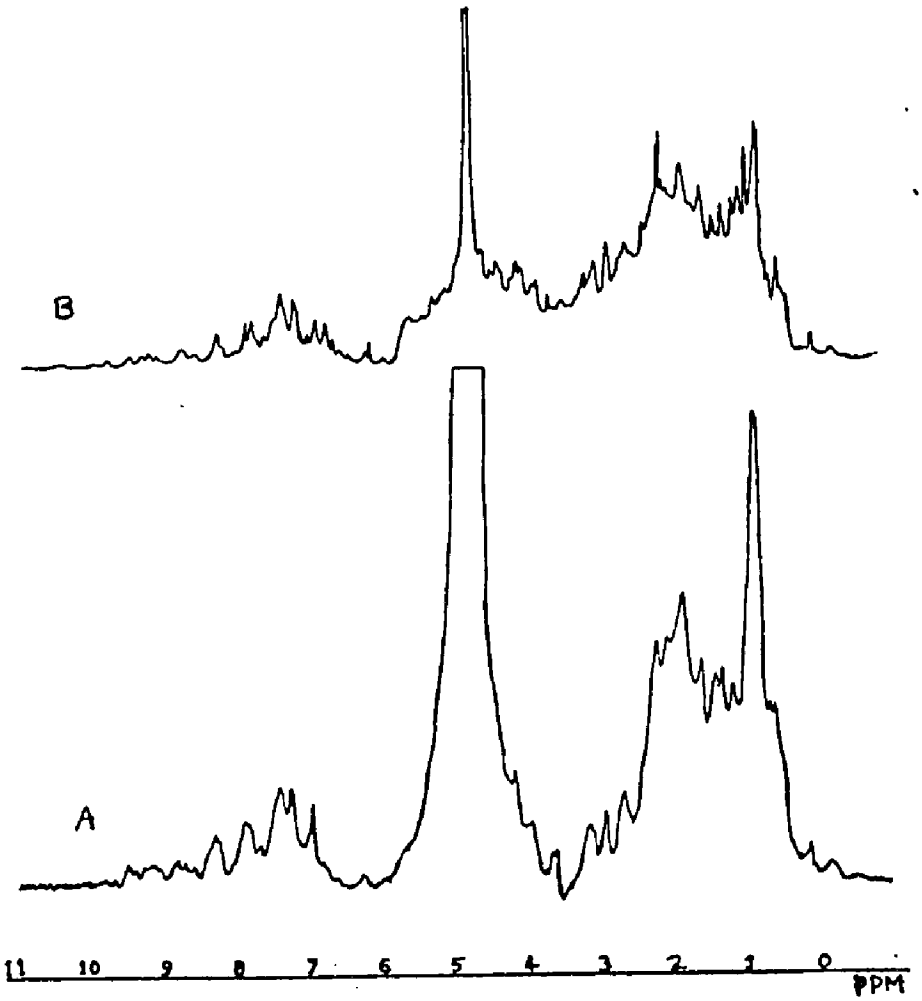
B
A
11
10
9
8
7
6
5
4
3
2
1
0
PPM

Figure XXXVI

A. 400 MHz PMR spectrum of FdI treated with a four fold moalr excess of potassium ferricyanide. Far downfield region. Solvent: 50 mM $KD_2PO_4/KDPO_4$, pD 7.39.

B. 400 MHz PMR spectrum of control FdI.

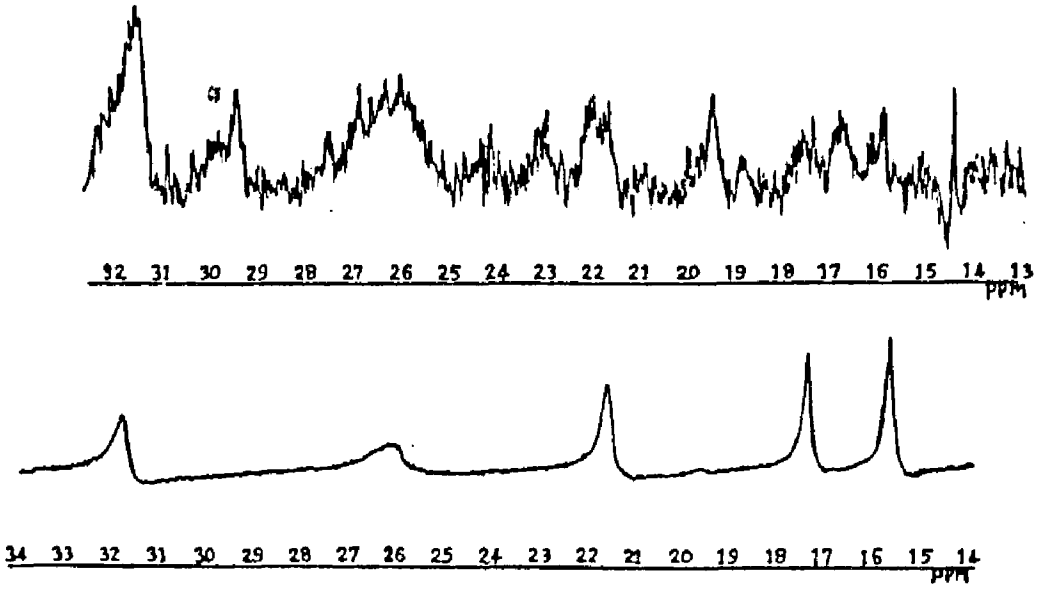
a
32 31 30 29 28 27 26 25 24 23 22 21 20 19 18 17 16 15 14 13
ppm
34 33 32 31 30 29 28 27 26 25 24 23 22 21 20 19 18 17 16 15 14
ppm

298 K. The other two hyperfine shifted resonances show a anti-Curie temperature dependence on chemical shifts. The latter behavior could be explained by a g-tensor anisotropy of the [Fe-S] cluster(s) due to thermal occupation of low-lying excited states.

Upon reduction of the 3Fe cluster, the three most downfield shifted resonances disappear. Therefore these resonances are presumably associated with the 3Fe cluster of the proetein. The association of the other two resonances to the 4Fe cluster is ambiguous since one of these resonances undergo a change in linewidth on reduction of the 3Fe cluster.

The spectrum undergoes significant changes when the 3Fe cluster and the 4Fe cluster are both reduced. Most of the changes in the upfield and the aromatic regions of the spectrum are best explained by a general protein conformational change upon reduction of the 4Fe cluster. The new hyperfine shiftes resonances in the fully reduced spectrum are presumably alpha and/or beta cysteinyl protons of the [Fe-S] clusters.

The spectrum undergoes reversible changes on mild oxidation with potassium ferricyanide. By comparison with similar behaviors of other 7Fe ferredoxins these

changes are attributed to the oxidation of the [4Fe-4S] cluster to the C^{3+} state of Carter's three state hypothesis.

CHARACTERIZATION OF THE GROWTH OF A. VINELANDII ON CYSTINE

Azotobacter vinelandii was grown on a synthetic growth medium that contained dl-cystine as the only sulfur source (cystine medium). The purpose of these experiments were to determine whether the cysteines of FdI could be specifically labelled with isotopes in order to facilitate the characterization of the proton magnetic resonance spectrum. In a ferredoxin from Clostridium acidi urici, approximately 95% of cysteines were isotopically labelled in similar experiments (41).

The dependence of the growth of the organism on cystine concentration present in the cystine medium was first studied. The lowest concentration of dl-cystine for the growth of cells at a rate comparable to the rate in normal medium was determined. A. vineladii was also grown on radioactive cystine medium (cystine medium containing beta ^{14}C-dl-cystine as an isotopic marker). The cell protein from the organism grown on the radioactive cystine medium was isolated by precipitation with trichloroacetic acid and was then hydrolyzed to the constituent amino acids. The protein hydrolysate was derivatized with o-phthalaldehyde and was analyzed by

high performance liquid chromatography (HPLC) to determine the ^{14}C distribution in the cell protein.

I. Growth characterization

A. vinelandii cultures were started from ATCC culture (OP strain) on agar plates. The agar medium contained, per liter,

$MgCl_2.6H_2O$	0.1650 g
$CaCl_2.2H_2O$	0.0427 g
$Na_2MoO_4.2H_2O$	1.2 mg
$FeCl_2.4H_2O$	5.5 mg
sugar (Domino, supermarket brand)	20.0 g
L-cystine	0.12 g
K_2HPO_4	0.64 g
KH_2PO_4	0.16 g
bactoagar	15.0 g

The phosphates were autoclaved separately from the medium and were added when the temperature of the medium dropped to approximately 50 ^{o}C. Plates were poured while the medium was still warm to avoid agar solidification. The plates were streaked with cells using a sterile platinum loop and were incubated at 30 ^{o}C. Cells were scraped off from fully grown plates to innoculate 100 ml of medium in a 1 L flask. This medium had the same ingredients as the agar medium except for the depletion of agar from it. The culture was grown in a constant temperature water bath at 32 ^{o}C with vigorous agitation. The fully grown medium was used to innoculate eight 100

ml growth media of varying dl-cysteine concentration. The cysteine concentration varied from 0 to 4 mM.

Figure XXXVII shows the klett turbidometric readings of cultures of varying dl-cysteine concentrations after 48 hours of growth. The organism did not grow in the absence of cysteine, as is evidenced by the steady klett reading in media of zero cysteine concentrations. A steady maximum cell density was observed in media of 10^{-4} M cysteine concentration and higher. However, cells collected from the medium of 10 cystune concentration were considerably less brown in color than cells from normal medium, presumably due to the inhibition of the biosynthesis of some electron transport proteins. Therefore 2.5 X 10^{-4} M cystine (equivalent to 5 X 10^{-4} M cysteine) was used in subsequent growths. At this cystine concentration the growth profile was indistinguishable from that in the normal medium described previously.

II. High performance liquid chromatography (HPLC)

The analysis of amino acids from protein hydrolysates has classically been carried out using ion exchange chromatography and post column derivatization and detection (56). This technique has the distinct

Figure XXXVII

Growth of A. vinelandii on cystine medium at varying cysteine concentrations.

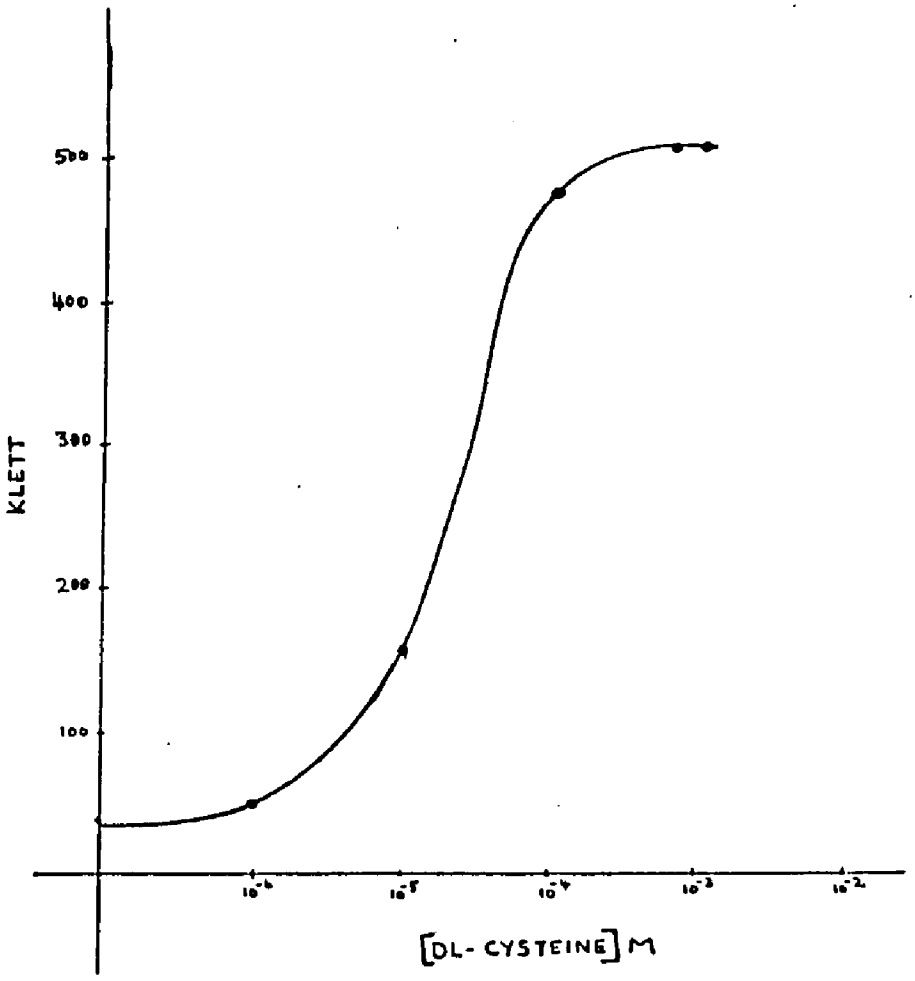
KLETT
500
400
300
200
100
10^{-6}
10^{-5}
10^{-4}
10^{-3}
10^{-2}
[DL- CYSTEINE] M

advantage of excellent resolving power and the ability to detect both primary and secondary amino acids. However, the high cost of operation, and the long time period of analysis are inherent drawbacks of this methodology. These limitations have been significantly circumvented by the use of high performance liquid chromatography as an alternate method for amino acid analysis (57,58,59,60).

Roth first described o-phthalaldehyde, in the presence of ethanethiol, as a reagent for the fluorometric detection of alpha amino acids (61,57). The reaction has been subsequently modified enabling the detection of amino acids in the picomole range (60). 1-alkylthio-2-alkyl-substituted isoindoles are formed in the reaction (62). These isoindoles have strong optical absorptions at 340 nm, and fluorescence at 455 nm.

HPLC analysis, with o-phthalaldehyde derivatization, of the total cell protein hydrolysate of A. vinelandii is described here.

Materials and methods

The HPLC anlyses were performed using a Beckman Model 332 Gradient Liquid Chromatograph system. The system comprised of a Altex Model 420 Microprocessor

System Controller, two Beckman Model 110A single-piston reciprocating pumps, a dynamically stirred gradient mixing chamber, a Model 210 sample injection valve, a Bondapak C_{18} column and a Beckman Model 155 variable wavelength detector with a 0.020 ml analytical flow cell. A Gilford fraction collector was used to collect 1 ml fractions from the detector.

All chromatograms were obtained under the following instrumental settings:

solvent programmer	15%B to 75%B in 60 minutes
flow rate	1.0 ml per minute
detection	340 nm
chart speed	4.0 inches per 60 minutes

All solutions were prepared in HPLC grade solvents. All solvents and samples were filtered using 6 micron filter paper and were thoroughly deaired immediately before injection into the column.

Preparation of reagents.

Borate buffer: 0.5 M potassium borate buffer was prepared by dissolving 31.0 g of boric acid (anhydrous) in 1.0 liter of HPLC grade water. The pH was adjusted to 10.5 with KOH pellets.

o-Phthalaldehyde: HPLC grade methanol was added to 10 mg of o-phthalaldehyde to a final volume of 1.0 ml.

This solution was prepared fresh immediately before use.

Ethanethiol: Ethanethiol reagent was prepared by adding HPLC grade methanol to 0.010 ml of ethanethiol to a final volume of 10.0 ml. This solution was freshly prepared for each use.

Stock 300 mM sodium phosphate buffer: HPLC grade water was added to 10.08 g of NaH_2PO_4 (anhydrous) and 30.67 g of Na_2HPO_4 (anhydrous) to a final volume of 1 liter. The pH of this solution was 7.2 at room temperature.

Solvent A: Solvent A was prepared by adding HPLC grade water to 50.0 ml of stock phosphate buffer to a final volume of 1.0 liter.

Solvent B: Solvent B was prepared by the addition of 50.0 ml stock phosphate buffer and 400.0 ml of HPLC grade water to 550.0 ml of acetonitrile.

Preparation of total cell protein

Cells were harvested from a one liter radioactive cystine medium (0.06 g dl-cystine and 10^{-3} mCi of beta ^{14}C-dl-cystine per liter of medium) by centrifugation at 8000 X G for twenty minutes. The cell paste was

suspended in 200 ml of 10% trichloroacetic acid that was precooled to ice bath temperature. The suspension was allowed to stand in an ice bath for one hour. The white precipitate formed was collected by centrifugation at 20000 X G for 50 minutes. The slightly yellow supernatant was discarded. The precipitate was suspended in 200 ml of 10% (W/V) trichloroacetic acid and placed in a hot water bath at 90 ^{o}C for 15 minutes to solubilize the nucleic acids. The suspension was spun at 20000 X G for 50 minutes. The clear supernatant, which showed a high 260 nm absorption, was discarded. The pellet was dissolved in 300 ml of 1.0 M Trizma base. This protein solution was dialyzed against 20 L of distilled deionized water for 48 hours. The solvent was removed by lyophilization.

Hydrolysis of cell protein

40 mg of the lyophilized cell protein was dissolved in 5 ml of 6N HCl in a 20 ml borosilicate test tube. The HCl solution was previously deaired and saturated with prepurified grade nitrogen. The test tube was immediately evacuated and filled with nitrogen. The cycle was repeated three times. 0.070 ml of deaired DMSO was added, and the container evacuated promptly and was refilled with nitrogen. The test tube was then sealed with an oxygen torch under a gentle flow of nitrogen gas.

The sealed test tube was then incubated at 110 ^{o}C for 24 hours. At the end of incubation the test tube was opened and the solvents were removed by rotary evaporation at 60^{o} C. The residue was redissolved in 5 ml of HPLC grade water and the solvent was again removed as before. The cycle was repeated two more times. The residue was finally dissolved in 0.60 ml of 300 mM stock potassium phosphate buffer. This sample was derivatized with o-phthalaldehyde by the following procedure.

Derivatization of amino acids

To 0.200 ml of the protein hydrolysate from the above step or to an equal volume of amino acid solution, 5 mg per ml of 300 mM stock potassium phosphate buffer, was added, in the following order: 0.050 ml of borate buffer, 0.050 ml of methanol, 0.100 ml of ethanethiol reagent, and 0.100 ml of o-phthalaldehyde. The reaction mixture was incubated at room temperature for 2 hours. For the derivatization of free amino acid this incubation was carried out only for 5 minutes. At the end of the incubation period the reaction mixture was filtered using a 6 micron filter paper and was thoroughly deaired by evacuation. 0.050 ml of this solution was used for injection into the HPLC column.

Results and discussion

A. vinelandii was grown on radioactive cystine medium. (0.06g of l-cystine and 10^{-3} mCi of beta ^{14}C-dl-cystine, per liter of medium). On a 5 minute counting of 1.0 ml of the medium, immediately before innoculation, a value of 1667 CPM was obtained. Approximately 40 hours after the innoculation time, cells were sedimented by centrifugation and the radioactivity of the supernatant was measured. On a 5 minute counting of 1.0 ml of the supernatant a value of 738 CPM (counts per minute) was obtained. When calibrated against a ^{14}C standard, the instrument demonstrated 80% counting efficiency immediately before either measurement. Thus it was calculated that the uptake of dl-cystine from the medium was approximately 56%.

In a separate experiment, in which the cells were grown only for 25 hours, 25% of the input radioactivity had disappeared from the growth medium. However, only 17% of the initial radioactivity was recovered in the cells. The remaining 8% of the initial radioactivity was unaccounted for, presumably due to the formation of $^{14}CO_2$, by cystine metabolism.

Figure XXXVIII demonstrates the resolving power of

Figure XXXVIII

HPLC chromatogram of a derivatized mixture of cyteic acid, aspartic acid, and glutamic acid.

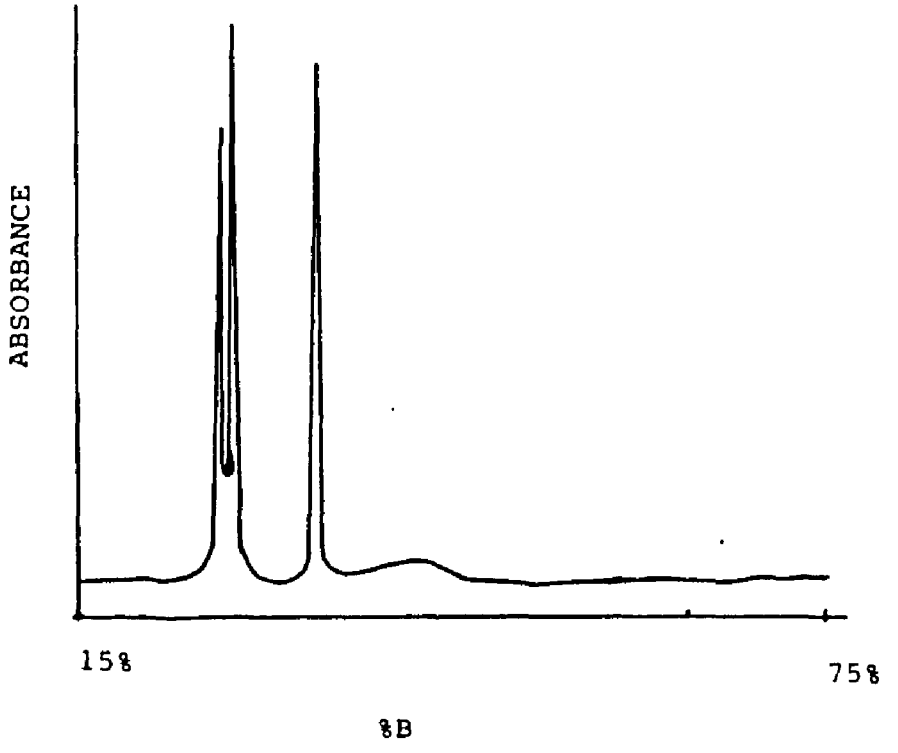
ABSORBANCE
15%
75%
%B

the HPLC column under conditions that were used for the separation of the protein hydrolysate. The injection sample consisted of 0.050 ml of a derivatized mixture of aspartic acid, cysteic acid, and glutamic acid. 0.200 ml of a solution that contained 3.0 mg of each amino acid in 1.0 ml of stock phosphate buffer was used for the derivatization. Because of their higher polarity than the remaining natural amino acids, these amino acids elute from the column in the above stated order as the earliest fractions. This order was verified by individual chromotography of single standard amino acids. The resolution between glutamic acid and the other two amino acids is good. However, cysteic acid and aspartic acid were not resolved from each other to the extent that they could be collected as pure fractions following detection. Amino acids were easily detected to the nanomole range.

Figure XXXIX shows the chromatogram of derivatized dl-cysteic acid. Figure XXXIX also shows the chromatogram of a derivatized sample of radioactive cystine (dl-cystine + beta ^{14}C-dl-cystine) that underwent the same hydrolysis treatment as the cell protein. Both samples had retention times of 10 minutes. This result shows that cystine is converted to cysteic acid upon acid hydrolysis in the presence of DMSO. This conclusion is

Figure XXXIX

A. HPLC chromatogram of derivatized cysteic acid.

B. HPLC chromatogram of derivatized dl-cystine that was previously hydrolyzed in the presence of DMSO.

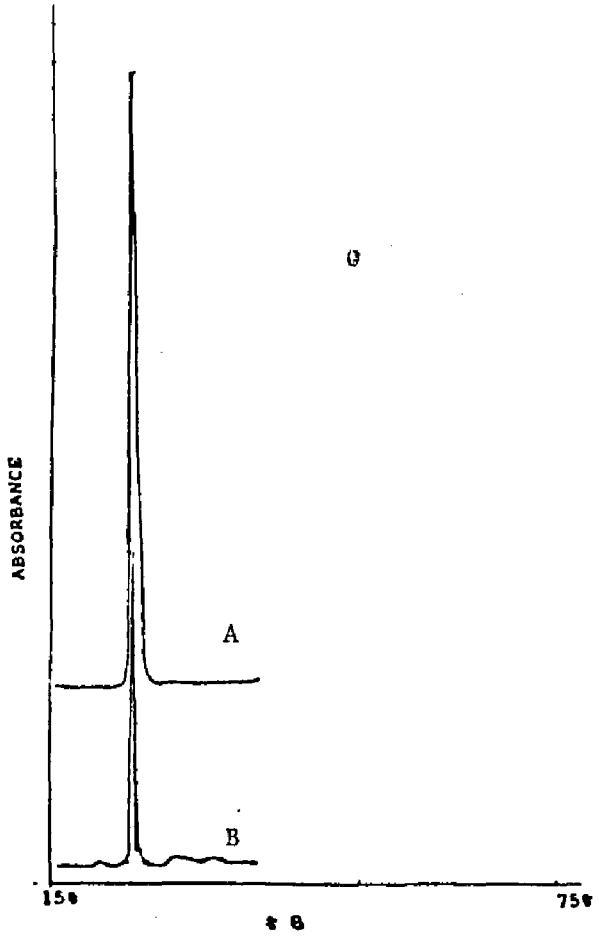
ABSORBANCE
A
B
15°
75°
θ

further corroborated by the ^{2}H NMR spectrum of a hydrolyzed sample of alpha ^{2}H-dl-cystine (Fig XL). However, in the chromatogram of the ^{14}C cysteic acid sample, only 3.4 % of the radioactivity of the injected sample was recovered in fraction number 10. No other fraction up to fraction number 60 contained any radioactivity. The last amino acid to emerge from the column, lysine, eluted as fraction number 60. The low recovery of the amino acid from the column is presumably due to the irreversible binding of material to the column as a result of the decomposition of the isoindole formed from the o-phthalaldehyde reaction. The isoindoles are reported to be unstable in acqueous solutions (62).

Figure XLI shows the chromatogram of A. vinelandii total cell protein hydrolysate, and Figure XLII shows the distribution of radioactivity of 1 ml fractions that was collected from the same sample. There was only one fraction that contained any radioactivity among fractions 1 to 65. This fraction, fraction number 3, contained 3.9% of the input radioactivity. However, in the chromatogram of the standard amino acids, the earliest amino acid, aspartic acid, eluted from the column as fraction number 9 (Figure XXXVIII). Figure XLIII shows the radioactivity distribution of a derivatized sample of radioactive cell protein that was hydrolyzed in the

Figure XL

^{2}H NMR spectrum of a alpha-^{2}H-dl-cysteic acid in 1N HCl.

The spectrum was recorded on a Bruker CXP-200 spectrometer at the Molecular Biophysics and Biochemistry department of Yale university. Deuterium was observed at 30 MHz through the lock channel without field lock. A cyclops pulse sequence was used. Reported chemical shifts are relative to external DSS.

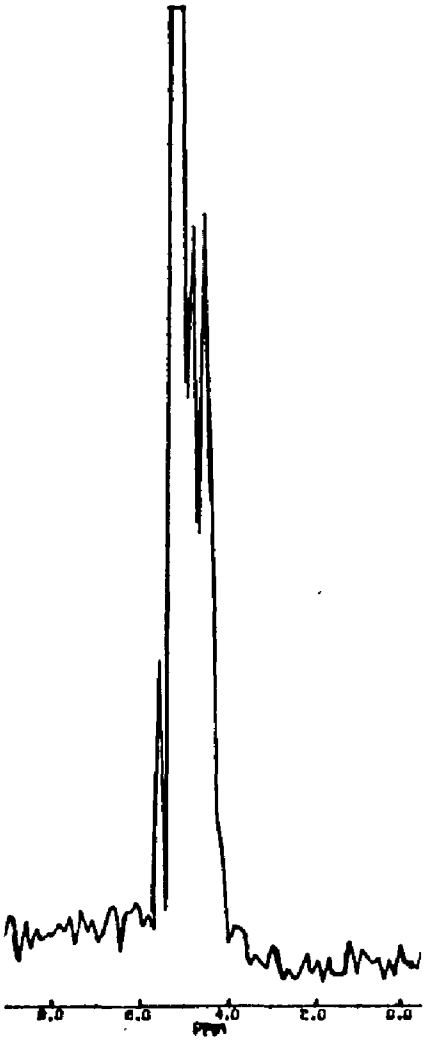
8.0
6.0
4.0
2.0
0.0
PPM

Figure XLI

HPLC chromatogram of derivatized hydrolyzate of the TCA-precipitable protein of A. vinelandii. Hydrolysis was in the presence of DMSO.

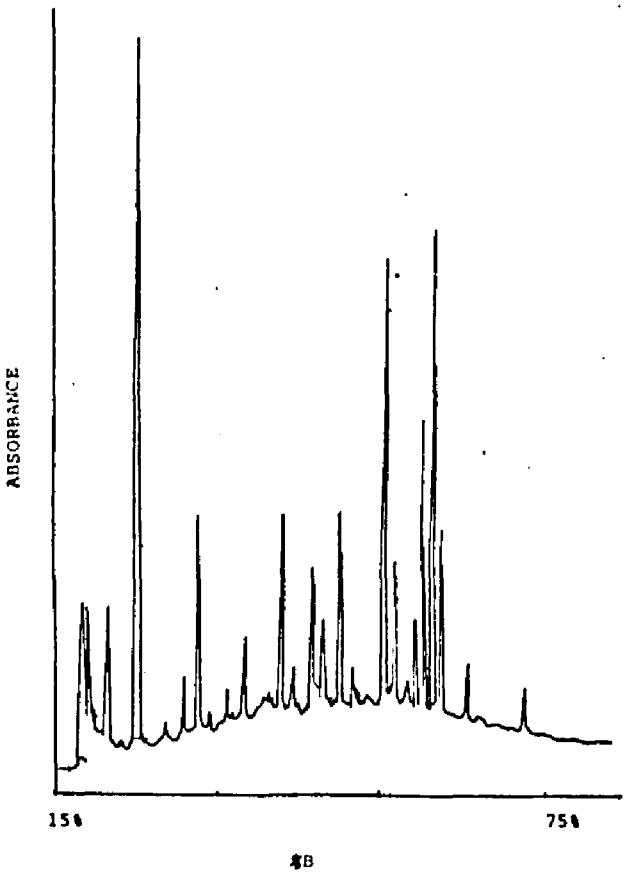
ABSORBANCE
15%
75%
%B

Figure XLII

^{14}C distribution in 1 ml fractions of derivatized TCA-precipitable protein of A. vinelandii

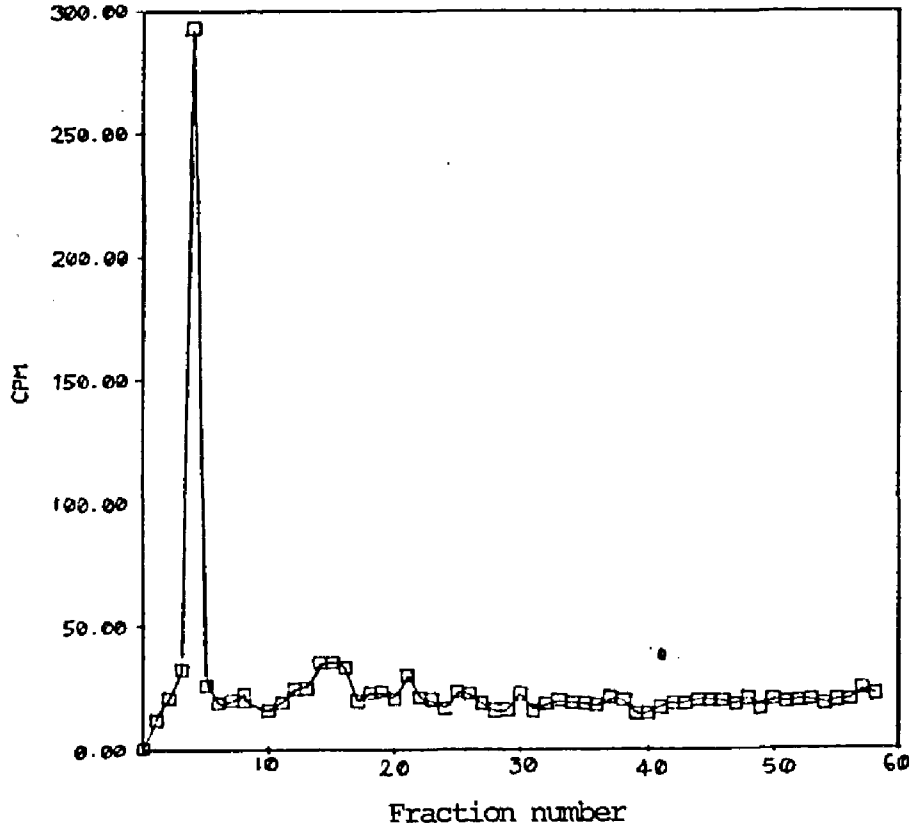
300.00
250.00
200.00
150.00
100.00
50.00
0.00
CPM
10
20
30
40
50
60
Fraction number

Figure XLIII

Radioactivity distribution in 1 ml HPLC fractions of a derivatized mixture of radioactive cell protein of A. vinelandii and beta ^{14}C-dl-cystine that was previously hydrolysed.

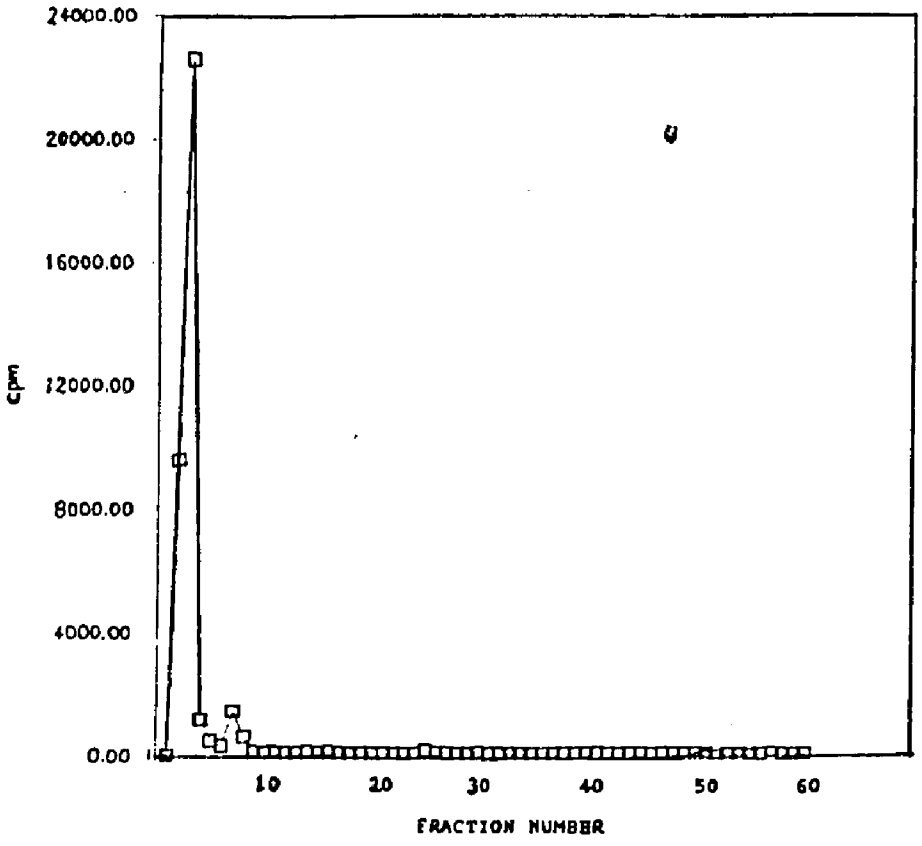
24000.00
20000.00
16000.00
12000.00
8000.00
4000.00
0.00
cpm
10
20
30
40
50
60
FRACTION NUMBER

presence of ^{14}C cystine (3mg l-cystine and 2.5×10^{-4} mCi beta ^{14}C-dl-cystine). The injection sample contained approximately 5.7×10^{5} CPM radioactivity from cysteine and 7.6×10^{3} CPM radioactivity from the cell protein. The peak radioactivity fraction was found in fraction number 3. In this instance 3.95% of the input radioactivity was recovered from the combined fractions 2,3 and 4.

The combined results presented above clearly show that free cystine in the absence of cell protein forms cysteic acid on hydrolysis in the presence of DMSO (Figure XXXIX and Figure XL). However, the fate of cysteine on hydrolysis in the presence of DMSO and the cell protein is not identified from the results presented above. Therefore these results cannot be interpreted to determine whether or not intact cysteines are incorporated into the cell protein of A. vinelandii when the organism is grown on cystine medium.

Conclusion

A. vinelandii was grown on a synthetic medium that contained dl-cystine as the sole sulfur source (cystine medium). Under these conditions the organism was able to grow by the uptake of cystine to meet its sulfur

requirements. The cells did not grow if cystine was depleted from the medium. Of the total beta ^{14}C radioactivity that disappeared from the medium, only 67% was recovered in the cells collected from the medium. This indicates that cystine was metabolised, presumably via the Kreb's cycle, with the liberation of CO_2. The cell protein from organism grown on ^{14}C-dl-cystine medium was hydrolyzed and analyzed by HPLC to determine radioacivity distribution in amino acids. The only fraction that contained any radioactivity had a retention time significantly shorter than that of any common amino acid. Since the idententity of this radioactive fraction could not be determined, these results cannot be interpreted to determine whether or not A. vinelandii incorporates intact cysteines into its cell protein when grown on cystine medium.

DEUTERIUM AND CARBON-13 NMR STUDIES

The five downfield resonances, in the region of +15 ppm to +32 ppm from DSS, in the ^{1}H NMR spectrum of FdI were reported to arise from cysteinyl protons of the [Fe-S] clusters. The three most downfield resonances were tentatively assigned to the alpha protons of cysteines ligated to the 3Fe center and the remaining two resonances were assigned to the beta protons of cysteines coordinating the 4Fe center (44). Experiments described here were attempts to assign the downfield resonances directly by specific isotope labelling of the cysteines in the protein.

The availability of high field spectrometers with pulse and Fourier transform capabilities made it possible to observe magnetic resonances of rare nuclei in biological samples. Deuterium magnetic resonance (DMR) spectroscopy has inherent advantages in the study of complex molecules such as proteins. Spin-spin coupling between a deuteron and the neighboring protons is 6.5 times smaller than the coupling between corresponding protons. Therefore the DMR spectrum is often not complicated by small couplings to protons. The spin-spin coupling between two deuterons (in enriched samples) is

42.4 times smaller than the corresponding proton coupling. Consequently, deuterium - deuterium coupling is seldom observed. Thus, if the quadrupole moment is averaged out by isotropic motion, a single resonance is observed for every inequivalent nuclei in the molecule. Due to the low natural abundance of deuterium (0.0156%) selected segments of the molecule could be studied, by specific labelling, without interference from the naturally abundant nuclei. The deuterium isotope effect on chemical shift is negligible, therefore the chemical shift in the DMR spectrum,expressed in parts per million is essentially same as that in the PMR spectrum (63).

For the study of contact shifted and pseudocontact shifted resonances of paramagnetic substances, DMR spectroscopy has the distinct advantage of narrower line width compared to PMR spectroscopy for corresponding nuclei in identical sites. Solomon and Bloembergen derived expressions for longitudinal and transverse relaxation times of nuclei in paramagnetic molecules (64,65). Accordingly:

$$1/T_1 = [(2/15r^6)S(S+1)\gamma_I^2 g^2 \beta^2][3\tau_c + 7\tau_c/(1+\omega_s^2\tau_c^2)] + 2/3[S(S+1)A^2/\hbar^2]\,[\,\tau_e / (1+\omega_s^2\tau_e^2)]$$

$$1/T_2 = [(1/15r^6)S(S+1)\gamma^{I2}g^2\beta^2][7\tau_c + 13\tau_c/(1+\omega_s^2\tau_c^2)] + 1/3[S(S+1)A^2/h^2][\tau_e + \tau_e/(1+\omega_s^2\tau_e^2)]$$

In these equations T_1 and T_2 are longitudinal and transverse relaxation times respectively, S is the electron spin quantum number, g is the Lande factor is the Bohr magneton, ω_I is the nuclear gyromagnetic ratio, r is the electron-nuclear distance, τ_c is the electron-nuclear dipolar interaction time, ω_S is the electron Larmor frequency, A is the hyperfine coupling constant, and τ_e is the correlation time for hyperfine coupling. The inherent assumptions of the above equations are that $\omega_I \ll \omega_S$ and $\omega_I^2\tau_c^2 \ll 1$ and that there is g factor isotropy (66). In addition, the equations make no distinction between longitudinal and transverse electron relaxation times (67,68). These conditions are not restrictive when the PMR and DMR spectra of identical molecules (except for isotopic labelling) are being compared.

A^2 is proportional to γ^2 through the equation:

$$A = (4/3)h\gamma_e\gamma_I\psi(0)]^2.$$

Thus a reexamination of the paramagnetic nuclear relaxation time expressions show that the relaxation rates and thereby the NMR linewidths are directly

proportional to the square of the gyromagnetic ratio of the nucleus under observation. If a proton in a paramagnetic molecule is substituted with a deuterium, the only parameter in the above expressions that change significantly is $_I$ and therefore the DMR line should be narrower than the corresponding proton line by a factor of $\gamma_H^2 / \gamma_D^2 = 42.4$. This prediction is on the basis of the assumption that signal broadening due to the nuclear quadrupole moment is negligible. This approximation is valid for small molecules where the rotational correlation time is ($_c$) is small because of fast molecular tumbling and thus the nuclear quadrupole moment is averaged out. A forty fold decrease in linewidth is reported for the Cr(III) acetylacetonate complex (63). The overall resolution enhancement of DMR resonance line compared to the PMR resonance line is expected to be 6.5 (63).

The rotational correlation time of FdI is not known. However, a value of 6 nanoseconds could be estimated since the molecular weight of the protein is approximately 14500 daltons (69). Little conformational flexibility is expected for the nuclei corresponding to the downfield shifted resonances in the PMR spectrum of FdI, if these resonances originate from the cysteinyl protons. The electron-nuclear correlation

times of the cysteinyl protons are thus expected to be governed by the rotational correlation time of the molecule. Based on an expected correlation time of 6 nanoseconds, a deuterium magnetic resonance linewidth in the vicinity of 365 Hz, could be calculated for the cysteinyl resonances (69). This value is exclusive of any paramagnetic contribution to linewidth. Therefore these resonances may not be observable in the DMR spectrum due to quadrupole line broadening. Selective deuterium substitution in the molecule is still a useful procedure, because assignments could be made based on the differences between the PMR spectra of labelled and unlabeled proteins.

Experimental attempts to incorporate alpha-^{2}H-cysteine, beta ^{2}H-cysteine and beta ^{13}C-cysteine into FdI are described here. Samples of FdI, isolated from these incorporation experiments, FDIA, FDIB, and FDIC respectively, were studied by ^{1}H, ^{2}H, and ^{13}C NMR spectroscopy.

Materials And methods

Alpha-^{2}H-dl-cystine was prepared in four steps. In the first step alpha-^{2}H-N-acetyl-S-benzyl-dl-cysteine was prepared by the method of Upson and Hruby (71). In the

second step the acetyl group was removed by acid hydrolysis. In the third step the benzyl group was removed by the method of Wood and Devigneaud (72). And in the final step cysteine was oxidized to cystine and the product was purified by recrystallization by the procedure of Wood and Devigneaud (72).

Results and discussion

Preparation of alpha-^{2}H-S-benzyl-dl-cysteine

50 g of S-benzyl-l-cysteine was weighed into a scrupulously dry 2L round bottom flask fitted with a drying tube. 750 ml of acetic anhydride were added immediately followed by 120 ml of D_2O (99.8 atom %). A 100 cm reflux condenser, fitted with a drying tube, was placed on the flask. The reaction mixture was allowed to stand with occasional swirling and extremely gentle heating, using a heating mantle, until all of the amino acid dissolved. The reaction vessel was then gently refluxed for 3 minutes. The solution could come to vigorous and explosive boiling unless extreme care is taken in heat regulation. Solution turned yellow on heating. The refluxed solution was cooled down to room temperature and an additional 50 ml of D_2O was added to convert any unreacted acetic anhydride to acetic acid. The solvent was removed by rotary evaporation at 60 ^{o}C.

The residue was taken up in 400 ml of 6N HCl. This acid mixture was refluxed at gentle boiling for 16 hours. A brown precipitate was formed upon cooling of the reflux mixture to room temperature. The pH of the solution layer was raised to 6 with Conc.NH_4OH. After 1 hour the precipitate was collected by vacuum filtration. The precipitate was washed with water, and then with ethyl alcohol. The alcohol wash was continued until the precipitate became nearly colorless. The precipitate was finally washed with diethyl ether and was dried in vacuuo over anhydrous $CaCl_2$ overnight at room temperature. A typical yield of this step was 95%.

The precipitate from the above step was recrystallized by the following procedure. 49.5 g of the dried precipitate from the above step was dissolved in 750 ml of 3N HCl by gentle heating. The solution was boiled with approximately 1 g of Norite for 5 minutes. Norite was removed by filtration. The procedure was repeated, if necessary, until the filtrate became colorless. The clear solution was allowed to cool down to room temperature. Conc. NH4OH was added, in small portions, until intense precipitation started. The reaction mixture was allowed to stand overnight at room temperature for complete precipitation. The colorless crystals were collected by vacuum filtration and were

washed with water, 10% ethyl alcohol and finally with diethyl ether. The washed crystals were dried in vacuo over anhydrous calcium chloride overnight. Upon drying colorless and fluffy crystals of S-benzyl-dl-cysteine was obtained. A typical yield of this step was 96%. A 60 MHz PMR spectrum of the product did not show the alpha hydrogen resonance.

Debenzylation of alpha-^{2}H-S-benzyl-dl-cysteine

Approximately 5 g of the 47.5 g of alpha-^{2}H-S-benzyl-dl-cysteine, from the above step, was added into 700 ml of liquid ammonia in a round bottomed flask. Strips of freshly shaven sodium metal were added until a very deep blue color developed in solution. The reaction mixture was swirled until most of the amino acid dissolved. Another 5 g portion of the amino acid was added and the procedure was repeated until all of the reactant was added. The deep blue color of the solution was maintained for an additional 20 minutes. The solvent was removed by evaporation in a cold water bath. The reaction vessel was cooled to icebath temperature and the residue was taken up in 300 ml of ice/water mixture. The mixture was transferred into a 1 L separatory funnel and was extracted with three 250 ml portions of diethyl ether. Dissolved ether was removed from the acqueous

phase by evaporation in a hot waterbath at 50 ^{o}C. pH of the solution was adjusted to 10.5. Two drops of 10% ferric chloride (W/V) was added and the solution was gently bubbled with air for 24 hours. The pH was adjusted to 7.0 and the solution was left overnight at room temperature for precipitation. The precipitate was filtered, washed with water and was dissolved in a minimum amount of 1N HCl. The solution was decolorized by Norite treatment as described before. Conc. NH4OH was added to the clear solution until intense precipitation started. The precipitating solution was left overnight at room temperature. The precipitate was collected by filtration, and was washed with water, 10% ethyl alcohol (V/V), and finally with diethyl ether. The product was dried in vacuuo over anhydrous calcium chloride. The yield from this step was 85%.

Figure XLIV shows the ^{1}H NMR spectra of alpha-^{2}H-dl-cystine prepared by the procedure described above. A comparison of the spectrum with that of dl-cystine provide proof for deuterium labelling at the alpha position. The resonance line corresponding to the alpha hydrogen has diminished in intensity approximately by 90% and the splitting pattern of the beta hydrogen resonances show considerable simplification. Figure XLV shows the solid state Raman spectrum of alpha-^{2}H-dl-cystine

Figure XLIV

Bottom: 500 MHz ^{1}H NMR spectrum of DL-cystine in 1 N DCl.

Top: 500 MHz ^{1}H NMR spectrum of alpha-^{2}H-dl-cystine in 1 N DCl.

Spectra were recorded on a Bruker AM-500 spectrometer at the Magnetic Resonance center of Yale university. HDO resonance is set to 5 ppm.

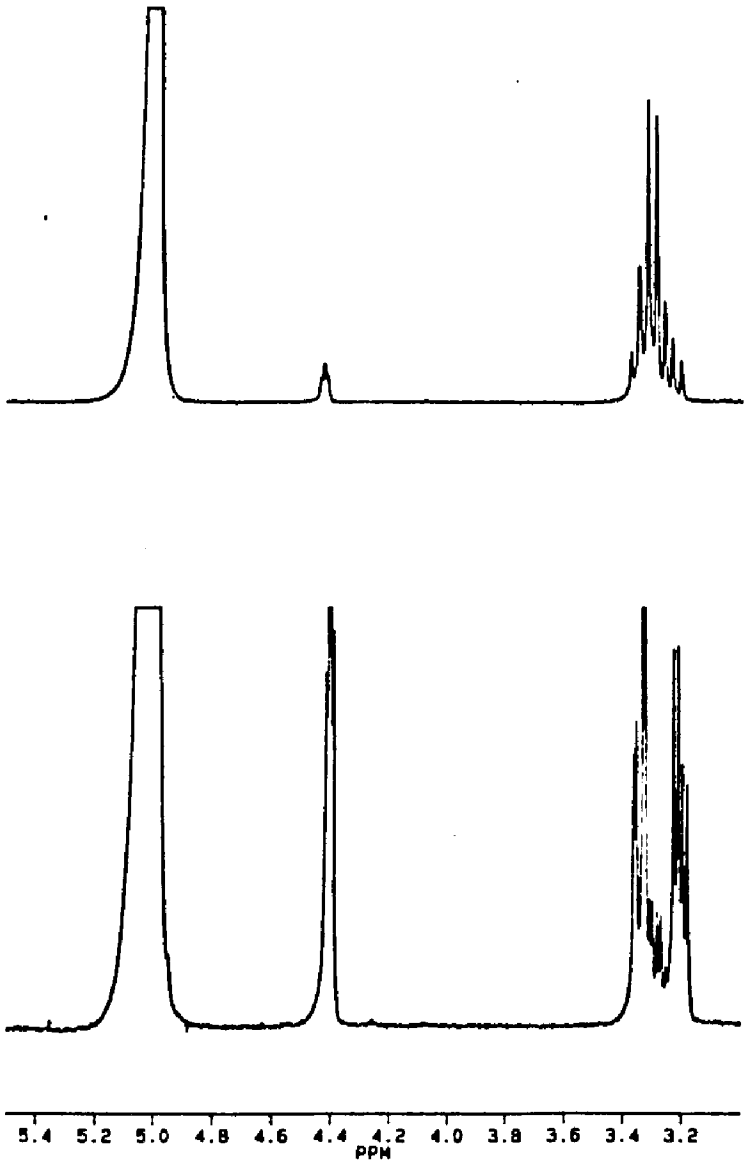
5.4 5.2 5.0 4.8 4.6 4.4 4.2 4.0 3.8 3.6 3.4 3.2
PPM

Figure XLV

Solid state Raman spectra of alpha-^{2}H-dl-cystine (top) and dl-cystine. (Courtesy of Prof. Max Diem).

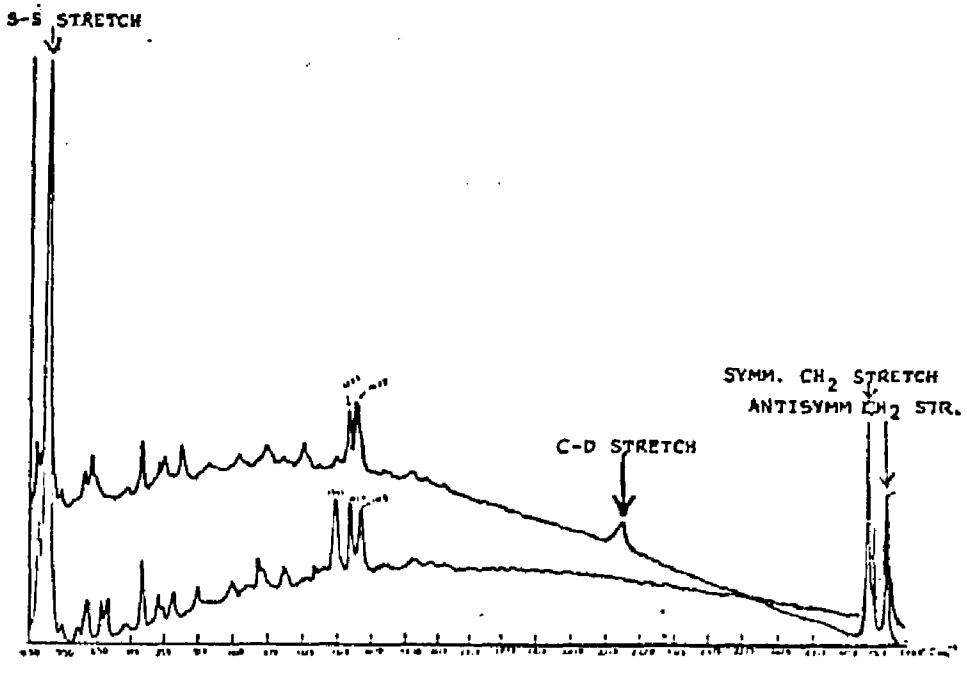
S-S STRETCH
C-D STRETCH
SYMM. CH_2 STRETCH
ANTISYMM CH_2 STR.

(courtesy of Prof. Max Diem). The C-D vibrational band is easily observed in the spectrum.

Preparation of beta-^{2}H-dl-cystine and beta-^{13}C dl-cystine

Beta-^{2}H-dl-cystine and beta-^{13}C-dl-cystine were prepared by Prof. Klaus Grohman (Hunter College, Department of Chemistry) by the procedure of Devigneaud (72).

Figure XLVI and XLVII respectively show the 400 MHz ^{1}H NMR spectra of of beta-^{2}H-dl-cystine, and beta-^{13}C-dl-cystine. Deuterium labelling of the beta position in the former spectrum is evidenced by the diminishment of the multiplet intensity between -1 ppm and -2 ppm in Figure XLVIA. Furthermore the multiplet structure of the alpha protons, between 0 ppm and -1 ppm, has coalesced because of the absence of spin-spin proton coupling. ^{13}C labelling in the latter spectrum is easily identified by the observed 135 Hz beta CH spin-spin coupling in Figure XLVIIA.

Preparation of FDIA, FDIB, and FDIC

A. vinelandii cultures were started from agar plates on cystine media as previously described. The agar medium was prepared with commercially obtained dl-cystine

FIGURE XLVI

Top: 400 MHz ^{1}H NMR spectrum of DL-cystine in 50 mM DCl.

Bottom: 400 MHz ^{1}H NMR spectrum of beta-^{2}H-dl-cystine in 50 mM DCl.
HDO resonance is assigned to 0 ppm.

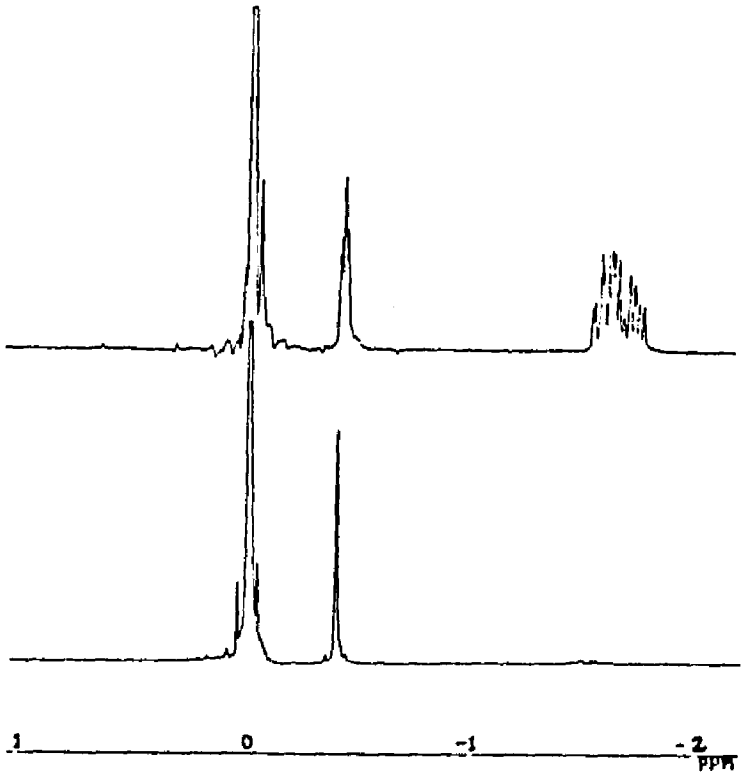
1
0
-1
-2
ppm

Figure XLVII

Top: 400 MHz ^{1}H NMR spectrum of DL-cystine in 25 mM DCl.

Bottom: 400 MHz ^{1}H NMR spectrum of beta-^{13}C--dl-cystine in 25 mM DCl.

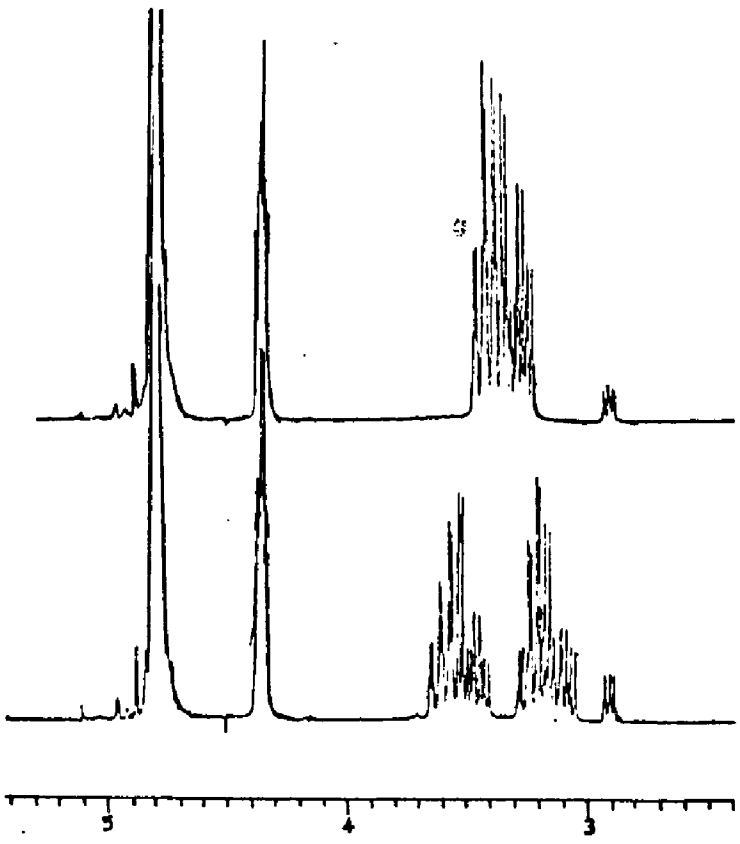
5
4
3

(Sigma Chemicals). Subsequent media were prepared with 4.0×10^{-4} M alpha-^{2}H-dl-cystine. Approximately 10% (V/V) fully grown innoculum was used in each transfer. The alpha-^{2}H-dl-cystine culture was grown to a volume of 4 liters. This culture was used to innoculate 25 L of medium containing 4.0×10^{-4} M alpha-^{2}H-dl-cystine in the fermentor. The starting Klett turbidometric reading of this culture was 100. When the Klett reading reached 250, in 24 hours, 80 L of preautoclaved medium containing 5.0 g of alpha-^{2}H-dl-cystine and 0.0185 mCi beta-^{14}C-dl-cystine were added. A 5 minute scintillation counting of a 0.5 ml of this medium gave a value of 162 CPM immediately before innoculation. In 18+ hours the klett reading and the CPM reading of the medium reached steady readings of 425 and 72 respectively. The culture was harvested at 20 hours. 425 g of cells were obtained. FdI was isolated as previously described .

To prepare FDIB or FDIC, a 90 L cystine medium containing 6.0 g of the specifically labelled amino acid was innoculated with 40 g of 1 week old frozen cells that were grown on dl-cystine medium (Sigma Chemicals). The cells reached a steady Klett of 450 in 18 hours and were harvested. FdI was isolated as described previously. Uptake of cysteine was not followed in this instance unlike in the previous experiment.

Figure XLVIII compares the ^{1}H NMR spectra of FDIA and FDIB with that of the unlabeled FdI. Figure IL shows the spectral comparison between FDI and FDIC. In either case no change in resonance intensities or splitting patterns is obvious between the spectra. These results show that either there were no label incorporation in FDIA, FDIB and FDIC or that none of the resolved reonances in the ^{1}H NMR spectrum of FdI are from cysteinyl protons. The spin-spin coupling between the beta carbon and the beta protons in free cysteine is approximately 135 Hz (see Figure XLVII). Therefore, the presence of cysteinyl beta ^{13}C nucleus in FDIC is expected to be easily identifiable in the ^{1}H NMR spectrum if the beta proton resonances are present in the spectrum.

Deuterium magnetic resonance study of FDIA

After recording the ^{1}H NMR spectrum, FdIA was dialysed against water for 24 hours at 4 ^{o}C with one solvent change (approximately 0.5 ml of FdI solution against 20 L of water). The dialysis water was pH adjusted to pH 7.0 with 1.0M tris buffer (0.1M trizma, pH 7.4). The protein sample was then dialysed against 25 ml of deuterium free water overnight. The solvent was finally exchanged five times with deuterium free water

Figure XLVIII

Bottom: 400 MHz ^{1}H NMR spectrum of FdI

Middle: 400 MHz ^{1}H NMR spectrum of FdIA

Top: 400 MHz ^{1}NMR spectrum of FdIB

All spectra were recored in 50 mM $KD_2PO_4/KDPO_4$, pD 7.39. Protein concentration in each case was approximately 0.5 mM. 32768 transients of 64K time domain points were collected with a spectral width of 40000 Hz and a pulse repeat time of 0.5 seconds. An exponential window of 3 Hz was applied prior to the Fourier transform.

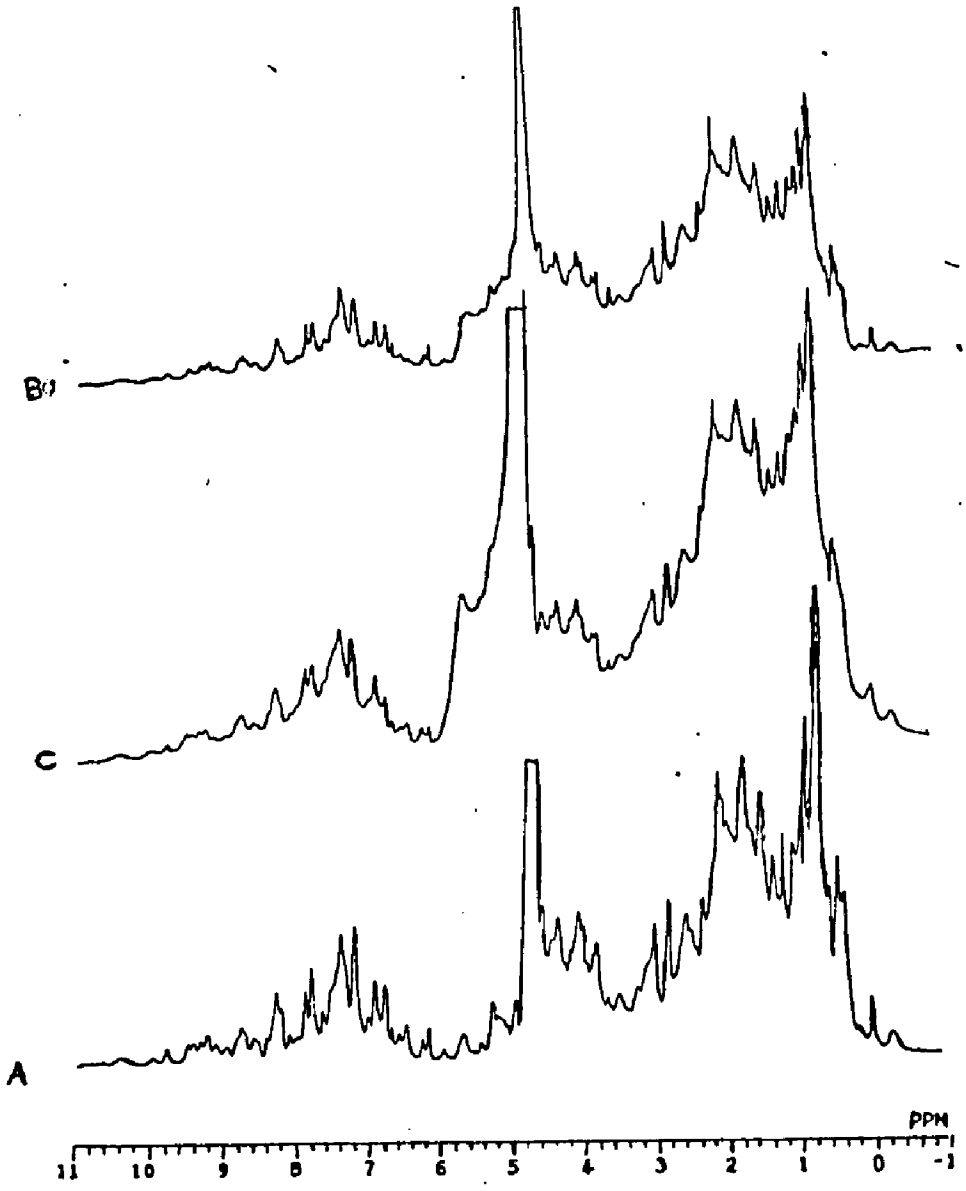
B
C
A
PPM
11
10
9
8
7
6
5
4
3
2
1
0
-1

Figure IL

Bottom: 400 MHz ^{1}H NMR spectrum of FdI

Top: 400 MHz ^{1}H NMR spectrum of FdIC

Conditions were same as in the previous figure.

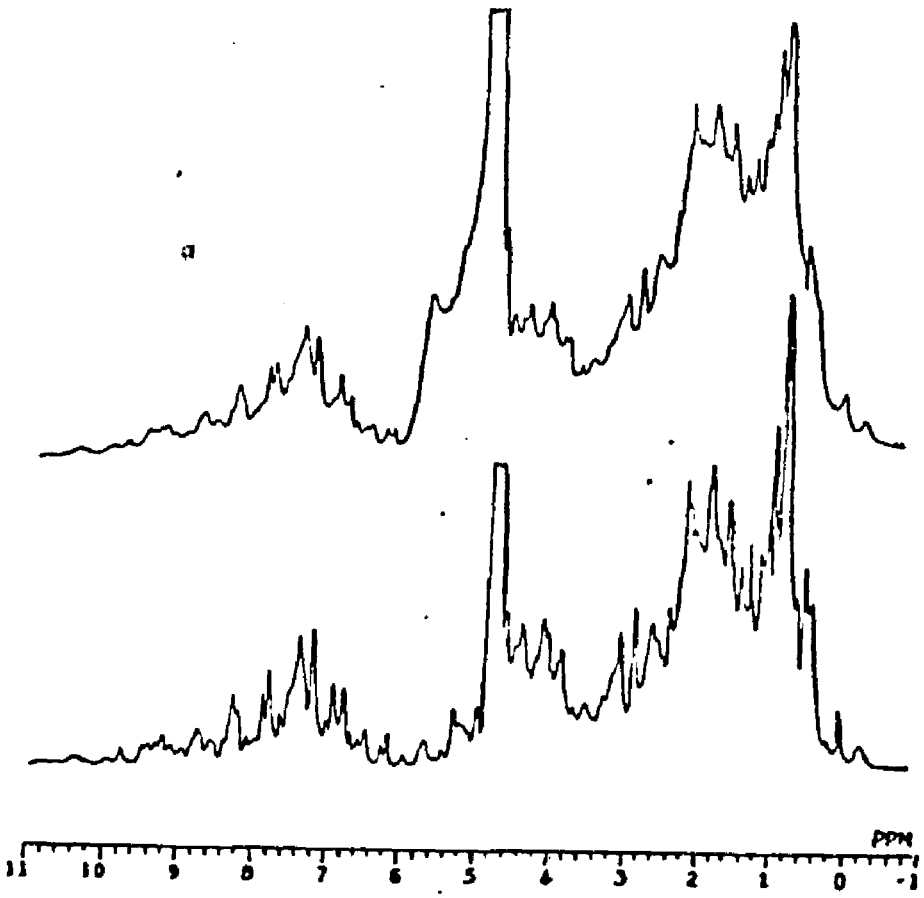
a
PPM
11
10
9
8
7
6
5
4
3
2
1
0
-1

finally transferred into a 10 mm (O.D) NMR tube (Wilmad) and the final volume was adjusted to 1.2 ml with deuterium free water.

Figure L shows the ^{2}H NMR spectrum of FdIA. No resonances were observed in the far downfield region or the aromatic region of the spectrum. Only a low intensity line was observed near -1 ppm from DSS. Direct observation of the hyperfine shifted resonances in the DMR spectrum was not expected to be easy, even if the protein was deuterium labelled at the cysteines, because of the large expected linewidth.

^{2}H NMR spectra of the hydrolysates of FdIA and FdIB

Both FdIA and FdIB were finally hydrolyzed in the presence of 0.21 M DMSO by the procedure described earlier. The hydrolysis solvent was then removed by rotary evaporation at 60 ^{o}C. The residue was taken up in 5 ml water and the cycle was repeated twice. The FdIA hydrolysate was finally taken up in 1.3 ml of 1 N HCl. However, the FdIB hydrolysate was taken up in water and was then pH adjusted to 1.5 with ammonium hydroxide. Both samples were loaded into 10 mm NMR tubes (Wilmad) to record their DMR spectra.

Figure L

60 MHz ^{2}H NMR spectrum of FdIA.

Solvent: 50 mM $KD_2PO_4/KDPO_4$, pD 7.39, prepared in deuterium free water (Aldrich Chemicals).

Spectral region shown is from 3 ppm downfield from HDO resonance to 13 ppm upfield from HDO resonance.

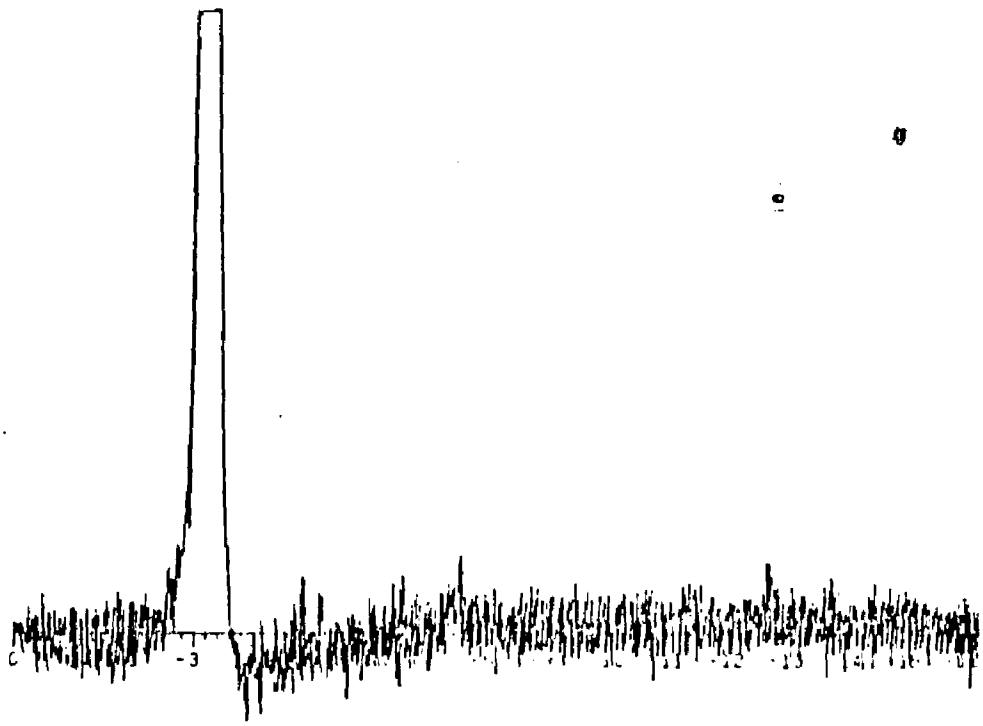
-3

Figure LI compares the ^{2}H NMR spectra of the hydrolysate of FdIAwith that of a sample of alpha ^{2}H-dl-cystine that was subjected to an identical hydrolysis treatment in a simultaneous experiment. In the latter case ^{2}H NMR spectrum of the hydrolysis mixture was recorded directly. Thus, because of the difference in pHs, the two spectra cannot be compared directly. The resonance near 0 ppm was established to be the HDO resonance by comparing the spectra recorded in deuterium depleted water (Aldrich Chemicals) and in natural abundance water.

Figure LII shows the ^{1}H NMR spectra of l-cysteic acid at varying pH conditions. From these spectra one could measure the chemical shift separation between the HDO resonance and the alpha deuterium resonance at the appropriate pH conditions of the above ^{2}H NMR spectra. Thus, this separation should be 0.67 ppm in 1N HCl and 3.11 ppm in 6N HCl. These results indicate that the resonances near 2 ppm in the ^{2}H NMR spectrum shown in Figure LII do not arise from cysteic acid, indicating lack of cysteine labelling in FdIA.

Figure LIII shows the ^{2}H NMR spectra of FDIB hydrolyzate, pH 1.5, and beta-^{2}H-dl-cystine hydrolyzate, pH 2.5. A similar analysis of this spectrum as in the

Figure LI

Bottom: 60 MHz ^{2}H NMR spectrum of hydrolyzed FdIA.

Top: 60 MHz ^{2}H NMR spectrum of hydrolyzed alpha ^{2}H-dl-cystine.

Solvent: Deuterium free water (Aldrich).

HDO resonance is assigned to 0 ppm.

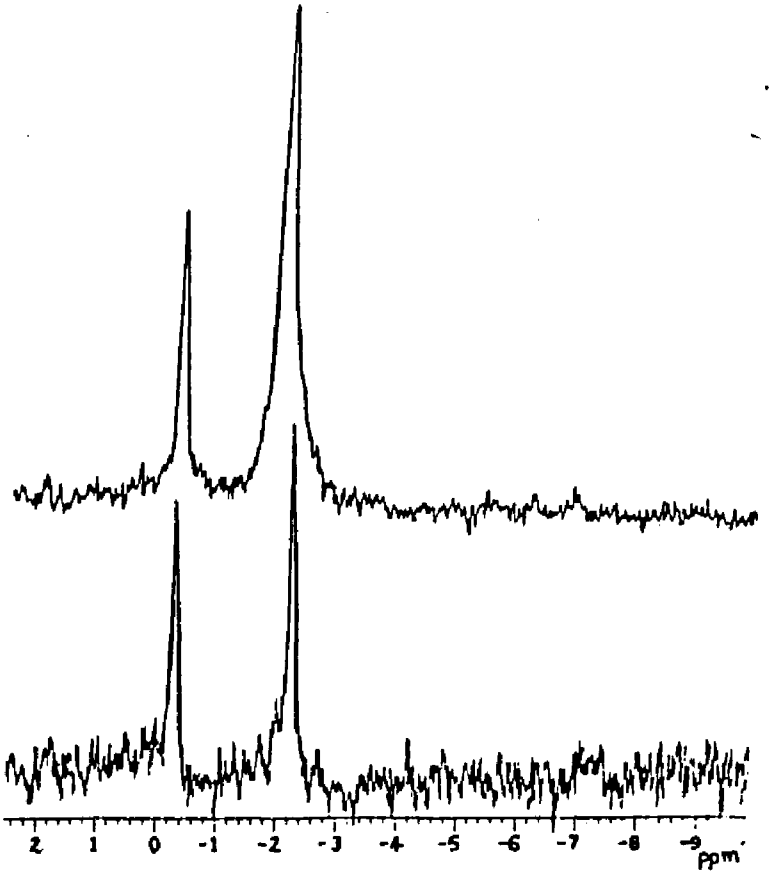
2
1
0
-1
-2
-3
-4
-5
-6
-7
-8
-9
ppm

Figure LII

pH dependence of the chemical ^{1}H chemical shifts of cysteic acid. Spectra were collected at 200 MHz on a Bruker CXP-200 spectrometer at Yale university. 0 ppm = DSS.

Spectrum shown is that in 1 N DCl.

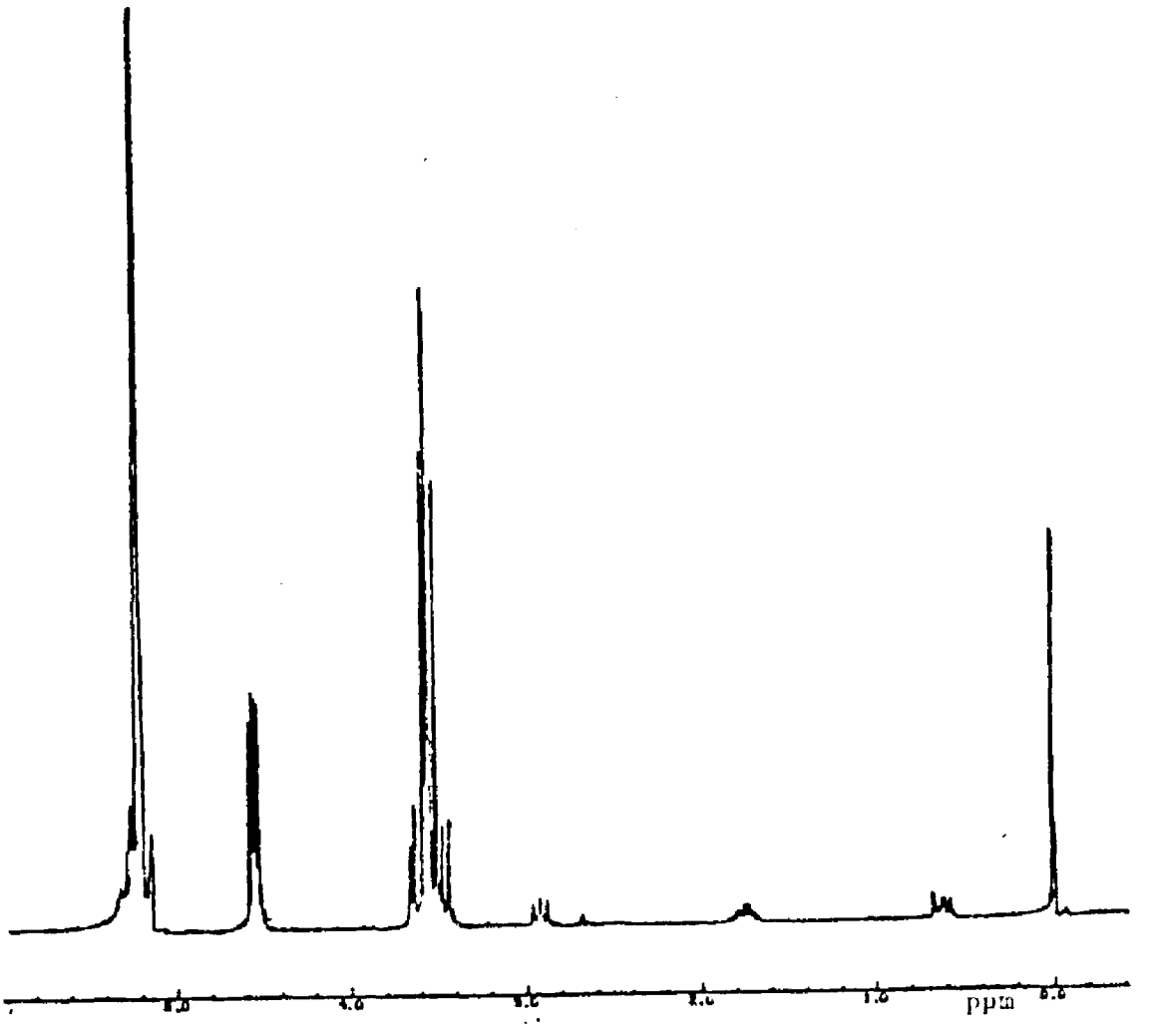

^{1}H Chemical shifts of dl-cysteic acid

Solvent	alpha	beta	HDO
6N DCl	4.64	3.66	7.25
1N DCl	4.54	3.56	5.21
DCl (pH 1.44)	4.46	3.51	4.77
DCl (pH 2.56)	4.22	3.46	4.75

Figure LIII

Bottom: 60 MHz ^{2}H NMR spectrum of hydrolyzed FdIB.

Top: 60 MHz ^{2}H NMR spectrum of hydrolyzed beta ^{2}H-dl-cystine.

Solvent: Natural abundance water.

HDO resonance is assigned to 5 ppm.

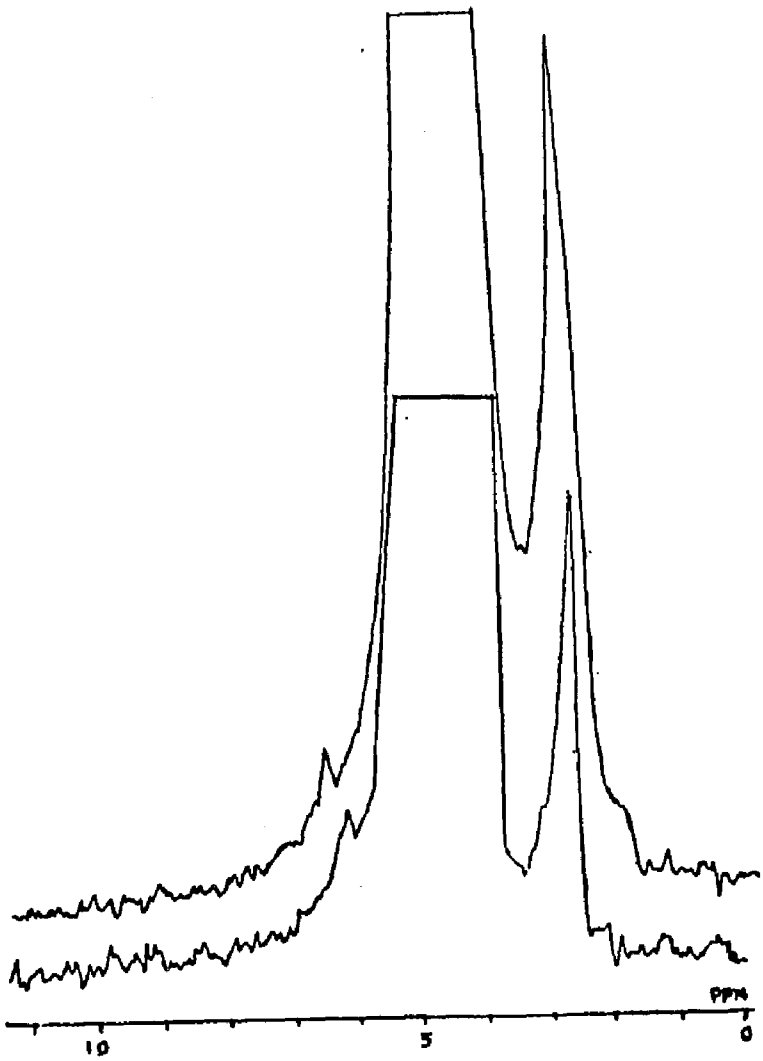
PPM
10
5
0

previous case show that the upfield resonances in the spectrum are not from the beta deuteriums of cysteic acid.

Figure LIV shows the proton decoupled ^{13}C NMR spectrum of FdIC in 10 mM tris.HCl buffer at pH 7. The resonance at 0 ppm is from the tris buffer. The other two broad resonances in the spectrum are the natural abundance resonances of aliphatic and the carbonyl carbons. These resonances lack any fine structure due to the poor signal to noise ratio of the spectrum. No additional resonaces were observed in the spectrum of apoferredoxin prepared from FdIC. This result clearly show the lack of ^{13}C label in FdIC.

Mass spectroscopy of apoferredoxin prepared from FdIB

0.5 mg of FdIB was converted into apoferredoxin as follows. The protein solution was made 10% (W/V) in trichloroacetic acid by the addition of the solid reagent at ice-bath temperature. The reaction mixture was allowed to stand at the ice-bath temperature for 1 hour. The milky white reaction mixture was centrifuged at 10000 X G for 20 minutes. The supernatant was discarded. The precipitate was taken up in 1.0 ml of 1.0 M trizma base. This protein solution was then dialysed against 20 L of

Figure LIV

Proton decoupled (broad band) ^{13}C NMR spectrum of FdIC. Spectra were recorded at 100 MHz collecting 64K time domain points with a spectral width of 25000 Hz and a pulse repetition time of 0.6 seconds.

Solvent: 10 mM tris.HCl in D_2O. The resonance at 0 ppm is due to tris buffer.

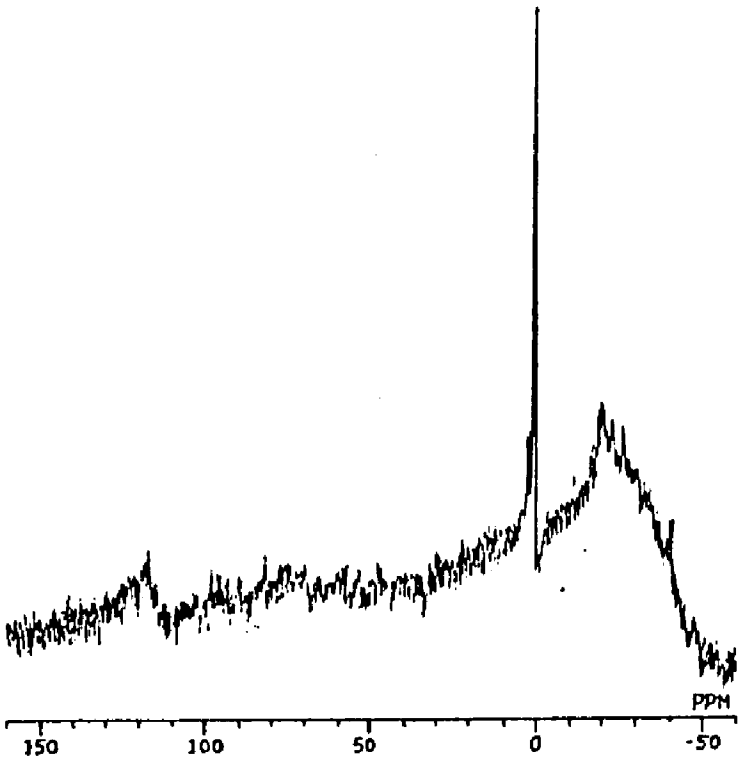
PPM
150
100
50
0
-50

distilled and deionised water for 48 hours with one solvent change. The solvent was then removed by lyophilization. The lyophilized apoferredoxin sample was sent to the Mass Spectroscopy Laboratory of Massachussets Institute of Technology for deuterium analysis by fast atom bombardment mass spectrometry (FAB-MS).

The apoferredoxins from FdI and FdIB were subjected to mild tryptic digestion for 4 hours at 40 ^{o}C. The primary peptide with the sequence AFVVTDNCIK (MH^{+} = 1109) was isolated from the hydrolyzed product by reverse phase liquid chromatography. The FAB spectra of this fragment from both FdI and FdIB were recorded. Spectra of both fragments showed the same ions with no apparent mass shift indicating that Cys^{8} and Cys^{11} of the fragment from FdIB was not labeled.

Conclusion

Ferredoxin I were isolated A. vinelandii grown on cystine media that contained alpha-^{2}H-dl-cystine, beta-^{2}H-dl-cystine, or beta-^{13}C-dl-cystine. FdI from these sources, designated FdIA, FdIB, and FdIC respectively, were analyzed by NMR methods. ^{1}H NMR spectra of FdIA, FdIB, and FdIC were indistinguishable from that of FdI. ^{2}H NMR spectra of hydrolyzates of FdIA and FdIB showed a

line upfield from HDO resonance. However, by analysis of ^{1}H NMR spectra of cysteic acid under similar conditions it was shown that the origins of these resonances were not the cysteines of FDIA and FdIB. ^{13}C spectrum of FdIC did not show cysteinyl carbon resonances either. Mass spectrum of apoferredoxin prepared from FdIB rendered further proof for the absence of deuterium labelling in FdIB. Thus these results, in conjunction with the results presented in the previous chapter, show that FdIA, FdIB, and FdIC were devoid of the anticipated isotopic labels on thier cysteines.

BIBLIOGRAPHY

1. Ghosh, D., O'Donnell, S., Furey, W., Jr., Robbins, A.H., and Stout, C.D. (1982) J. Mol. Biol. 158: 73.

2. Fee, J.A., Findling, K.L., Yoshida, T., Hille, R., Tarr, G.E., Hearshen, D.O., Dunham, W.R., Day, E.P., Kent, T.A., Münck, E. (1984) J. Biol. Chem. 259: 124.

3. Beinert H., Emptage, M.H., Dreyer, Jean-Luc., Scott,R.A., Hahn, J.E., Hodgson, K.O., and Thomson, A.J. (1983) Proc. Natl. Acad. Sci. USA 80: 393.

4. Johnson, M.K., Czernuszewicz, R.S., Spiro, T.G., Fee, J.A., and Sweeney, W.V. (1983) J. Amer. Chem. Soc. 105: 6671.

5. Robbins, A.H., and Stout, C.D. (1984) J. Biol. Chem. 260: 2328.

6. Emptage, M.H., Kent, T.A., Huynh, B.H., Rawlings, J., Orme-Johnson, W.H., and Munck, E. (1980) J.Biol. Chem. 255: 1793.

7. Stout, C.D., Ghosh, D., Pattabi, V., and Robbins, A.H. (1980) J. Biol. Chem. 255: 1797.

8. Moura, J.J.G., Moura, I., Kent, T.A., Lipscomb, J.D., Huynh, B.H., LeGall, J., Xavier, A.V., and Munck, E.(1982) J. Biol. Chem. 257: 6259.

9. Kent, T.A., Dreyer, J.-L., Emptage, M.H., Moura, I., Moura, J.J.G., Huynh, B.H., Xavier, A.V., Legall, J., Beinert, H., Orme-Johnson, W.H., and Munk, E.

10. Kent, T.A., Huynh, B.H., and Munck, E. (1980) Proc. Natl. Acad. Sci. USA 77: 6574.

11. Thomson, A.J., Robinson, A.E., Johnson, M.K., Moura, M.K., Moura, J.J.G., Xavier, A.V., and Legall. J. (1981) Biochim. Biophys. Acta. 670: 93.

12. Johnson, M.K., Thomson, A.J., Richards, A.J.M., Peterson, J., Robinson, A.E., Ramsay, R.R., and Singer, T.P. (1984) J. Biol. Chem. 259, 2274.

13. Shethna, Y.I. (1970) Biochim. Biophys. Acta 205: 58

14. Yoch, D.C., Benneman, J.R., Valentine R.C., and Arnon, D.I. (1969) Proc. Natl. Acad. Sci. USA 64: 1404.

15. Yoch, D.C., and Arnon, D.I. (1972) J. Biol. Chem. 247: 4514

16. Sweeney, W.V., Rabinowitz, J.C., and Yoch, D.C. (1975) J. Biol. Chem. 250: 7842.

17. Que, L Jr., Bobrik, M.A., Ibers, J.A., and Holm, R.H.(1974) J. Amer. Chem. Soc. 96: 168.

18. Howard, J.B., Lorsbach, T., and Que, L. (1976) Biochem. Biophys. Res. Commun. 70: 582.

19. Averill, B.A., Bale, J.R., and Orme-Johnson, W.H. (1978) J. Amer. Chem. Soc. 100: 3034.

20. Howard, B.A., Lorsbach, T.W., Ghosh, D., Melis, K., and Stout, C.D. (1983) J. Biol. Chem. 258: 508.

21 Nagayama, K., Ohmori, D., Imai, T., and Oshima, T. (1983) FEBS Lett. 158, 208.

22. Rabinowitz, J.C. (1972) Methods Enzymol 24: 431.

23. Lode, E.T., Murray, C.L., and Rabinowitz, J.C. (1976) J. Biol. Chem 251: 1683.

24. Sweeney, W.V., Rabinowitz, J.C., and Yoch, D.C. (1975) J. Biol. Chem. 250: 7842.

25. Covington, A.K., Paabo, M., Robinson, R.A., and Bates R.G. (1968) Anal. Chem. 40: 700

26. Wallace, E.F., and Rabinowitz, J.C. (1971) Arch. Biochem. Biophys. 146: 400.

27. Malkin, R., and Rabinowitz, J.C. (1966) Biochemistry 5: 1262.

28. Mcdonald, C.C., Philip, W.D., Lovenberg, W., and Holm, R.H. (1973) Ann. N.Y. Acad. Sci. 222: 789.

29. Malkin, R., and Rabinowitz, J.C. (1967) Biochemistry 6: 3880.

30. Peisach, J., Mims, W.B., and Davis, J.L. (1984) J. Biol. Chem. 259: 2704.

31. Mims, W.B., and Peisach, J. (1981) in Biological Magnetic Resonance (Berlinger, L.J. and Reuben J., eds.) Vol. III, 213.

32. Lerch, K., Mims, W.B., and Peisach, J. (1981) J. Biol. Chem. 256: 10088.

33. Peisach, J., Mims, W.B., and Davis, J.L. (1979) J. Biol. Chem. 254: 12379.

34. Orme-Johnson, N.R., Mims, W.B., Orme-Johnson, W.H., Bartsch, R.G., Susanovich, M.A. and Peisach, J. (1983) Biochim. Biophys. Acta. 748: 68.

35. Peisach, J., Orme-Johnson, N.R., Mims, W.B., and Orme-Johnson, W.H. (1977) J. Biol. Chem. 252: 5643.

36. Carter, C.W., Jr., Kraut, J., Freer, S.T., and

Alden, R.A. (1974) J. Biol. Chem. 249: 6339.

37. Cammack, R., Dickson, D.P.E., and Johnson, C.E. (1977) *Iron sulfur Proteins III* (Lovenberg, W., ed) 283.

38. Holm, R.H., Philips, W.D., Averill, B.A., Mayerele, J.J., and Herskowitz, T. (1974) J. Am. Chem. Soc. 96: 2109

39. Que, L., Jr., Anglin, J.R., Bobrik.=, M.A., Davison, A., and Holm, R.H. (1974) J. Am. Chem. Soc. 96, 6042.

40. Reynolds, J.G., Laskowski, E.J., and Holm, R.H. (1978) J. Am. Chem. Soc. 100, 5315.

41. Packer, E.L., Sweeney, W.V., Rabinowitz, J.C., Sternlicht, H., and Shaw, E.N. (1977) J. Biol. Chem. 252, 2245.

42. Phillips, W.D., and Poe, M. (1973) in Iron sulfur Proteins II (Lovenberg, W., ed). Academic Press, New York, 255.

43. Nettesheim, D.G., Meyer, T.E., Feinberg, B.A., and Otvos, J.D. (1983) J. Biol. Chem. 258, 8235.

44. Sweeney, W.V. (1980) J. Biol. Chem. 256, 12222.

45. Malikayil, J.A., Sweeney, W.V., McCracken, J., and Peisach, J. (1985) Biochem. Biophys. Res. Commun. 133: 1119

46. Nagayama, K., and Ohmori, D. (1984) FEBS Lett. 173: 15.

47. Jesson, J.P. (1973) in NMR of Paramagnetic Molecules, Academic Press, 1.

48. Ohnishi, T., Blum, H., Sato, S., Nakasawa, K., Hon-Nami, K., and Oshima, T. (1980) J. Biol. Chem. 255: 345.

49. Imai, T., Matsumoto, T., Ohta, S., Ohmori, D., Suzuki, K., Tanaka, J., Tsukioka, M., and Tobari, J. (1983) Biochim. Biophys. Acta. 743: 91.

50. Carter, C.W., Jr. Kraut, J., Freer, S.T., Alden, R.A., Seiker, L.C., Adman, E.T., and Jensen, L.H. (1972) Proc. Natl. Acad. Sci. U.S.A. 69: 3526.

51. Nagayama, K., Imai, T., Ohmori, D., and Oshima, T. (1984) FEBS Lett. 169: 79.

52. Nagayama, K., Ozaki,Y., Kyoguku, Y., Hase, T., and Matsubara, H. (1983) J. Biochem. 94: 893.

53. Johnson, M.K., Spiro, T.G., and Mortenson, L.E., (1982) J. Biol. Chem. 257: 2447.

54. Fee, J.A., Mayhew, S.G., and Palmer, G. (1971) Biochim. Biophys. Acta. 245: 196.

55. Ingledew, W.J., and Ohnishi, T. (1980) Biochem. J. 186: 111.

56. Hamilton, P.B. (1963) Anal. Chem. 35: 2055.

57. Roth, M. and Hampai, A. (1973) J. Chromatography. 83: 353.

58. Lee, K.S., and Drescher, D.G. (1978) Inter. J. Biochem. 9: 457.

59. Ishida, Y., Fugita, T., and Asai, K. (1981) J. Chromatography. 204: 143.

60. Hill, D.W., Walters, F.H., Wilson,T.D., and Stuart,

J.D. (1979) Anal. Chem. 51: 1338.

61. Roth, M. (1971) Anal. Chem. 43: 880.

62. Simmons, S.S., Jr., and Johnson, D.F. (1976) J. Am. Chem. Soc. 98: 7098.

63. Johnson, A., and Everett, G.W., Jr. ((1972) J. Am. Chem. Soc. 94: 1419.

64. Solomon, I. (1955) Phys. Rev. 99: 559.

65. Bloembergen, N. (1957) J. Chem. Phys. 27: 572.

66. Sternlicht, H. (1965) J. Chem. Phys. 42: 2250.

67. Chmelnick, A.M., and Fiat, D. (1968) J. Chem. Phys. 49: 2101.

68. Reuben, J., Reed, G.H., and Cohn, M. (1970) J. Chem. Phys. 52: 1617.

69. Cantor, C.R., and Shimmel, P.R. (1980) in Biophysical Chemistry Part II: Techniques for the study of biological structure and function (W.H. Freeman And Company) 461.

70. Schramm, S., and Oldfield, E. (1983) Biochemistry 22: 2908.

71. Upson, D.A., and Hruby, V.J. (1977) J. Org. Chem. 42: 2329

72. Wood, J.L., and Du Vigneaud, V. (1939) J. Biol. Chem. 131: 267.

73. Ghosh, D., Furey, W., O'Donnell, S., and Stout, C.D. (1981) J. Biol. Chem. 256: 4185.

74. Carter, C.W., Jr., Kraut, J., Freer, S.T., and Alden, R.A. (19740 J. Biol. Chem. 249: 6339.

75. Adman, E., Watenpaugh, K.D., and Jessen, L.H. (1975) Proc. Natl. Acad. Sci. U.S.A. 72; 5854.